Universidade do Minho
Escola de Medicina

Luísa da Rocha Santa Marinha

Lipid signaling determinants of physiology and pathology along the longitudinal hippocampal axis

setembro de 2020

Lipid signaling determinants of physiology and pathology along the longitudinal hippocampal axis
Luísa da Rocha Santa Marinha
UMinho | 2020

Universidade do Minho
Escola de Medicina

Luísa da Rocha Santa Marinha

Lipid signaling determinants of physiology and pathology along the longitudinal hippocampal axis

Tese de Doutoramento
Doutoramento em Medicina

Trabalho efetuado sob a orientação do
Professor Doutor Tiago Gil Rodrigues Oliveira

setembro de 2020

Agradecimentos/Acknowledgements

À minha família, sempre. Aos meus pais e irmão pelo carinho incondicional e apoio sempre presentes. À minha mãe por ser o exemplo de força maior, ao meu pai por ser o exemplo de coragem e perseverança e ao meu irmão por nunca deixar que eu não acreditasse em mim.

Ao meu orientador, Professor Doutor Tiago Gil Oliveira, que me acompanhou desde as aulas de anatomia até este doutoramento. Obrigada pelo incentivo no princípio, meio e fim desta caminhada. Obrigada pelo apoio incondicional e pelo telefonema sempre disponível, científico ou não.

Ao Doutor Vítor Pinto, que muito me ensinou sobre eletrofisiologia e sobre ser pessoa.

À equipa TGO que muito me deu. Obrigada especial à Francisca Vaz Bravo, Isabel Castanho, André Miranda e Rafaela Ribeiro pela ajuda, integração e companhia. Ao Torcato Meira, meu amigo que me ensinou acerca de CA2 e memória social.

Aos que estiveram sempre por perto, aos "Milões", à Marisa, ao Carlos, ao André Viana e ao João Pereira. Aos amigos que o doutoramento me trouxe e que comigo partilharam sucessos, dificuldades e cafés. Obrigada especial à Sónia Guerra Gomes, Tiago Rosa, Cláudia Antunes, Vanessa Sardinha, Jorge Silva, Diana Nascimento, João Viana, Sara Silva, Sofia Neves e Marco Guimarães.

À Tuna de Medicina da Universidade do Minho, minha família durante a minha passagem na Escola de Medicina da Universidade do Minho.

Aos constituintes da minha comissão de tese, Doutor Carlos Bandeira Duarte, Doutora Patrícia Monteiro e Doutor João Carlos Sousa pelas discussões científicas sempre relevantes.

À Escola de Medicina da Universidade do Minho/Instituto de Investigação em Ciências da Vida e Saúde, que me acolheu enquanto aluna de Mestrado em Medicina e me proporcionou as condições para me tornar aluna de Doutoramento em Medicina.

Ao João, o meu porto seguro.

This work was supported by Programa Operacional Regional do Norte (NORTE2020) (fellowship UMINHO/BD/52/2017) and the BIAL Foundation, Portugal (253/14) and by national funds, through the Foundation for Science and Technology (FCT) - project UIDB/50026/2020 and UIDP/50026/2020; and by the projects NORTE-01-0145-FEDER-000013 and NORTE-01-0145-FEDER-000023, supported by Norte Portugal Regional Operational Programme (NORTE 2020), under the PORTUGAL 2020 Partnership Agreement, through the European Regional Development Fund (ERDF).

STATEMENT OF INTEGRITY

I hereby declare having conducted this academic work with integrity. I confirm that I have not used plagiarism or any form of undue use of information or falsification of results along the process leading to its elaboration.

I further declare that I have fully acknowledged the Code of Ethical Conduct of the University of Minho.

Resumo

O hipocampo é uma estrutura do lobo temporal do cérebro presente em todos os mamíferos, fundamental para a aprendizagem, memória e navegação espacial. A sua arquitetura transversal é constituída pelo giro denteado e Cornu Ammonis (CA), que se divide em CA1, CA2 e CA3, e é preservada ao longo do eixo longitudinal e em todas as espécies. Os lípidos fazem parte dos principais constituintes do cérebro e os distúrbios no seu conteúdo e metabolismo têm sido propostos como sendo de particular importância em várias doenças. A análise por espectrometria de massa das porções dorsal (HD), intermédia e ventral (HV) do hipocampo revelou um gradiente lipídico contínuo ao longo do eixo longitudinal, com maior distinção entre o HD e HV. O HD apresenta níveis superiores de ácido fosfatídico e níveis reduzidos de fosfatidilcolina em comparação com o HV, potencialmente implicando a via da fosfolipase D (PLD) na regulação do eixo HD-HV. A superfamília da PLD possui seis membros (PLD1-PLD6), mas apenas a PLD1 e a PLD2 hidrolisam fosfatidilcolina em ácido fosfatídico.

O nosso principal objetivo foi estudar o impacto da modulação genética da PLD na organização e função do eixo HD-HV. Em primeiro lugar, mostramos que a PLD1 e a PLD2 são os únicos contribuintes para a atividade total da PLD no cérebro de ratinho, embora a PLD1 seja uma fonte maioritária de ácido fosfatídico no HD e HV em comparação com a PLD2. A seguir, abordamos como a PLD1 afeta diferencialmente a organização e o funcionamento do hipocampo em cada subregião. A ablação da PLD1 afeta predominantemente o lipidoma do HD e os ratinhos *Pld1* knockout (KO) apresentam déficits específicos no reconhecimento de objetos novos e interação social e também disrupção na diferenciação da arborização dendrítica do HD e HV em neurónios piramidais de CA1/CA3. Apresentam ainda diminuição na indução de depressão de longo-prazo (LTD) e redução dos níveis das proteínas GluN2A e SNAP-25 no HD. De seguida, abordamos os efeitos da ablação PLD2 no comportamento social e na potenciação sináptica hipocampal. Mostramos que a ablação PLD2 leva a défices de discriminação social, nomeadamente no reconhecimento de ratinhos da mesma ninhada, diminuição da exploração social e redução de potenciação de longo-prazo (LTP) no HV.

Com nosso trabalho mostramos como a PLD regula o hipocampo e a sua função, mostrando que, embora a PLD1 e a PLD2 catalisem a mesma reação, a sua ablação específica promove fenótipos diferentes. Isto tem possíveis implicações em doenças neurodegenerativas, como a doença de Alzheimer, na qual PLD tem um papel importante para a sua patologia.

Palavras-chave: Fosfolipase D, Hipocampo, Lípidos, Memória

Abstract

The hippocampus is a brain temporal lobe structure present in all mammals fundamental for learning, memory and spatial navigation. Its cross-sectional architecture, constituted by the dentate gyrus (DG) and Cornu Ammonis (CA) subfields, CA1, CA2 and CA3, is preserved along the longitudinal axis and in every species. Lipids are major constituents of the brain and disturbances in brain lipid content and metabolism have been proposed to be of particular importance in several diseases. A mass spectrometry analysis of dorsal (DH), intermediate and ventral (VH) portions of the hippocampus revealed a continuous lipid gradient along the longitudinal axis, with greater distinction between DH and VH. DH presents increased phosphatidic acid (PA) and decreased phosphatidylcholine (PC) compared to the VH, potentially implicating the phospholipase D (PLD) pathway in DH-VH axis regulation. The PLD superfamily has six members (PLD1-PLD6), but only PLD1 and PLD2 hydrolyze PC into PA.

Our main goal was to study the impact of PLD genetic modulation on the DH-VH axis organization and function. First, we showed that PLD1 and PLD2 are the only contributors to total PLD activity in the mouse brain, although PLD1 is a major source of PA in both DH and VH when compared to PLD2. Next, we addressed how PLD1 differentially affects hippocampal organization and functioning in a region-specific manner. PLD1 ablation affects predominantly the lipidome of the DH and *Pld1* knockout (KO) mice present specific deficits in novel object recognition and social interaction, disruption in the DH-VH dendritic arborization differentiation in CA1/CA3 pyramidal neurons, along with reduced long-term depression (LTD) induction and reduced GluN2A and SNAP-25 protein levels in the DH. Then, we address the effects of PLD2 ablation in social behavior and hippocampal synaptic potentiation. We showed that PLD2 ablation leads to social discrimination deficits, namely littermate recognition impairment, decreases social exploration and reduces long-term potentiation (LTP) in the VH.

With our work we show how PLD differentially regulates the hippocampus, showing that, although PLD1 and PLD2 catalyze the same reaction, their specific ablation promotes different phenotypes. This leads to potential implications in neurodegenerative diseases, such as Alzheimer's disease, in which PLD is an important player.

Keywords: Hippocampus, Lipids, Memory, Phospholipase D

Table of Contents

Abbreviations List

AA – Arachidonic acid

ACSF – Artificial cerebrospinal fluid

APP – Amyloid precursor protein

ARF – ADP ribosylation factor

AVP – Arginine vasopressin

AVPR – Arginine vasopressin receptor

Aβ – Amyloid Beta

BACE1 – β-secretase β-site APP cleavage enzyme 1

BDNF – Brain-derived neurotrophic factor

C. elegans – *Caenorhabditis elegans*

CA – Cornu Ammonis

CDP-DAG – Cytidine diphosphate-diacylglycerol

CDS – Cytidine diphosphate-diacylglycerol synthase

CL – Cardiolipin

DAG – Diacylglycerol

DG – Dentate gyrus

DGK – Diacylglycerol kinase

DH – Dorsal hippocampus

dhCer – Dihydroceramide

DKO– Double knock out

d*Pld* – *Drosophila* Phospholipase D (gene)

dPLD – *Drosophila* Phospholipase D (protein)

EC – Entorhinal cortex

EPM – Elevated plus maze test

FC – Fear conditioning test

GluA – α-amino-3-hydroxy-5-methyl-4-isoxazolepropionic acid (AMPA) receptor (also known as GluR)

GluN – N-methyl-D-aspartate receptor (also known as NMDAR or NR)

HKD – HxKxxxxD

hPLD – human PLD

KO – Knockout

LC-MS – Liquid chromatography-mass spectrometry

LPA – Lysophosphatidic acid

LPAAT – Lysophosphatidic acid acyltransferase

LPC – Lysophosphatidylcholine

LPCe – Ether lysophosphatidylcholine

LPI – Lysophosphatidylinositol

LTD – Long-term depression

LTP – Long-term potentiation

MG – Monoacylglycerol

MS – Mass spectrometry

mTOR – Mammalian target of rapamycin

mTORC – Mammalian target of rapamycin complex

MWM – Morris water maze test

NOR – Novel object recognition test

OF – Open field test

OXT – Oxytocin

OXTR – Oxytocin receptor

PA – Phosphatidic acid

PAP– Phosphatidic acid phosphatase

PC – Phosphatidylcholine

PE – Phosphatidylethanolamine

PEtOH – Phosphatidylethanol

PG – Phosphatidylglycerol

PH– Pleckstrin homology

PI – Phosphatidylinositol

$PI(4,5)P_2$ – Phosphoinositide 4,5-bisphosphate

PIP – Phosphatidylinositol phosphate

PIP_2 – Phosphatidylinositol bisphosphate

PIP_3 – Phosphatidylinositol triphosphate

PKC – Protein kinase C

PLA – Phospholipase A

PLB – Phospholipase B

PLC – Phospholipase C

Pld – Phospholipase D (gene)

PLD – Phospholipase D (protein)

PP – Paired pulse

PS – Phosphatidylserine

PS1 – Presenilin 1

PX – Phox

RhoA – Ras homolog family member A

SNARE – N-ethylmaleimide sensitive factor attachment protein receptor

TRAAK – TWIK-related arachdonic acid stimulated K+ channel

TREK – TWIK-related K channel

VH – Ventral hippocampus

WT – Wild type

Figures, Tables and Boxes

Chapter 1

Chapter 2

Chapter 2 – Supplementary Information

Chapter 3

Chapter 3 – Supplementary Information

Chapter 4

CHAPTER 1

General Introduction

1.1. Hippocampus

The hippocampus is a brain temporal lobe structure present in all mammals fundamental for learning, memory and spatial navigation (Strange et al., 2014). Classically, memory can be divided in short-term (working) memory and long-term memory, which, in its turn, can be subdivided in non-declarative (implicit) memory and declarative (explicit) memory (see Figure 1). Both episodic (memory for events or episodes in a specific spatial and temporal context) and semantic memory (generic memory about people, objects, places, new word meanings and the world in general) compose the declarative long-term type of memory (Kandel et al., 2000). The processing of declarative memory involve encoding (where new information is attended and linked to existing information in memory), storage (mechanism by which memory is retained over time), consolidation (the mechanism that makes the temporarily stored and still labile information more stable, which implicates expression of genes and protein synthesis that give rise to structural changes at synapses) and retrieval (the process by which stored information is recalled) (Kandel et al., 2000).

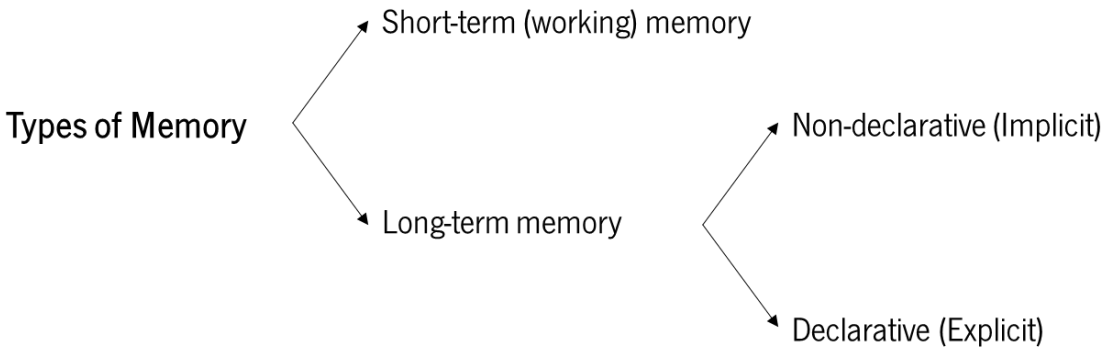

Figure 1. Types of memory.

The hippocampal role in declarative memory was first considered with the work of Scoville and Milner with the patient H.M., after a bilateral temporal resection in an attempt to treat temporal lobe epilepsy (Scoville and Milner, 1957). As a result, the seizures were controlled but severe anterograde amnesia emerged as a side effect, with deficient acquisition of episodic and semantic knowledge (Corkin, 2002).

The hippocampal role in spatial navigation was contemplated with the discovery of “place cells”, which are pyramidal neurons that become activate when a subject is in a particular environment or “place field” (O'Keefe and Dostrovsky, 1971; O'Keefe and Speakman, 1987), and with the realization that hippocampal lesions cause a profound and lasting impairment in place-navigation (Morris et al., 1982). Later, entorhinal grid cells were also proposed to encode the spatial map (Hafting et al., 2005). These neurons fire in hexagonal grid patterns and transmit information to place cells (Hafting et al., 2005). Conjointly, these two types of cells from the hippocampal and parahippocampal formations work to grant positioning awareness and spatial representations (Moser et al., 2008).

The hippocampus is curved-shaped and its cross-sectional architecture is preserved along the longitudinal axis and in every species (Strange et al., 2014). The hippocampal formation consists of dentate gyrus (DG), hippocampus proper – Cornu Ammonis (CA), consisting of CA1, CA2 and CA3 – and subiculum (Strange et al., 2014; van Strien et al., 2009). It has a three-layered appearance histologically. The deep layer, constituted by afferent and efferent fibers and interneurons, is the hilus in the DG and the stratum oriens in the CA (van Strien et al., 2009). The intermediate layer is the cell layer, mainly with cells and interneurons, and it is called granule layer (with granular cells that present only apical dendrites in mice) in the DG and stratum pyramidale (with pyramidal neurons that express both apical and basal dendrites) in the CA and the subiculum (Kandel et al., 2000; van Strien et al., 2009). The superficial layer is called the stratum moleculare in the DG and in the subiculum (van Strien et al., 2009). In CA3, the superficial layer is subdivided in three: the stratum lucidum, the stratum radiatum and the stratum lacunosum-moleculare (van Strien et al., 2009). The first receives input from the DG; the second shelters the apical dendrites from stratum pyramidale neurons; and the last comprises the apical tufts of the apical dendrites (van Strien et al., 2009). In CA1 and CA2 the stratum lucidum is missing (van Strien et al., 2009). All these structures interconnect in complex intrahippocampal circuits.

The entorhinal cortex (EC) is a hippocampal nearby structure that sends sensory and spatial information to the hippocampus through the perforant direct and indirect pathways (see Figure 2) (Kandel et al., 2000; Strange et al., 2014; van Strien et al., 2009). The monosynaptic direct pathway is originated in the layer III of the EC and its neurons form synapses on the distal apical dendrites of CA1 neurons (Kandel et al., 2000; van Strien et al., 2009). The indirect pathway has its origins in the layer II of the EC and reaches the more proximal regions of CA1 through the

trisynaptic pathway: neurons from layer II of EC synapse onto DG granule cells (synapse 1) whose axons project in the mossy fiber pathway to excite the pyramidal cells in the CA3 (synapse 2) and then axons of the neurons from CA3 region project through the Schaffer collateral pathway to make excitatory synapses on CA1 pyramidal cell dendrites (synapse 3) (Kandel et al., 2000; van Strien et al., 2009). Both pathways are necessary for normal learning and memory. Inactivation of the indirect pathway impairs the competence to perform complex spatial learning and memory tasks while lesions of the direct pathway impair episodic memory and interfere with the ability to consolidate memory (Kandel et al., 2000). The major output of the hippocampus are the pyramidal neurons in CA1 region, which have projections to the layer V of EC and to the subiculum (which also projects to layer V of the EC), closing the circuit (Kandel et al., 2000). Regarding EC connections, it is known that cells from EC layer II also project to CA3 (Tamamaki and Nojyo, 1993) and that neurons from EC layer III project to the subiculum in addition to CA1 (direct pathway) (Honda et al., 2012).

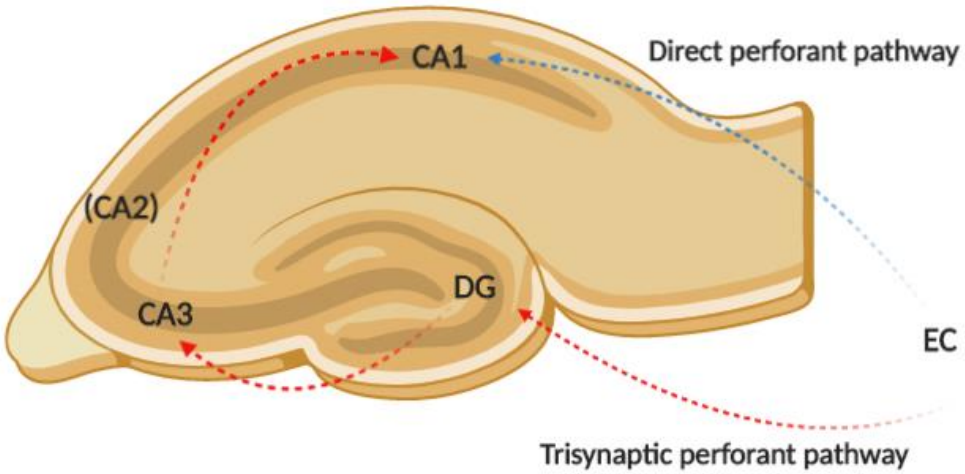

Figure 2. Classical cortico-hippocampal synaptic circuitry. Schematic representation of the intra-hippocampal connectivity and connection with EC. The trisynaptic pathway is highlighted in red and the direct (monosynaptic) pathway is highlighted in blue. CA, Cornu Ammonis; DG, dentate gyrus; EC, entorhinal cortex.

Afterward, studies focusing on CA2 revealed other cortico-hippocampal pathways. CA2 pyramidal neurons receive strong input from layer II of the EC and are weekly activated by CA3 neurons. In

their turn, CA2 neurons strongly activate CA1 neurons (Chevaleyre and Siegelbaum, 2010). Thus, CA2 provides a disynaptic link between the cortical input to the hippocampus to its CA1 neuronal output (Chevaleyre and Siegelbaum, 2010). Moreover, DG neurons form monosynaptic inputs to CA2 pyramidal neurons (Kohara et al., 2014). In addition, there are CA3-CA2 connections dominated by feedforward inhibition (Chevaleyre and Siegelbaum, 2010; Kohara et al., 2014).

Inhibition or genetic lesions of each of these structures improved the knowledge about their function. Deletion of N-methyl-D-aspartate receptor 1 (GluN1, also known as the NMDAR1 or NR1) in CA1 pyramidal neurons leads to impaired spatial memory, because of impairment in CA1 long-term potentiation (LTP) (see below), without disruption of nonspatial learning (Tsien et al., 1996). Dorsal CA1 and subiculum are involved in contextual memory (Goshen et al., 2011; Roy et al., 2017) and inhibition of dorsal CA1, sparing other hippocampal regions, such as dorsal DG and CA3 and ventral CA1, impairs remote memory recall (Goshen et al., 2011). Dorsal CA1 inhibition with muscimol, a selective $GABA_A$ receptor agonist, also impairs spatial and object memory (Stackman et al., 2016). On the other hand, ventral CA1 (and its projections to the nucleus accumbens) is implicated in the storage of social memory (Okuyama et al., 2016). In fact, dorsal CA2 projections to ventral CA1 are necessary for social memory (Meira et al., 2018). Deletion of GluN1 in CA3 pyramidal cells also leads to deficits in social memory and, ventral, but not dorsal, CA3 is necessary for the encoding of a social memory (Chiang et al., 2018). Targeted manipulation of GluN receptors in CA3 showed that the output from CA3 in the trisynaptic pathway is dispensable for spatial learning, but the full trisynaptic pathway containing CA3 was required for rapid one-trial contextual learning and for pattern completion recall (Nakashiba et al., 2008).

The DG is a brain region where neurogenesis persists into adulthood (Altman and Das, 1965; Anacker and Hen, 2017; Hochgerner et al., 2018). A transgenic mouse model in which output of old granule cells was specifically inhibited while leaving a substantial portion of young granule cells intact displayed enhanced or normal contextual and spatial pattern separation (ability to distinguish between two similar contexts), which was reduced following ablation of young granule cells. In addition, these animals exhibited deficits in contextual and spatial pattern completion (ability to recall a memory based on incomplete information). This indicates that pattern separation depends on adult-born young granule cells, while recall by pattern completion needs older granule cells (Nakashiba et al., 2012).

Genetic ablation of layer III inputs from EC to the hippocampus leads to an impairment in hippocampal-dependent temporal association memory (the ability to associate temporally discontinuous elements) assessed by trace fear conditioning (Suh et al., 2011).

Despite the preservation of the same basic intrinsic circuit, anatomical features (such as cortical and subcortical connections) and electrophysiological, gene expression and functional studies distinguish a longitudinal dorsal-ventral (DH-VH) axis in rodents, that segregate into DH-VH poles, which correspond in primates to posterior-anterior poles, respectively (Strange et al., 2014). Despite the sharply demarcated dichotomous segregation into dorsal-ventral portions, it has also been enrolled a gradual biochemical and functional transition between the two poles (Strange et al., 2014).

The classical dichotomic view associates predominantly the DH in spatial navigation and episodic memory and the VH in emotional stress-related behaviors (Bannerman et al., 2014; Fanselow and Dong, 2010; Kheirbek et al., 2013; McHugh et al., 2011; Strange et al., 2014) and also in motivational behaviors because of its connections with the amygdala and hypothalamus (see Figure 3) (van Strien et al., 2009). On the other hand, DH-VH organization of extrinsic connectivity follows topographically organized projections along the hippocampus (Strange et al., 2014).

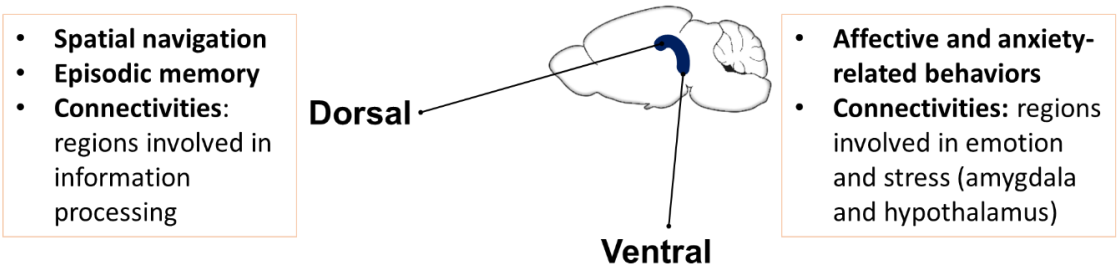

Figure 3. Hippocampus dichotomic view.

Expression of specific genes also support this long-axis organization (Strange et al., 2014), for example, NMDAR expression decreases from dorsal to ventral in CA1 (Maruki et al., 2001) and hippocampal gene expression analysis predicted functional differentiation across the full longitudinal axis of the hippocampus (Bienkowski et al., 2018; Shah et al., 2017; Thompson et

al., 2008). Also, low-affinity glucocorticoid receptors are more expressed in the DH, while high-affinity mineralocorticoid receptors are more expressed in the VH (Segal et al., 2010).

Chronic unpredictable stress also has a different impact along the DH-VH axis of the hippocampus. In the DH, stress triggers a volumetric reduction as a result of atrophy of CA3 and CA1 apical dendrites, whereas in the VH there is an increase in hippocampal volume concurrent with the increase of CA3 apical dendrites. Moreover, electrophysiological data revealed that stress leads to a decrease in VH long-term depression (LTD) (see below) (Maggio and Segal, 2007; Pinto et al., 2015).

Regarding other electrophysiological features, when dividing the hippocampus along its septotemporal axis into five sections, LTP is specifically reduced in the more ventral portion, compared with the rest of the hippocampus (Maggio and Segal, 2007). This was reversed by an exposure to acute stress, allowing VH to express a large LTP, whereas in the rest of the hippocampus it was much suppressed (Maggio and Segal, 2007). Nonetheless, LTD in VH is of similar magnitudes as the ones expressed in DH (Pinto et al., 2015). Short-term plasticity is also different between DH and VH, with DH presenting higher levels of paired pulse (PP) facilitation (Maruki et al., 2001; Pinto et al., 2015).

Concerning lipid composition, a broad-scale analysis of dorsal, intermediate and ventral portions of the hippocampus revealed a continuous gradient along the longitudinal axis, with greater distinction between DH and VH (Miranda et al., 2019). Treatment with corticosterone in rats also led to region-specific modulation of lipid species, displaying VH as more sensitive to corticosterone (Miranda et al., 2019).

Altogether, these findings provide insight for hippocampal organization and functioning in a region-specific manner.

1.2. Synaptic Plasticity

One of the most important characteristics of the mammalian brain is its plasticity. It has been proposed that associative memories are stored as changes in the strength of synaptic connections between neurons, also called synaptic plasticity (Bannerman et al., 2014; Citri and Malenka, 2008). Numerous forms of synaptic plasticity have been characterized. Synaptic

transmission can last from milliseconds to several minutes (short-term synaptic plasticity) or longer (long-term synaptic plasticity) (Citri and Malenka, 2008).

Short-term plasticity is important for short-term adaptations to sensory inputs, transient changes in behavioral states and short-lasting forms of memory (Citri and Malenka, 2008). It is triggered by short bursts of activity, causing a transient accumulation of calcium in presynaptic nerve terminals, leading to changes in the probability of neurotransmitter release (Citri and Malenka, 2008). When two stimuli are delivered within a short interval, the response to the second stimulus can be enhanced or depressed relative to the response to the first stimulus – PP facilitation or depression. One synapse can display either facilitation or depression depending on the previous activation or modulation (Citri and Malenka, 2008). PP depression occurs within short interstimulus intervals (less than 20ms) and can be caused by depletion of some pool of readily releasable vesicles (Zucker and Regehr, 2002) or it can arise from feedback activation of presynaptic receptors and from postsynaptic processes such as receptor desensitization (Citri and Malenka, 2008; Zucker and Regehr, 2002). Longer interstimulus intervals (20–500ms) are responsible for PP facilitation, since the residual calcium left over from the invasion of the first action potential contributes to additional release during the second stimulation (Zucker and Regehr, 2002) or due to the activation of protein kinases that regulate the activity of presynaptic phosphoproteins (Citri and Malenka, 2008). Longer-lasting forms of plasticity can be seen after tetanic stimulation with prolonged (200ms to 5s) trains of stimulation applied at high frequencies (10-200 Hz) – augmentation and post-tetanic potentiation (Zucker and Regehr, 2002).

Memory relies on changes in synaptic strength, which can take the form of persistent enhancements, such as LTP of LTD (Bear, 1996; Kemp and Manahan-Vaughan, 2004). Most hippocampal studies regarding long-term plasticity are focused on LTP in CA1, but it is known that the majority of synapses that exhibit LTP also exhibit LTD (Citri and Malenka, 2008). A brief high-frequency train of stimuli gives rise to LTP and distinct forms of LTP diverge in the relative importance of diverse receptors and ion channels and each one may be able to recruit distinct second-messenger signaling pathways (Kandel et al., 2000). Postsynaptic NMDAR are necessary for LTP at the Schaffer collateral, mossy fiber and entorhinal inputs to CA1, although its contribution diverges in the three pathways (Kandel et al., 2000). Therefore, inhibition of LTP in the hippocampus interferes with spatial memory (Kandel et al., 2000). LTP can also be split into a short and long-term phases, this last requiring the synthesis of new proteins and mRNA for its persistence (Kauderer and Kandel, 2000).

LTD is a mechanism that downregulates synaptic function and it was first identified in the cerebellum, with relevance for motor learning (Kandel et al., 2000). LTD induction requires longer periods of low-frequency synaptic stimulation (Kandel et al., 2000) and can also be divided in phases, depending an early-phase of covalent modifications of preexisting proteins, whereas a late-phase requires transcription and translation (Kauderer and Kandel, 2000).

1.3. Lipids

Lipids can be defined as fat-soluble molecules based on their solubility in non-polar solvents (Lam and Shui, 2013). Lipids are a naturally occurring group of amphipathic molecules, which means they hold both a hydrophobic/apolar domain and a hydrophilic domain, which interacts with water (Simons and Sampaio, 2011). This hydrophobic effect results from the hydrocarbon domains that distort the stable hydrogen-bonded structure of water by inducing cage-like structures around the apolar domains (Simons and Sampaio, 2011). Moreover, the lipids degree of length and saturation provides different physical properties to membranes, such as thickness, fluidity, and microdomain assembly (Holthuis and Menon, 2014).

Based on their functional backbone structure, a commonly used classification divides lipids into eight categories: fatty acyls, glycerolipids, glycerophospholipids, sphingolipids, sterol lipids, prenol lipids, saccharolipids and polyketides (Fahy et al., 2009). Fatty acyls possess a carboxylic group attached to an aliphatic chain; saturated fatty acids do not contain double bonds, whereas monounsaturated and polyunsaturated fatty acids contain one or more cis double bonds. Glycerolipids are fatty acid esters of glycerol and comprise mono-, di- and tri-acylglycerols. Glycerophospholipids contain phosphoric acid in ester form with a glycerolipid and are subdivided into distinct classes based on the nature of the head group linked to the phosphate. Sphingolipids contain a common sphingoid base backbone and are acylated to form ceramides, which are modified to generate phosphosphingolipids and glycosphingolipids. Sterol lipids, of which cholesterol and its derivatives are the most widely studied in mammalian systems, contain a fused four-ring core and are subdivided based on the number of carbons in the core skeleton. Prenols are synthesized from the five carbon precursors isopentenyl diphosphate and dimethylallyl diphosphate that are produced mainly via the mevalonic acid pathway. Saccharolipids are compounds in which fatty acids are linked directly to a sugar backbone (the sugar substitutes for the glycerol backbone that is present in glycerolipids and

glycerophospholipids). Polyketides are natural compounds containing alternating carbonyl and methylene groups (Fahy et al., 2005; Piomelli et al., 2007). In mammalian cellular membranes, the main lipid categories are glycerophospholipids, sphingolipids and sterols (Fahy et al., 2005).

Considered major components of cellular membranes serving largely structural functions (Lam and Shui, 2013) and viewed as a reservoir for carbon storage (Wenk, 2005), lipids are crucial to all aspects of life. For example, they are key regulators of brain function (Cermenati et al., 2015) and lipid anabolism and catabolism are key molecular integrators of energy homeostasis, membrane structure and dynamics and signaling (Cermenati et al., 2015; Vattulainen and Rog, 2011; Wenk, 2005). Furthermore, the plasma membrane comprises lipid rafts, specialized regions containing high concentrations of the most abundant sterol, cholesterol, and glycosphingolipids, also including ordered assemblies of specific proteins, as well as consequential specific lipid-lipid, protein-lipid, and protein-protein interactions with a crucial role in specific cell signaling events (Simons and Sampaio, 2011).

Over half of the human brain dry weight is represented by lipids, which is in accordance with the role as key players in the physiology and pathophysiology of different diseases (Piomelli et al., 2007). Moreover, glycerophospholipids account for about 20–25% of the dry weight in adult brain (Farooqui et al., 2000). Major lipid classes of the nervous system are cholesterol, phosphatidylcholine, sphingomyelin, ceramide, glucosyl-ceramide, and sulfatide and less abundant lipids are derivatives of cholesterol such as oxysterols and neuroactive steroids, derivatives of long chain fatty acids such as prostaglandins, endocannabinoids, neuroprotectins and resolvins, that are localized in myelin, in the plasma membranes of neurons and glial cells, or intracellularly, where they exhibit signaling and regulatory functions (Cermenati et al., 2015). Particularly, in the nervous system, lipids play functions on synaptogenesis, neurogenesis, insulation, rapid saltatory nerve impulse conduction, among many others (Cermenati et al., 2015). Disturbances in brain lipid content and metabolism have been proposed to be of particular importance in disorders such as Alzheimer's disease (AD) (Di Paolo and Kim, 2011), Parkinson's disease (Ruiperez et al., 2010), multiple sclerosis (Ho et al., 2012) and amyotrophic lateral sclerosis (Schmitt et al., 2014).

Lipids are now an emerging field of research. There is a growing number of drugs that target lipid metabolic and signaling pathways, ranging from inflammation and cancer to metabolic diseases (Wenk, 2005). In addition, different tools are being used for lipid research, such as nuclear

magnetic resonance, chromatographic tools, mass spectrometry based lipidomics (defined as the large-scale characterization and quantification of lipids and modifications in various physiological and pathological conditions) and *in vivo* manipulation of lipid signaling pathways, that are expanding our understanding of the functions of the different lipid species (Checa et al., 2015; Lam and Shui, 2013; Wenk, 2005).

Lipids are not genetically encoded and are generated and metabolized by enzymes (that are influenced by the environment of the biological system, for example, by temperature and diet) (Wenk, 2005). Among these enzymes, phospholipases play a key role in lipid signaling and have been shown to be implicated in disease processes when dysregulated.

1.4. Phospholipids and Phospholipases

Phospholipids are ubiquitous in nature and well-known for their importance as major components of lipid bilayer of cell membranes. They provide neural membranes with stability, fluidity, and permeability. In addition to serving as a primary component of cellular membranes and binding sites for intracellular and intercellular proteins, they are also either precursors of, or are themselves, membrane-derived second messengers (Fahy et al., 2005).

Structurally, all phospholipids present a hydrophilic head composed of a phosphate group linked to either glycerol or sphingosine, and two or one hydrophobic tail of fatty acyl chains, respectively (Fahy et al., 2005). Glycerol-based phospholipids are known as glycerophospholipids and sphingosine-based phospholipids are named phosphosphingolipids.

Regarding glycerophospholipids, they are constituted by four components: fatty acyl chains, a glycerol backbone to which the fatty acyl chains are attached, a phosphate head group, and a radical group that defines the specific classes of phospholipids (see Figure 4 and Table 1). For example a phosphocholine, phosphoserine, or a phosphoinositol ring originate phosphatidylcholine (PC), phosphatidylserine (PS), and phosphatidylinositol (PI), respectively (Fahy et al., 2005). More complex phospholipids, such as cardiolipin, can be synthesized by adding more than two glycerol units (Miranda and Oliveira, 2015). According to the geometry of their polar heads, lipids can assume cylindrical or conical shapes, which determine the form of membranes, inducing planar or curved membrane structures, respectively (Fahy et al., 2005).

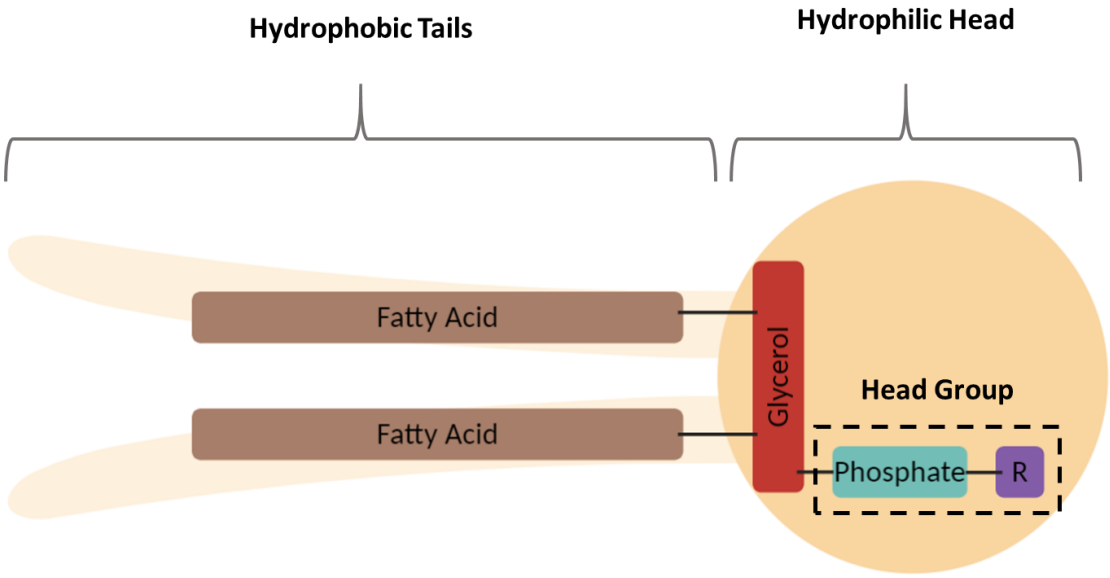

Figure 4. Schematic representation of the main structure of glycerophospholipids. R - radical group.

Table 1. Examples of glycerophospholipids and their correspondent head groups.

Head group	Glycerophospholipid
Hydroxyl	Phosphatidic acid (PA)
Ethanolamine	Phosphatidylethanolamine (PE)
Choline	Phosphatidylcholine (PC)
Serine	Phosphatidylserine (PS)
Glycerol	Phosphatidylglycerol (PG)
Phosphatidylglycerol	Cardiolipin (CL)
Inositol	Phosphatidylinositol (PI)
Inositol-phosphate	Phosphatidylinositol phosphate (PIP)[1]
Inositol-bisphosphate	Phosphatidylinositol bisphosphate (PIP_2)[2]
Inositol-triphosphate	Phosphatidylinositol triphosphate (PIP_3)[3]

[1] PI(3)P, PI(4)P or PI(5)P
[2] $PI(4,5)P_2$
[3] $PI(3,4,5)P_3$

Phospholipases are enzymes that cleave the various bonds in glycerophospholipids, differing in the site of action on the molecules, physiological function, mode of action, and their regulation

(Aloulou et al., 2012). These enzymes act in different sites on the glycerophospholipid structure and are generally grouped into four classes: A, B, C and D (Aloulou et al., 2012). The phospholipases A1 and A2 (PLA1 and PLA2) produce free fatty acids, (including arachidonic and docosahexaenoic acid) and 2-acyl lysophospholipid or 1-acyl lysophospholipid, respectively. The fatty acid linked to the lysophospholipid is cleaved by lysophospholipase activity of phospholipase B (PLB). Phospholipases C (PLC) are defined as phosphodiesterases that cleave the glycerophosphate bond, forming diacylglycerols and a phospho-base. Finally, the base group of the phospholipid is removed by phospholipase D (PLD) (Aloulou et al., 2012; Farooqui and Horrocks, 2005). For example, the cylindrical phospholipid PC can be converted into conical lipids, such as diacylglycerol (DAG) by PLC, or phosphatidic acid (PA) by PLD. It can also be converted into the inverted cone-shaped lysophosphatidylcholine (lysoPC) with the release of a fatty acyl chain by PLA (Miranda and Oliveira, 2015).

Phospholipases convert phospholipids into lipid mediators or second messengers important for membrane trafficking, signal transduction, cell proliferation and apoptosis (Aloulou et al., 2012). Therefore, phospholipases have been identified as therapeutic targets for prevention and treatment of diseases, since their dysregulation contributes to several human diseases.

1.5. Phospholipase D

PLD is a signal-activated enzyme existent in virus, bacteria, plants and lower and higher eukaryotes and catalyzes the hydrolysis of phospholipids with generation of lipid head group and phosphatidic acid. Even though there are PLD enzymes with broader substrate selectivity present in plants and some bacteria, PLD is primarily known for hydrolyzing in mammals, in the presence of water, PC, the most abundant membrane phospholipid, to metabolically active PA, a second messenger signaling lipid, and free choline (see Figure 5) (Jenkins and Frohman, 2005; Oliveira et al., 2010). However, in the presence of primary alcohols, PLD preferentially uses these as a substrate, resulting in the formation of a specific phosphatidylalcohol, such as phosphatidylethanol (PEtOH) in the presence of ethanol. This property has been used to measure PLD activity (Gustavsson, 1995; Oliveira et al., 2010; Scott et al., 2013). PLD superfamily is classified based on the two highly conserved HKD catalytic motifs. HKD denotes for an HxxxxKxD sequence, where H corresponds to histine, K for lysine, D for aspartic acid and x for any amino acid (Frohman et al., 1999; Raghu et al., 2009b).

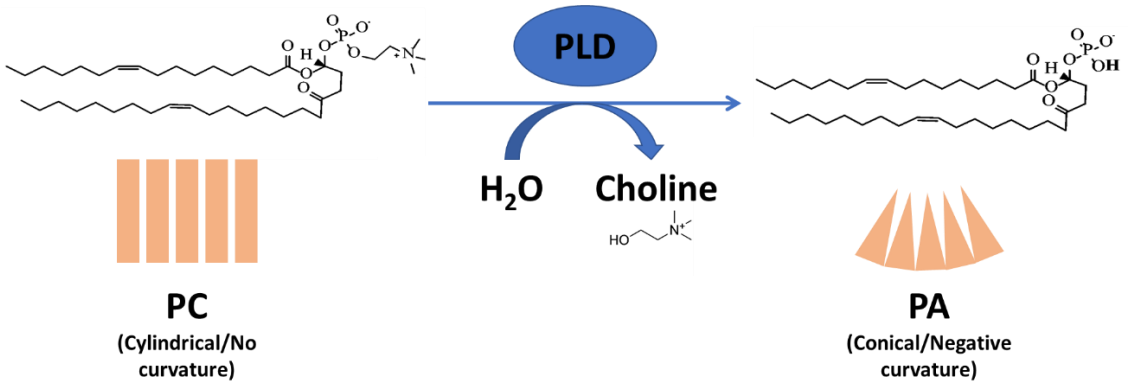

Figure 5. PLD hydrolyses cylindrical PC into conical PA. PA is negatively charged and promotes a negative membrane curvature. Structures above represent ones of many possible.

The first evidence for PLD-like activity was reported by Hanahan and Chaikoff in carrot extracts in 1947 (Hanahan and Chaikoff, 1947), and was afterward described in virus, prokaryotes and eukaryotes (Selvy et al., 2011). The mammalian PLD activity was first described by Saito and Kanfer in 1973 in rat brain extracts (Saito and Kanfer, 1973). Later, the yeast *Spo14* gene was shown to encode a protein with PLD activity (Rose et al., 1995) and the human sequence was eventually isolated (Hammond et al., 1995).

In yeast, PLD (spo14) is essential for meiosis and sporulation by directing vesicular transport to form the membrane surrounding the nucleus of the nascent spore (Rose et al., 1995) and the loss of the protein leads to a sporulation defect (Rudge et al., 2001) and accumulation of undocked membrane vesicles in the spindle pole body (Nakanishi et al., 2006).

In the nematode *Caenorhabditis elegans* (*C. elegans*) there is only one PLD gene (*Pld-1*), which encodes a protein structurally similar to its mammalian ortholog, sharing 6 of its 7 domains. It is abundant in neurons and pharyngeal muscles, whereas expression in epithelial cells, body-wall muscles and the excretory canal is weaker (Park et al., 2018). It is also the main source of PA in this model (Bravo et al., 2018). The ablation of PLD in this model causes no major phenotype, since the progeny, development and survival, as well as the motor behavior, chemotactic responses and learning are not affected (Bravo et al., 2018). Despite these data, PLD downregulation has been shown to shorten longevity and induce age-related biomarkers through reactive oxygen species accumulation (Park et al., 2018). Moreover PLD modulates *C. elegans*

body size, since the ablation of this enzyme leads to increased size and lipid stores of the nematodes (Bravo et al., 2018).

In *Drosophila melanogaster* there is also a single *Pld* gene, which encodes a protein with a domain structure conserved with mammalian PLD protein; this includes an N-terminal phox (PX) and pleckstrin homology (PH) domain as well as two HxKxxxxD (HKD) domains and a phosphoinositide 4,5 bisphosphate ($PI(4,5)P_2$) binding site (see below) (Raghu et al., 2009b). In this model, loss of function of PLD also decreases the levels of PA (Thakur et al., 2016). In order to detect photons, ocular photoreceptors of animals generate an expanded region of the plasma membrane that is packed with the receptor of light rhodopsin. Either the increase or decrease of PLD levels have a functional impact in fly rhabdomeres. It was found that photoreceptors contain a light-dependent PLD activity that balances membrane internalization and recycling to maintain the size and rhodopsin composition of the membrane (Thakur et al., 2016). On the other hand, high levels of PA during development in *Drosophila* photoreceptors disrupts rabdhomere biogenesis with associated endomembrane defects (Raghu et al., 2009a).

Six different isoforms sharing an HKD structure have been identified in mammals to date, but PLD1 and PLD2 (120 KDa and 106 KDa respectively) are the only isoforms with proposed canonical activity, meaning they are the only with the ability to hydrolyze PC to generate PA. PLD1 and PLD2 structure share many domains: two HKD motifs, a PX consensus sequence and a PH domain, which are phosphoinositide-binding modules that are required for proper targeting of PLD and a PIP2-binding site, fundamental for enzymatic activity. The distinction between PLD1 and PLD2 structure remains in the presence of a loop region in PLD1, which has been proposed to function as a negative regulatory element for catalysis, that is absent in PLD2 (Jenkins and Frohman, 2005). Although PLD1 and PLD2 catalyze the same biochemical reactions they differ in their cellular localization and in the mechanisms by which their catalytic activities are regulated. PLD1 locates on perinuclear, Golgi and endosomal vesicles and, upon cell stimulation, translocates to the plasma membrane or late endosomes (Liscovitch et al., 1999; Oliveira and Di Paolo, 2010; Selvy et al., 2011), while PLD2 resides mainly in the plasma membrane under non-stimulated conditions and translocates to recycle vesicles or partly to the cytosol with agonist-stimulated and desensitized receptors (Colley et al., 1997; Hiroyama and Exton, 2005; Oliveira et al., 2010). Baseline activity increases as a consequence of extracellular stimuli such as engagement of G-protein-coupled receptors and receptor tyrosine kinases and downstream

activation of small GTPases, such as Ras homolog family member A (RhoA) and ADP ribosylation factor (ARF) family members, and protein kinase C (PKC). Other regulatory mechanisms including phosphorylation, availability of the lipid cofactor $PI(4,5)P_2$, and other protein activators have been proposed (Bruntz et al., 2014; Jenkins and Frohman, 2005; Salazar and Frohman, 2020).

With the emergence genetic PLD mouse models, namely *Pld1* knock-out (KO) (Elvers et al., 2010) and *Pld2* KO (Oliveira et al., 2010) mice, it was possible to study the mammalian phenotypes upon PLD ablation. Studies in *Pld1* and/or *Pld2* KO mice result in homozygous viable adults, although it has been reported by some authors that *Pld1* KO and *Pld2* KO animals present increased body weight and body fat content, accompanied by an increased food intake (Trujillo Viera et al., 2016). Other reported observations mentioned PLD1 and/or PLD2 deficient mice to have reduced brain growth at 14-27 days after birth, but that is eventually caught up with WT mice at day 33 (Burkhardt et al., 2014). Moreover, *Pld2* KO mice have an increased number of ectopic cerebellar Purkinje cells and olfactory defects after 13 weeks of age (Vermeren et al., 2016). Regarding mice behavior, conflicting results have been reported upon PLD1 or PLD2 ablation. Oliveira et al. reported that *Pld2* KO mice have no memory or learning deficits when compared to control mice (Oliveira et al., 2010). However, Burkhardt et al. showed a deficit at the level of discrimination in long-term novel object recognition test in *Pld2* and double *Pld* KO and a social recognition deficit in *Pld1* and/or *Pld2* KO (Burkhardt et al., 2014).

The hallmarks of AD are the extracellular amyloid beta (Aβ) deposition (generated from amyloid precursor protein (APP) by sequential cleavages mediated by the β-secretase β-site APP cleavage enzyme 1, BACE1, and the γ-secretase complex) as senile plaques and the intracellular accumulation of hyperphosphorylated tau as neurofibrillary tangles (Di Paolo and Kim, 2011). Several studies have addressed the link between PLD1/PLD2 and AD, either in Aβ signaling (Bravo et al., 2018; Oliveira et al., 2010) and amyloid precursor protein APP processing and trafficking (Cai et al., 2006a; Cai et al., 2006b). Kanfer et al. found an increase in PLD activity in AD brain extracts (Kanfer et al., 1996). PLD1 has been implicated in APP processing and trafficking. For instance PLD1 has been shown to regulate the intracellular trafficking of presenilin 1(PS1)/γ-secretase (Liu et al., 2009). Moreover, it has been suggested that reducing the APP trafficking back to the trans-Golgi network results in an increase of amyloidogenesis and several studies implicate PLD1 as well as its product PA in the budding of secretory vesicles from the

trans-Golgi network (Chen et al., 1997; Ktistakis et al., 1995; Riebeling et al., 2009). In fact, Cai et al. showed that PS1 physically interacts with PLD1, recruiting it to the Golgi complex/trans-Golgi network (Cai et al., 2006a). Also, overexpression of PLD1 decreases the levels of Aβ whereas silencing PLD1 produces the opposite effect (Cai et al., 2006a). In a companion publication, PLD1 overexpression was shown to promote the formation of APP-containing secretory vesicles from trans-Golgi network and inhibition of PLD1 activity decreases APP trafficking (Cai et al., 2006b). PLD1 is able to correct the impaired APP trafficking and neurite outgrowth in familiar AD-linked PS1 mutant neurons (Cai et al., 2006b). Aberrant elevated synaptosomal PLD1 was observed in AD hippocampi compared to age-matched controls and this elevated PLD1 plays a key detrimental role in facilitating both Aβ and tau oligomer-driven synaptic dysfunction and underlying memory deficits (Krishnan et al., 2018) and, also, the use of a PLD1 inhibitor (VU0 155069) is sufficient to prevent the progression of synaptic dysfunction during early stages in the 3xTg-AD mouse model (Bourne et al., 2019). Oliveira and colleagues showed that Aβ oligomers induce total PLD activity in primary cortical neurons, which is abolished in mouse cultured neurons lacking PLD2, and that genetic ablation of PLD2 leads to attenuation of AD pathogenesis by increasing resistance to Aβ oligomer insult and memory deficit protection in the SwAPP mouse model (Oliveira et al., 2010).

In addition to these findings relating PLD to AD, it is also known that synucleins interact with and inhibit PLD (Ahn et al., 2002; Jenco et al., 1998; Payton et al., 2004). Moreover, ablation of these enzymes promotes other phenotypes regarding autophagy (Dall'Armi et al., 2010), tumor biology (Chen et al., 2012; Wang et al., 2017), neurobiology (Ammar et al., 2015; Oliveira et al., 2010; Vermeren et al., 2016) and platelet function (Elvers et al., 2010; Thielmann et al., 2012).

Canonical enzymatic activity has not been described for non-classical PLDs, such as PLD3, PLD4, PLD5 and PLD6. These members lack the two functional domains PX and PH which are found in the N-terminal regions of PLD1 and PLD2 and instead contain a putative transmembrane (TM) domain (Yoshikawa et al., 2010). PLD3 (*Hu-K4* in humans, *SAM-9* in murines) and PLD4 are 5' exonucleases glycosylated type II transmembrane proteins (Fazzari et al., 2017; Gavin et al., 2018; Gonzalez et al., 2018; Otani et al., 2011). PLD3 is a located in endoplasmatic reticulum and endolysosomes (Frohman, 2015; Gavin et al., 2018; Munck et al., 2005; Osisami et al., 2012). In 2014, a genome wide-association study identified a rare variant of PLD3 (Val232Met) that doubled the risk for late-onset AD. In addition, two other PLD3 variants,

Ala442Ala and Met6Arg, were reported to be nominally associated with AD risk. This study showed that PLD3 is highly expressed in the hippocampus and cortex, brain regions vulnerable to AD pathology, and that AD brains have lower levels of PLD3 in their neurons (Cruchaga et al., 2014). Moreover, Cruchaga et al. observed that overexpression of PLD3 leads to a significant decrease in intracellular APP and extracellular Aβ42 and Aβ40 and PLD3 knockdown had an opposite effect (Cruchaga et al., 2014). These data led to propose PLD3 loss-of-function as an AD risk factor by affecting APP processing but, although there are studies in agreement with some of these data (van der Lee et al., 2015), several reports have questioned some of the findings regarding molecular association between PLD3 and AD (Hooli et al., 2015; Lambert et al., 2015). In addition, Fazzari et al. observed no alterations in full-length APP, C-terminal APP fragments and the ratio between full-length and C-terminal fragments expression under genetic deletion of *Pld3*. In addition, they found that PLD3 was localized in late and endosomes and lysosomes (visualized with the lysosomal-associated membrane protein 1 (LAMP1) marker) and lysosomes from PLD3-deficient CA1 neurons displayed an increase in density, size and in total area occupied with lipid droplets inclusions (Fazzari et al., 2017). Later, another study showed that PLD3 is a lysosomal protein that becomes proteolytically cleaved in acidic compartments and inhibitors of intracellular trafficking or lysosomal acidification abolished this processing (Gonzalez et al., 2018). Gonzalez et al. also proposed that the biosynthetic route of PLD3 depends on the endosomal sorting complex required for transport (ESCRT) machinery to reach lysosomes in mammalian cells (Gonzalez et al., 2018). In 2019 two other rare variants of *Pld3* were described in late-onset AD, which could lead to reduced PLD3 activity and affect Aβ levels in cellular model of AD, via autophagy-dependent mammalian target of rapamycin (mTOR) pathway (Tan et al., 2019). Since disruption of endolysomal membrane trafficking flux has been shown to lead to neurodegeneration and impairment in APP trafficking and processing (Miranda et al., 2018), the role of PLD3 in lysosome functioning is a strong biological hypothesis for the reported human genetic association in AD (Cruchaga et al., 2014).

PLD4 is localized in organelle membranes, including the endoplasmatic reticulum and Golgi complex (Yoshikawa et al., 2010) and also in phagosomes (Otani et al., 2011). Its biological function has not been fully elucidated, but some studies associate PLD4 to autoimmune diseases. *Pld4* risk allele was associated with anti-double stranded DNA antibodies production, implying PLD4 contribution to systemic lupus erythematosus by hyperactivating B-cells (Akizuki et al., 2019). *Pld4* mutant mice have low body weight and also autoimmune phenotypes

corresponding to systemic lupus erythematosus, including nephritis (Akizuki et al., 2019). Moreover, it has been demonstrated that PLD4 promotes kidney fibrogenesis by modulating innate and adaptative immune responses (Trivedi et al., 2017). Other studies linked PLD4 polymorphisms to systemic sclerosis (Terao et al., 2013) and rheumatoid arthritis (Okada et al., 2012). Lastly, Gavin et al. presented evidence that the endolysosomal proteins PLD3 and PLD4 are 5′ exonucleases that break down toll-like receptor (TLR) 9 ligands, thus degrading them and limiting their ability to stimulate TLR9. Hence, macrophages from PLD3-deficient mice have exaggerated TLR9 responses (Gavin et al., 2018) and PLD4-deficient mice display a TLR9-driven inflammatory syndrome and splenomegaly (Chen et al., 2017; Gavin et al., 2018).

PLD5 is encoded by an autosomal gene (Yao et al., 2020) and has nonconservative substitutions in its putative catalytic site, making it unlikely to be enzymatically active and definitive cellular or physiological roles have not yet been recognized (Nelson and Frohman, 2015). One study correlates a single-nucleotide polymorphism in the *Pld5* gene with verbal performance in autism patients, but the clinical importance of this finding is not clear (Anney et al., 2010).

PLD6 (also known as mitoPLD) encodes only one HKD motif and dimerizes to exhibit catalytic activity (Nelson and Frohman, 2015). It is anchored by an N-terminal transmembrane tail into the outer surface of mitochondria (Choi et al., 2006) and hydrolyzes cardiolipin on the outer surface of the mitochondria to generate PA (Choi et al., 2006). It also acts as an endonuclease of RNA to generate specialized microRNAs known as P-element-induced wimpy testis (piwi)-interacting RNAs (Voigt et al., 2012), that control gene modification and stability (Moyano and Stefani, 2015), which are critical during spermatogenesis (Huang et al., 2011; Kabayama et al., 2017).

PLD is still a rapidly rising field of research with recent major technical advances. For instance, it was recently developed a method named IMPACT (Imaging Phospholipase D Activity with Clickable Alcohols via Transphosphatidylation), which is a chemical method for imaging phosphatidyl-alcohols synthesized by PLD enzymes in live cells, relying in azidoalcohols as reporters in a transphosphatidylation reaction (Bumpus and Baskin, 2016; Bumpus et al., 2018) and also an optogenetic PLD which allows the visualization of cellular PLD activity (Tei and Baskin, 2020). Moreover, crystal structures of PLD are emerging, either in plants (Li et al., 2020) and humans (Metrick et al., 2020), providing explanations for structural insights and promoting structure-based drug discoveries.

1.6. Phosphatidic Acid Signaling

PA has important physiological and signaling roles, since it contributes to membrane biogenesis and is also a signaling molecule. It is composed of a three-carbon glycerol backbone, two fatty acid chains and a small phosphate headgroup, thus referred to as a "cone shape" lipid (i.e., a lipid with a small head groups relative to a large hydrophobic domain) (Cazzolli et al., 2006; Jenkins and Frohman, 2005). PA is negatively charged, promoting a negative membrane curvature and making it possible to alter the properties of the membranes (Jenkins and Frohman, 2005). PA is involved in important cellular processes such as membrane biogenesis and trafficking events and different PA species exhibit different structural properties, which is related to the acyl chain length and unsaturation of the fatty acyl chain at sn-1 and sn-2 positions, leading to distinct repercussion on membrane structure, for example membrane curvature (van Meer, 2005). In fact, PA saturation level influences its functions in neurosecretory pathway (Tanguy et al., 2020). While mono-unsaturated PA regulates the number of exocytotic events, poly-unsaturated PA regulates fusion pore stability and expansion (Tanguy et al., 2020).

PA is a critical element in signaling pathways as a second messenger and it can also be further metabolized to other signaling lipids such as DAG by PA phosphatases, lysophosphatidic acid (LPA) by phospholipase A and other lipids such as PI (Oliveira and Di Paolo, 2010; Sonoda et al., 2002). On the other hand, PLD is not the only source of PA, since it can also be obtained from DAG by a reaction catalyzed by DAG kinase, from LPA as a result of LPA acyltransferases (LPAAT) activity, from cardiolipin catalyzed by mitoPLD and other enzymes in the biosynthetic pathway (see Figure 6) (Choi et al., 2006; Haucke and Di Paolo, 2007).

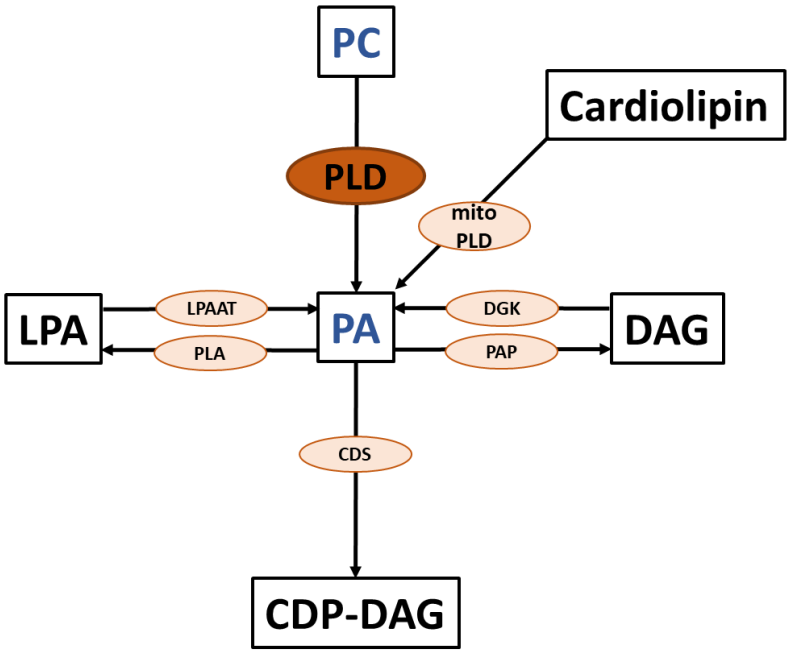

Figure 6. PA metabolism. PA can be generated from other sources and further metabolized. PA, phosphatidic acid; PLD, Phospholipase D; PC, phosphatidylcholine; LPA, lysoPA; DAG, diacylglycerol; CDP-DAG, cytidine diphosphate-DAG; PLA, phospholipase A; LPAAT, LPA acyltransferase; PAP, PA phosphatase; DGK, DAG kinase; CDS, CDP-DAG synthase; mitoPLD, mito-phospholipase D.

PA plays an important role in membrane trafficking, for example, in phagocytosis (Corrotte et al., 2006; Tanguy et al., 2019), autophagy (Holland et al., 2016), synaptic transmission (Humeau et al., 2001; Raben and Barber, 2017), among others, since it may recruit specific proteins and/or facilitate fusion because of higher curvature of PA-enriched membranes (Tanguy et al., 2020). PA is crucial for many activation pathways of intracellular signaling transduction events, such as PI phosphate kinases, activation of mTOR, and direct binding with Rapidly Accelerated Fibrosarcoma (Raf) kinase, soluble N-ethylmaleimide sensitive factor attachment protein receptor (SNARE) proteins and sphingosine kinases (Cazzolli et al., 2006; Jenkins and Frohman, 2005; Stace and Ktistakis, 2006). In fact, specific PLD-derived PA modulates subcellular processes such as vesicular transport (Cai et al., 2006b; Choi et al., 2002; Huang et al., 2005; Raghu et al., 2009a; Vitale et al., 2001), NADPH oxidase activity (Zhang et al., 2009), mTOR and S6K activity (Fang et al., 2003).

1.7. Aims of the thesis

Recently, a mass spectrometry study revealed that the DH presents increased PA and decreased PC compared to the VH, potentially implicating the PLD pathway in DH-VH axis regulation (Miranda et al., 2019). Since the cell biology and pathophysiology involving PLD1 and PLD2 remain a topic of investigation, our main goal was to study the impact of PLD genetic modulation on the DH-VH axis organization and function.

In chapter 2, we address how PLD1 ablation differentially affects hippocampal organization and functioning in a region-specific manner.

In chapter 3, we address the effects of PLD2 ablation in social behavior and hippocampal synaptic potentiation.

References

Ahn, B.H., Rhim, H., Kim, S.Y., Sung, Y.M., Lee, M.Y., Choi, J.Y., Wolozin, B., Chang, J.S., Lee, Y.H., Kwon, T.K., *et al.* (2002). alpha-Synuclein interacts with phospholipase D isozymes and inhibits pervanadate-induced phospholipase D activation in human embryonic kidney-293 cells. The Journal of biological chemistry *277*, 12334-12342.

Akizuki, S., Ishigaki, K., Kochi, Y., Law, S.M., Matsuo, K., Ohmura, K., Suzuki, A., Nakayama, M., Iizuka, Y., Koseki, H., *et al.* (2019). PLD4 is a genetic determinant to systemic lupus erythematosus and involved in murine autoimmune phenotypes. Annals of the rheumatic diseases *78*, 509-518.

Aloulou, A., Ali, Y.B., Bezzine, S., Gargouri, Y., and Gelb, M.H. (2012). Phospholipases: an overview. Methods in molecular biology (Clifton, NJ) *861*, 63-85.

Altman, J., and Das, G.D. (1965). Autoradiographic and histological evidence of postnatal hippocampal neurogenesis in rats. The Journal of comparative neurology *124*, 319-335.

Ammar, M.R., Thahouly, T., Hanauer, A., Stegner, D., Nieswandt, B., and Vitale, N. (2015). PLD1 participates in BDNF-induced signalling in cortical neurons. Scientific reports *5*, 14778.

Anacker, C., and Hen, R. (2017). Adult hippocampal neurogenesis and cognitive flexibility - linking memory and mood. Nature reviews Neuroscience *18*, 335-346.

Anney, R., Klei, L., Pinto, D., Regan, R., Conroy, J., Magalhaes, T.R., Correia, C., Abrahams, B.S., Sykes, N., Pagnamenta, A.T., *et al.* (2010). A genome-wide scan for common alleles affecting risk for autism. Human molecular genetics *19*, 4072-4082.

Bannerman, D.M., Sprengel, R., Sanderson, D.J., McHugh, S.B., Rawlins, J.N., Monyer, H., and Seeburg, P.H. (2014). Hippocampal synaptic plasticity, spatial memory and anxiety. Nature reviews Neuroscience *15*, 181-192.

Bear, M.F. (1996). A synaptic basis for memory storage in the cerebral cortex. Proceedings of the National Academy of Sciences of the United States of America *93*, 13453-13459.

Bienkowski, M.S., Bowman, I., Song, M.Y., Gou, L., Ard, T., Cotter, K., Zhu, M., Benavidez, N.L., Yamashita, S., Abu-Jaber, J., *et al.* (2018). Integration of gene expression and brain-wide connectivity reveals the multiscale organization of mouse hippocampal networks. Nature neuroscience *21*, 1628-1643.

Bourne, K.Z., Natarajan, C., Perez, C.X.M., Tumurbaatar, B., Taglialatela, G., and Krishnan, B. (2019). Suppressing aberrant phospholipase D1 signaling in 3xTg Alzheimer's disease mouse model promotes synaptic resilience. Scientific reports *9*, 18342.

Bravo, F.V., Da Silva, J., Chan, R.B., Di Paolo, G., Teixeira-Castro, A., and Oliveira, T.G. (2018). Phospholipase D functional ablation has a protective effect in an Alzheimer's disease Caenorhabditis elegans model. Scientific reports *8*, 3540.

Bruntz, R.C., Lindsley, C.W., and Brown, H.A. (2014). Phospholipase D signaling pathways and phosphatidic acid as therapeutic targets in cancer. Pharmacological reviews *66*, 1033-1079.

Bumpus, T.W., and Baskin, J.M. (2016). A Chemoenzymatic Strategy for Imaging Cellular Phosphatidic Acid Synthesis. Angewandte Chemie (International ed in English) *55*, 13155-13158.

Bumpus, T.W., Liang, F.J., and Baskin, J.M. (2018). Ex Uno Plura: Differential Labeling of Phospholipid Biosynthetic Pathways with a Single Bioorthogonal Alcohol. Biochemistry *57*, 226-230.

Burkhardt, U., Stegner, D., Hattingen, E., Beyer, S., Nieswandt, B., and Klein, J. (2014). Impaired brain development and reduced cognitive function in phospholipase D-deficient mice. Neuroscience letters *572*, 48-52.

Cai, D., Netzer, W.J., Zhong, M., Lin, Y., Du, G., Frohman, M., Foster, D.A., Sisodia, S.S., Xu, H., Gorelick, F.S.*, et al.* (2006a). Presenilin-1 uses phospholipase D1 as a negative regulator of beta-amyloid formation. Proceedings of the National Academy of Sciences of the United States of America *103*, 1941-1946.

Cai, D., Zhong, M., Wang, R., Netzer, W.J., Shields, D., Zheng, H., Sisodia, S.S., Foster, D.A., Gorelick, F.S., Xu, H.*, et al.* (2006b). Phospholipase D1 corrects impaired betaAPP trafficking and neurite outgrowth in familial Alzheimer's disease-linked presenilin-1 mutant neurons. Proceedings of the National Academy of Sciences of the United States of America *103*, 1936-1940.

Cazzolli, R., Shemon, A.N., Fang, M.Q., and Hughes, W.E. (2006). Phospholipid signalling through phospholipase D and phosphatidic acid. IUBMB life *58*, 457-461.

Cermenati, G., Mitro, N., Audano, M., Melcangi, R.C., Crestani, M., De Fabiani, E., and Caruso, D. (2015). Lipids in the nervous system: from biochemistry and molecular biology to patho-physiology. Biochim Biophys Acta *1851*, 51-60.

Checa, A., Bedia, C., and Jaumot, J. (2015). Lipidomic data analysis: tutorial, practical guidelines and applications. Analytica chimica acta *885*, 1-16.

Chen, Q., Hongu, T., Sato, T., Zhang, Y., Ali, W., Cavallo, J.A., van der Velden, A., Tian, H., Di Paolo, G., Nieswandt, B.*, et al.* (2012). Key roles for the lipid signaling enzyme phospholipase d1 in the tumor microenvironment during tumor angiogenesis and metastasis. Science signaling *5*, ra79.

Chen, W.C., Wang, W.C., Okada, Y., Chang, W.P., Chou, Y.H., Chang, H.H., Huang, J.D., Chen, D.Y., and Chang, W.C. (2017). rs2841277 (PLD4) is associated with susceptibility and rs4672495 is associated with disease activity in rheumatoid arthritis. Oncotarget *8*, 64180-64190.

Chen, Y.G., Siddhanta, A., Austin, C.D., Hammond, S.M., Sung, T.C., Frohman, M.A., Morris, A.J., and Shields, D. (1997). Phospholipase D stimulates release of nascent secretory vesicles from the trans-Golgi network. The Journal of cell biology *138*, 495-504.

Chevaleyre, V., and Siegelbaum, S.A. (2010). Strong CA2 pyramidal neuron synapses define a powerful disynaptic cortico-hippocampal loop. Neuron *66*, 560-572.

Chiang, M.C., Huang, A.J.Y., Wintzer, M.E., Ohshima, T., and McHugh, T.J. (2018). A role for CA3 in social recognition memory. Behavioural brain research *354*, 22-30.

Choi, S.Y., Huang, P., Jenkins, G.M., Chan, D.C., Schiller, J., and Frohman, M.A. (2006). A common lipid links Mfn-mediated mitochondrial fusion and SNARE-regulated exocytosis. Nature cell biology *8*, 1255-1262.

Choi, W.S., Kim, Y.M., Combs, C., Frohman, M.A., and Beaven, M.A. (2002). Phospholipases D1 and D2 regulate different phases of exocytosis in mast cells. Journal of immunology (Baltimore, Md : 1950) *168*, 5682-5689.

Citri, A., and Malenka, R.C. (2008). Synaptic plasticity: multiple forms, functions, and mechanisms. Neuropsychopharmacology : official publication of the American College of Neuropsychopharmacology *33*, 18-41.

Colley, W.C., Sung, T.C., Roll, R., Jenco, J., Hammond, S.M., Altshuller, Y., Bar-Sagi, D., Morris, A.J., and Frohman, M.A. (1997). Phospholipase D2, a distinct phospholipase D isoform with novel regulatory properties that provokes cytoskeletal reorganization. Current biology : CB *7*, 191-201.

Corkin, S. (2002). What's new with the amnesic patient H.M.? Nature reviews Neuroscience *3*, 153-160.

Corrotte, M., Chasserot-Golaz, S., Huang, P., Du, G., Ktistakis, N.T., Frohman, M.A., Vitale, N., Bader, M.F., and Grant, N.J. (2006). Dynamics and function of phospholipase D and phosphatidic acid during phagocytosis. Traffic (Copenhagen, Denmark) *7*, 365-377.

Cruchaga, C., Karch, C.M., Jin, S.C., Benitez, B.A., Cai, Y., Guerreiro, R., Harari, O., Norton, J., Budde, J., Bertelsen, S.*, et al.* (2014). Rare coding variants in the phospholipase D3 gene confer risk for Alzheimer's disease. Nature *505*, 550-554.

Dall'Armi, C., Hurtado-Lorenzo, A., Tian, H., Morel, E., Nezu, A., Chan, R.B., Yu, W.H., Robinson, K.S., Yeku, O., Small, S.A.*, et al.* (2010). The phospholipase D1 pathway modulates macroautophagy. Nature communications *1*, 142-142.

Di Paolo, G., and Kim, T.W. (2011). Linking lipids to Alzheimer's disease: cholesterol and beyond. Nature reviews Neuroscience *12*, 284-296.

Elvers, M., Stegner, D., Hagedorn, I., Kleinschnitz, C., Braun, A., Kuijpers, M.E., Boesl, M., Chen, Q., Heemskerk, J.W., Stoll, G.*, et al.* (2010). Impaired alpha(IIb)beta(3) integrin activation and shear-dependent thrombus formation in mice lacking phospholipase D1. Science signaling *3*, ra1.

Fahy, E., Subramaniam, S., Brown, H.A., Glass, C.K., Merrill, A.H., Jr., Murphy, R.C., Raetz, C.R., Russell, D.W., Seyama, Y., Shaw, W.*, et al.* (2005). A comprehensive classification system for lipids. J Lipid Res *46*, 839-861.

Fahy, E., Subramaniam, S., Murphy, R.C., Nishijima, M., Raetz, C.R., Shimizu, T., Spener, F., van Meer, G., Wakelam, M.J., and Dennis, E.A. (2009). Update of the LIPID MAPS comprehensive classification system for lipids. J Lipid Res *50 Suppl*, S9-14.

Fang, Y., Park, I.H., Wu, A.L., Du, G., Huang, P., Frohman, M.A., Walker, S.J., Brown, H.A., and Chen, J. (2003). PLD1 regulates mTOR signaling and mediates Cdc42 activation of S6K1. Current biology : CB *13*, 2037-2044.

Fanselow, M.S., and Dong, H.W. (2010). Are the dorsal and ventral hippocampus functionally distinct structures? Neuron *65*, 7-19.

Farooqui, A.A., and Horrocks, L.A. (2005). Signaling and interplay mediated by phospholipases A2, C, and D in LA-N-1 cell nuclei. Reproduction, nutrition, development *45*, 613-631.

Farooqui, A.A., Horrocks, L.A., and Farooqui, T. (2000). Glycerophospholipids in brain: their metabolism, incorporation into membranes, functions, and involvement in neurological disorders. Chemistry and physics of lipids *106*, 1-29.

Fazzari, P., Horre, K., Arranz, A.M., Frigerio, C.S., Saito, T., Saido, T.C., and De Strooper, B. (2017). PLD3 gene and processing of APP. Nature *541*, E1-e2.

Frohman, M.A. (2015). The phospholipase D superfamily as therapeutic targets. Trends Pharmacol Sci *36*, 137-144.

Frohman, M.A., Sung, T.C., and Morris, A.J. (1999). Mammalian phospholipase D structure and regulation. Biochim Biophys Acta *1439*, 175-186.

Gavin, A.L., Huang, D., Huber, C., Martensson, A., Tardif, V., Skog, P.D., Blane, T.R., Thinnes, T.C., Osborn, K., Chong, H.S.*, et al.* (2018). PLD3 and PLD4 are single-stranded acid exonucleases that regulate endosomal nucleic-acid sensing. Nature immunology *19*, 942-953.

Gonzalez, A.C., Schweizer, M., Jagdmann, S., Bernreuther, C., Reinheckel, T., Saftig, P., and Damme, M. (2018). Unconventional Trafficking of Mammalian Phospholipase D3 to Lysosomes. Cell reports *22*, 1040-1053.

Goshen, I., Brodsky, M., Prakash, R., Wallace, J., Gradinaru, V., Ramakrishnan, C., and Deisseroth, K. (2011). Dynamics of retrieval strategies for remote memories. Cell *147*, 678-689.

Gustavsson, L. (1995). ESBRA 1994 Award Lecture. Phosphatidylethanol formation: specific effects of ethanol mediated via phospholipase D. Alcohol and alcoholism (Oxford, Oxfordshire) *30*, 391-406.

Hafting, T., Fyhn, M., Molden, S., Moser, M.B., and Moser, E.I. (2005). Microstructure of a spatial map in the entorhinal cortex. Nature *436*, 801-806.

Hammond, S.M., Altshuller, Y.M., Sung, T.C., Rudge, S.A., Rose, K., Engebrecht, J., Morris, A.J., and Frohman, M.A. (1995). Human ADP-ribosylation factor-activated phosphatidylcholine-specific phospholipase D defines a new and highly conserved gene family. The Journal of biological chemistry *270*, 29640-29643.

Hanahan, D.J., and Chaikoff, I.L. (1947). The phosphorus-containing lipides of the carrot. The Journal of biological chemistry *168*, 233-240.

Haucke, V., and Di Paolo, G. (2007). Lipids and lipid modifications in the regulation of membrane traffic. Curr Opin Cell Biol *19*, 426-435.

Hiroyama, M., and Exton, J.H. (2005). Localization and regulation of phospholipase D2 by ARF6. Journal of cellular biochemistry *95*, 149-164.

Ho, P.P., Kanter, J.L., Johnson, A.M., Srinagesh, H.K., Chang, E.J., Purdy, T.M., van Haren, K., Wikoff, W.R., Kind, T., Khademi, M.*, et al.* (2012). Identification of naturally occurring fatty acids of the myelin sheath that resolve neuroinflammation. Science translational medicine *4*, 137ra173.

Hochgerner, H., Zeisel, A., Lonnerberg, P., and Linnarsson, S. (2018). Conserved properties of dentate gyrus neurogenesis across postnatal development revealed by single-cell RNA sequencing. Nature neuroscience *21*, 290-299.

Holland, P., Knævelsrud, H., Søreng, K., Mathai, B.J., Lystad, A.H., Pankiv, S., Bjørndal, G.T., Schultz, S.W., Lobert, V.H., Chan, R.B.*, et al.* (2016). HS1BP3 negatively regulates autophagy by modulation of phosphatidic acid levels. Nature communications *7*, 13889.

Holthuis, J.C., and Menon, A.K. (2014). Lipid landscapes and pipelines in membrane homeostasis. Nature *510*, 48-57.

Honda, Y., Sasaki, H., Umitsu, Y., and Ishizuka, N. (2012). Zonal distribution of perforant path cells in layer III of the entorhinal area projecting to CA1 and subiculum in the rat. Neuroscience research *74*, 200-209.

Hooli, B.V., Lill, C.M., Mullin, K., Qiao, D., Lange, C., Bertram, L., and Tanzi, R.E. (2015). PLD3 gene variants and Alzheimer's disease. Nature *520*, E7-8.

Huang, H., Gao, Q., Peng, X., Choi, S.Y., Sarma, K., Ren, H., Morris, A.J., and Frohman, M.A. (2011). piRNA-associated germline nuage formation and spermatogenesis require MitoPLD profusogenic mitochondrial-surface lipid signaling. Developmental cell *20*, 376-387.

Huang, P., Altshuller, Y.M., Hou, J.C., Pessin, J.E., and Frohman, M.A. (2005). Insulin-stimulated plasma membrane fusion of Glut4 glucose transporter-containing vesicles is regulated by phospholipase D1. Molecular biology of the cell *16*, 2614-2623.

Humeau, Y., Vitale, N., Chasserot-Golaz, S., Dupont, J.L., Du, G., Frohman, M.A., Bader, M.F., and Poulain, B. (2001). A role for phospholipase D1 in neurotransmitter release. Proceedings of the National Academy of Sciences of the United States of America *98*, 15300-15305.

Jenco, J.M., Rawlingson, A., Daniels, B., and Morris, A.J. (1998). Regulation of phospholipase D2: selective inhibition of mammalian phospholipase D isoenzymes by alpha- and beta-synucleins. Biochemistry *37*, 4901-4909.

Jenkins, G.M., and Frohman, M.A. (2005). Phospholipase D: a lipid centric review. Cellular and molecular life sciences : CMLS *62*, 2305-2316.

Kabayama, Y., Toh, H., Katanaya, A., Sakurai, T., Chuma, S., Kuramochi-Miyagawa, S., Saga, Y., Nakano, T., and Sasaki, H. (2017). Roles of MIWI, MILI and PLD6 in small RNA regulation in mouse growing oocytes. Nucleic acids research *45*, 5387-5398.

Kandel, E.R., Schwartz, J.H., Jessell, T.M., Biochemistry, D.o., Jessell, M.B.T., Siegelbaum, S., and Hudspeth, A. (2000). Principles of neural science, Vol 4 (McGraw-hill New York).

Kanfer, J.N., Singh, I.N., Pettegrew, J.W., McCartney, D.G., and Sorrentino, G. (1996). Phospholipid metabolism in Alzheimer's disease and in a human cholinergic cell. Journal of lipid mediators and cell signalling *14*, 361-363.

Kauderer, B.S., and Kandel, E.R. (2000). Capture of a protein synthesis-dependent component of long-term depression. Proceedings of the National Academy of Sciences of the United States of America *97*, 13342-13347.

Kemp, A., and Manahan-Vaughan, D. (2004). Hippocampal long-term depression and long-term potentiation encode different aspects of novelty acquisition. Proceedings of the National Academy of Sciences of the United States of America *101*, 8192-8197.

Kheirbek, M.A., Drew, L.J., Burghardt, N.S., Costantini, D.O., Tannenholz, L., Ahmari, S.E., Zeng, H., Fenton, A.A., and Hen, R. (2013). Differential control of learning and anxiety along the dorsoventral axis of the dentate gyrus. Neuron *77*, 955-968.

Kohara, K., Pignatelli, M., Rivest, A.J., Jung, H.Y., Kitamura, T., Suh, J., Frank, D., Kajikawa, K., Mise, N., Obata, Y.*, et al.* (2014). Cell type-specific genetic and optogenetic tools reveal hippocampal CA2 circuits. Nature neuroscience *17*, 269-279.

Krishnan, B., Kayed, R., and Taglialatela, G. (2018). Elevated phospholipase D isoform 1 in Alzheimer's disease patients' hippocampus: Relevance to synaptic dysfunction and memory deficits. Alzheimer's & dementia (New York, N Y) *4*, 89-102.

Ktistakis, N.T., Brown, H.A., Sternweis, P.C., and Roth, M.G. (1995). Phospholipase D is present on Golgi-enriched membranes and its activation by ADP ribosylation factor is sensitive to brefeldin A. Proceedings of the National Academy of Sciences of the United States of America *92*, 4952-4956.

Lam, S.M., and Shui, G. (2013). Lipidomics as a principal tool for advancing biomedical research. Journal of genetics and genomics = Yi chuan xue bao *40*, 375-390.

Lambert, J.C., Grenier-Boley, B., Bellenguez, C., Pasquier, F., Campion, D., Dartigues, J.F., Berr, C., Tzourio, C., and Amouyel, P. (2015). PLD3 and sporadic Alzheimer's disease risk. Nature *520*, E1.

Li, J., Yu, F., Guo, H., Xiong, R., Zhang, W., He, F., Zhang, M., and Zhang, P. (2020). Crystal structure of plant PLDalpha1 reveals catalytic and regulatory mechanisms of eukaryotic phospholipase D. Cell research *30*, 61-69.

Liscovitch, M., Czarny, M., Fiucci, G., Lavie, Y., and Tang, X. (1999). Localization and possible functions of phospholipase D isozymes. Biochim Biophys Acta *1439*, 245-263.

Liu, Y., Zhang, Y.W., Wang, X., Zhang, H., You, X., Liao, F.F., and Xu, H. (2009). Intracellular trafficking of presenilin 1 is regulated by beta-amyloid precursor protein and phospholipase D1. The Journal of biological chemistry *284*, 12145-12152.

Maggio, N., and Segal, M. (2007). Striking variations in corticosteroid modulation of long-term potentiation along the septotemporal axis of the hippocampus. The Journal of neuroscience : the official journal of the Society for Neuroscience *27*, 5757-5765.

Maruki, K., Izaki, Y., Nomura, M., and Yamauchi, T. (2001). Differences in paired-pulse facilitation and long-term potentiation between dorsal and ventral CA1 regions in anesthetized rats. Hippocampus *11*, 655-661.

McHugh, S.B., Fillenz, M., Lowry, J.P., Rawlins, J.N., and Bannerman, D.M. (2011). Brain tissue oxygen amperometry in behaving rats demonstrates functional dissociation of dorsal and ventral hippocampus during spatial processing and anxiety. The European journal of neuroscience *33*, 322-337.

Meira, T., Leroy, F., Buss, E.W., Oliva, A., Park, J., and Siegelbaum, S.A. (2018). A hippocampal circuit linking dorsal CA2 to ventral CA1 critical for social memory dynamics. Nature communications *9*, 4163.

Metrick, C.M., Peterson, E.A., Santoro, J.C., Enyedy, I.J., Murugan, P., Chen, T., Michelsen, K., Cullivan, M., Spilker, K.A., Kumar, P.R.*, et al.* (2020). Human PLD structures enable drug design and characterization of isoenzyme selectivity. Nature chemical biology *16*, 391-399.

Miranda, A.M., Bravo, F.V., Chan, R.B., Sousa, N., Di Paolo, G., and Oliveira, T.G. (2019). Differential lipid composition and regulation along the hippocampal longitudinal axis. Transl Psychiatry *9*, 144.

Miranda, A.M., Lasiecka, Z.M., Xu, Y., Neufeld, J., Shahriar, S., Simoes, S., Chan, R.B., Oliveira, T.G., Small, S.A., and Di Paolo, G. (2018). Neuronal lysosomal dysfunction releases exosomes harboring APP C-terminal fragments and unique lipid signatures. Nature communications *9*, 291.

Miranda, A.M., and Oliveira, T.G. (2015). Lipids under stress–a lipidomic approach for the study of mood disorders. BioEssays : news and reviews in molecular, cellular and developmental biology *37*, 1226-1235.

Morris, R.G., Garrud, P., Rawlins, J.N., and O'Keefe, J. (1982). Place navigation impaired in rats with hippocampal lesions. Nature *297*, 681-683.

Moser, E.I., Kropff, E., and Moser, M.B. (2008). Place cells, grid cells, and the brain's spatial representation system. Annual review of neuroscience *31*, 69-89.

Moyano, M., and Stefani, G. (2015). piRNA involvement in genome stability and human cancer. Journal of hematology & oncology *8*, 38.

Munck, A., Bohm, C., Seibel, N.M., Hashemol Hosseini, Z., and Hampe, W. (2005). Hu-K4 is a ubiquitously expressed type 2 transmembrane protein associated with the endoplasmic reticulum. The FEBS journal *272*, 1718-1726.

Nakanishi, H., Morishita, M., Schwartz, C.L., Coluccio, A., Engebrecht, J., and Neiman, A.M. (2006). Phospholipase D and the SNARE Sso1p are necessary for vesicle fusion during sporulation in yeast. Journal of cell science *119*, 1406-1415.

Nakashiba, T., Cushman, J.D., Pelkey, K.A., Renaudineau, S., Buhl, D.L., McHugh, T.J., Rodriguez Barrera, V., Chittajallu, R., Iwamoto, K.S., McBain, C.J.*, et al.* (2012). Young dentate granule cells mediate pattern separation, whereas old granule cells facilitate pattern completion. Cell *149*, 188-201.

Nakashiba, T., Young, J.Z., McHugh, T.J., Buhl, D.L., and Tonegawa, S. (2008). Transgenic inhibition of synaptic transmission reveals role of CA3 output in hippocampal learning. Science (New York, NY) *319*, 1260-1264.

Nelson, R.K., and Frohman, M.A. (2015). Physiological and pathophysiological roles for phospholipase D. J Lipid Res *56*, 2229-2237.

O'Keefe, J., and Dostrovsky, J. (1971). The hippocampus as a spatial map. Preliminary evidence from unit activity in the freely-moving rat. Brain research *34*, 171-175.

O'Keefe, J., and Speakman, A. (1987). Single unit activity in the rat hippocampus during a spatial memory task. Experimental brain research *68*, 1-27.

Okada, Y., Terao, C., Ikari, K., Kochi, Y., Ohmura, K., Suzuki, A., Kawaguchi, T., Stahl, E.A., Kurreeman, F.A., Nishida, N.*, et al.* (2012). Meta-analysis identifies nine new loci associated with rheumatoid arthritis in the Japanese population. Nature genetics *44*, 511-516.

Okuyama, T., Kitamura, T., Roy, D.S., Itohara, S., and Tonegawa, S. (2016). Ventral CA1 neurons store social memory. Science (New York, NY) *353*, 1536-1541.

Oliveira, T.G., Chan, R.B., Tian, H., Laredo, M., Shui, G., Staniszewski, A., Zhang, H., Wang, L., Kim, T.W., Duff, K.E.*, et al.* (2010). Phospholipase d2 ablation ameliorates Alzheimer's disease-linked synaptic dysfunction and cognitive deficits. The Journal of neuroscience : the official journal of the Society for Neuroscience *30*, 16419-16428.

Oliveira, T.G., and Di Paolo, G. (2010). Phospholipase D in brain function and Alzheimer's disease. Biochim Biophys Acta *1801*, 799-805.

Osisami, M., Ali, W., and Frohman, M.A. (2012). A role for phospholipase D3 in myotube formation. PloS one *7*, e33341.

Otani, Y., Yamaguchi, Y., Sato, Y., Furuichi, T., Ikenaka, K., Kitani, H., and Baba, H. (2011). PLD$ is involved in phagocytosis of microglia: expression and localization changes of PLD4 are correlated with activation state of microglia. PloS one *6*, e27544.

Park, J.H., Park, J.W., Lee, J.H., Kim, D.Y., Hahm, J.H., and Bae, Y.S. (2018). Role of phospholipase D in the lifespan of Caenorhabditis elegans. Experimental & molecular medicine *50*, 8.

Payton, J.E., Perrin, R.J., Woods, W.S., and George, J.M. (2004). Structural determinants of PLD2 inhibition by alpha-synuclein. Journal of molecular biology *337*, 1001-1009.

Pinto, V., Costa, J.C., Morgado, P., Mota, C., Miranda, A., Bravo, F.V., Oliveira, T.G., Cerqueira, J.J., and Sousa, N. (2015). Differential impact of chronic stress along the hippocampal dorsal-ventral axis. Brain structure & function *220*, 1205-1212.

Piomelli, D., Astarita, G., and Rapaka, R. (2007). A neuroscientist's guide to lipidomics. Nature reviews Neuroscience *8*, 743-754.

Raben, D.M., and Barber, C.N. (2017). Phosphatidic acid and neurotransmission. Adv Biol Regul *63*, 15-21.

Raghu, P., Coessens, E., Manifava, M., Georgiev, P., Pettitt, T., Wood, E., Garcia-Murillas, I., Okkenhaug, H., Trivedi, D., Zhang, Q.*, et al.* (2009a). Rhabdomere biogenesis in Drosophila photoreceptors is acutely sensitive to phosphatidic acid levels. The Journal of cell biology *185*, 129-145.

Raghu, P., Manifava, M., Coadwell, J., and Ktistakis, N.T. (2009b). Emerging findings from studies of phospholipase D in model organisms (and a short update on phosphatidic acid effectors). Biochim Biophys Acta *1791*, 889-897.

Riebeling, C., Morris, A.J., and Shields, D. (2009). Phospholipase D in the Golgi apparatus. Biochim Biophys Acta *1791*, 876-880.

Rose, K., Rudge, S.A., Frohman, M.A., Morris, A.J., and Engebrecht, J. (1995). Phospholipase D signaling is essential for meiosis. Proceedings of the National Academy of Sciences of the United States of America *92*, 12151-12155.

Roy, D.S., Kitamura, T., Okuyama, T., Ogawa, S.K., Sun, C., Obata, Y., Yoshiki, A., and Tonegawa, S. (2017). Distinct Neural Circuits for the Formation and Retrieval of Episodic Memories. Cell *170*, 1000-1012.e1019.

Rudge, S.A., Pettitt, T.R., Zhou, C., Wakelam, M.J., and Engebrecht, J.A. (2001). SPO14 separation-of-function mutations define unique roles for phospholipase D in secretion and cellular differentiation in Saccharomyces cerevisiae. Genetics *158*, 1431-1444.

Ruiperez, V., Darios, F., and Davletov, B. (2010). Alpha-synuclein, lipids and Parkinson's disease. Progress in lipid research *49*, 420-428.

Saito, M., and Kanfer, J. (1973). Solubilization and properties of a membrane-bound enzyme from rat brain catalyzing a base-exchange reaction. Biochemical and biophysical research communications *53*, 391-398.

Salazar, C., and Frohman, M.A. (2020). Prospects for PLD Inhibition in Cancer and Thrombotic Disease. Handbook of experimental pharmacology *259*, 79-88.

Schmitt, F., Hussain, G., Dupuis, L., Loeffler, J.P., and Henriques, A. (2014). A plural role for lipids in motor neuron diseases: energy, signaling and structure. Front Cell Neurosci *8*, 25.

Scott, S.A., Xiang, Y., Mathews, T.P., Cho, H.P., Myers, D.S., Armstrong, M.D., Tallman, K.A., O'Reilly, M.C., Lindsley, C.W., and Brown, H.A. (2013). Regulation of phospholipase D activity

and phosphatidic acid production after purinergic (P2Y6) receptor stimulation. The Journal of biological chemistry *288*, 20477-20487.

Scoville, W.B., and Milner, B. (1957). Loss of recent memory after bilateral hippocampal lesions. Journal of neurology, neurosurgery, and psychiatry *20*, 11-21.

Segal, M., Richter-Levin, G., and Maggio, N. (2010). Stress-induced dynamic routing of hippocampal connectivity: a hypothesis. Hippocampus *20*, 1332-1338.

Selvy, P.E., Lavieri, R.R., Lindsley, C.W., and Brown, H.A. (2011). Phospholipase D: enzymology, functionality, and chemical modulation. Chemical reviews *111*, 6064-6119.

Shah, S., Lubeck, E., Zhou, W., and Cai, L. (2017). seqFISH Accurately Detects Transcripts in Single Cells and Reveals Robust Spatial Organization in the Hippocampus. Neuron *94*, 752-758.e751.

Simons, K., and Sampaio, J.L. (2011). Membrane organization and lipid rafts. Cold Spring Harbor perspectives in biology *3*, a004697.

Sonoda, H., Aoki, J., Hiramatsu, T., Ishida, M., Bandoh, K., Nagai, Y., Taguchi, R., Inoue, K., and Arai, H. (2002). A novel phosphatidic acid-selective phospholipase A1 that produces lysophosphatidic acid. The Journal of biological chemistry *277*, 34254-34263.

Stace, C.L., and Ktistakis, N.T. (2006). Phosphatidic acid- and phosphatidylserine-binding proteins. Biochim Biophys Acta *1761*, 913-926.

Stackman, R.W., Jr., Cohen, S.J., Lora, J.C., and Rios, L.M. (2016). Temporary inactivation reveals that the CA1 region of the mouse dorsal hippocampus plays an equivalent role in the retrieval of long-term object memory and spatial memory. Neurobiology of learning and memory *133*, 118-128.

Strange, B.A., Witter, M.P., Lein, E.S., and Moser, E.I. (2014). Functional organization of the hippocampal longitudinal axis. Nature reviews Neuroscience *15*, 655-669.

Suh, J., Rivest, A.J., Nakashiba, T., Tominaga, T., and Tonegawa, S. (2011). Entorhinal cortex layer III input to the hippocampus is crucial for temporal association memory. Science (New York, NY) *334*, 1415-1420.

Tamamaki, N., and Nojyo, Y. (1993). Projection of the entorhinal layer II neurons in the rat as revealed by intracellular pressure-injection of neurobiotin. Hippocampus *3*, 471-480.

Tan, M., Li, J., Ma, F., Zhang, X., Zhao, Q., and Cao, X. (2019). PLD3 Rare Variants Identified in Late-Onset Alzheimer's Disease Affect Amyloid-beta Levels in Cellular Model. Frontiers in neuroscience *13*, 116.

Tanguy, E., Costé de Bagneaux, P., Kassas, N., Ammar, M.R., Wang, Q., Haeberlé, A.M., Raherindratsara, J., Fouillen, L., Renard, P.Y., Montero-Hadjadje, M.*, et al.* (2020). Mono- and Poly-unsaturated Phosphatidic Acid Regulate Distinct Steps of Regulated Exocytosis in Neuroendocrine Cells. Cell reports *32*, 108026.

Tanguy, E., Tran Nguyen, A.P., Kassas, N., Bader, M.F., Grant, N.J., and Vitale, N. (2019). Regulation of Phospholipase D by Arf6 during FcγR-Mediated Phagocytosis. Journal of immunology (Baltimore, Md : 1950) *202*, 2971-2981.

Tei, R., and Baskin, J.M. (2020). Spatiotemporal control of phosphatidic acid signaling with optogenetic, engineered phospholipase Ds. The Journal of cell biology *219*.

Terao, C., Ohmura, K., Kawaguchi, Y., Nishimoto, T., Kawasaki, A., Takehara, K., Furukawa, H., Kochi, Y., Ota, Y., Ikari, K.*, et al.* (2013). PLD4 as a novel susceptibility gene for systemic sclerosis in a Japanese population. Arthritis and rheumatism *65*, 472-480.

Thakur, R., Panda, A., Coessens, E., Raj, N., Yadav, S., Balakrishnan, S., Zhang, Q., Georgiev, P., Basak, B., Pasricha, R.*, et al.* (2016). Phospholipase D activity couples plasma membrane endocytosis with retromer dependent recycling. eLife *5*.

Thielmann, I., Stegner, D., Kraft, P., Hagedorn, I., Krohne, G., Kleinschnitz, C., Stoll, G., and Nieswandt, B. (2012). Redundant functions of phospholipases D1 and D2 in platelet alpha-granule release. Journal of thrombosis and haemostasis : JTH *10*, 2361-2372.

Thompson, C.L., Pathak, S.D., Jeromin, A., Ng, L.L., MacPherson, C.R., Mortrud, M.T., Cusick, A., Riley, Z.L., Sunkin, S.M., Bernard, A.*, et al.* (2008). Genomic anatomy of the hippocampus. Neuron *60*, 1010-1021.

Trivedi, P., Kumar, R.K., Iyer, A., Boswell, S., Gerarduzzi, C., Dadhania, V.P., Herbert, Z., Joshi, N., Luyendyk, J.P., Humphreys, B.D.*, et al.* (2017). Targeting Phospholipase D4 Attenuates Kidney Fibrosis. Journal of the American Society of Nephrology : JASN *28*, 3579-3589.

Trujillo Viera, J., El-Merahbi, R., Nieswandt, B., Stegner, D., and Sumara, G. (2016). Phospholipases D1 and D2 Suppress Appetite and Protect against Overweight. PloS one *11*, e0157607.

Tsien, J.Z., Huerta, P.T., and Tonegawa, S. (1996). The essential role of hippocampal CA1 NMDA receptor-dependent synaptic plasticity in spatial memory. Cell *87*, 1327-1338.

van der Lee, S.J., Holstege, H., Wong, T.H., Jakobsdottir, J., Bis, J.C., Chouraki, V., van Rooij, J.G., Grove, M.L., Smith, A.V., Amin, N.*, et al.* (2015). PLD3 variants in population studies. Nature *520*, E2-3.

van Meer, G. (2005). Cellular lipidomics. The EMBO journal *24*, 3159-3165.

van Strien, N.M., Cappaert, N.L., and Witter, M.P. (2009). The anatomy of memory: an interactive overview of the parahippocampal-hippocampal network. Nature reviews Neuroscience *10*, 272-282.

Vattulainen, I., and Rog, T. (2011). Lipid simulations: a perspective on lipids in action. Cold Spring Harbor perspectives in biology *3*.

Vermeren, M.M., Zhang, Q., Smethurst, E., Segonds-Pichon, A., Schrewe, H., and Wakelam, M.J. (2016). The Phospholipase D2 Knock Out Mouse Has Ectopic Purkinje Cells and Suffers from Early Adult-Onset Anosmia. PloS one *11*, e0162814.

Vitale, N., Caumont, A.S., Chasserot-Golaz, S., Du, G., Wu, S., Sciorra, V.A., Morris, A.J., Frohman, M.A., and Bader, M.F. (2001). Phospholipase D1: a key factor for the exocytotic machinery in neuroendocrine cells. The EMBO journal *20*, 2424-2434.

Voigt, F., Reuter, M., Kasaruho, A., Schulz, E.C., Pillai, R.S., and Barabas, O. (2012). Crystal structure of the primary piRNA biogenesis factor Zucchini reveals similarity to the bacterial PLD endonuclease Nuc. RNA (New York, NY) *18*, 2128-2134.

Wang, Z., Zhang, F., He, J., Wu, P., Tay, L.W.R., Cai, M., Nian, W., Weng, Y., Qin, L., Chang, J.T.*, et al.* (2017). Binding of PLD2-Generated Phosphatidic Acid to KIF5B Promotes MT1-MMP Surface Trafficking and Lung Metastasis of Mouse Breast Cancer Cells. Developmental cell *43*, 186-197.e187.

Wenk, M.R. (2005). The emerging field of lipidomics. Nature reviews Drug discovery *4*, 594-610.

Yao, Y., Wang, X., Li, H., Fan, J., Qian, X., Li, H., and Xu, Y. (2020). Phospholipase D as a key modulator of cancer progression. Biological reviews of the Cambridge Philosophical Society.

Yoshikawa, F., Banno, Y., Otani, Y., Yamaguchi, Y., Nagakura-Takagi, Y., Morita, N., Sato, Y., Saruta, C., Nishibe, H., Sadakata, T.*, et al.* (2010). Phospholipase D family member 4, a transmembrane glycoprotein with no phospholipase D activity, expression in spleen and early postnatal microglia. PloS one *5*, e13932.

Zhang, Y., Zhu, H., Zhang, Q., Li, M., Yan, M., Wang, R., Wang, L., Welti, R., Zhang, W., and Wang, X. (2009). Phospholipase dalpha1 and phosphatidic acid regulate NADPH oxidase activity and production of reactive oxygen species in ABA-mediated stomatal closure in Arabidopsis. The Plant cell *21*, 2357-2377.

Zucker, R.S., and Regehr, W.G. (2002). Short-term synaptic plasticity. Annual review of physiology *64*, 355-405.

CHAPTER 2

Phospholipase D1 Ablation Disrupts Mouse Longitudinal Hippocampal Axis Organization and Functioning

Article

Cell Reports

Phospholipase D1 Ablation Disrupts Mouse Longitudinal Hippocampal Axis Organization and Functioning

Graphical Abstract

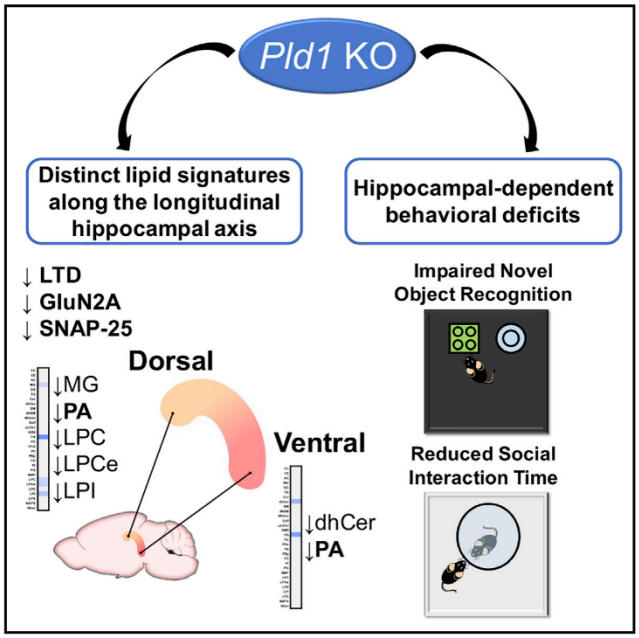

Authors

Luísa Santa-Marinha, Isabel Castanho, Rita Ribeiro Silva, ..., Gilbert Di Paolo, Vítor Pinto, Tiago Gil Oliveira

Correspondence

tiago@med.uminho.pt

In Brief

Santa-Marinha et al. show that PLD1 and PLD2 contribute differentially to the mouse hippocampal lipidomic profile. Their data highlight PLD1-derived PA reduction as a major modulator of dorsal-ventral hippocampal organization and functioning.

Highlights

- PLD1 is a major phosphatidic acid source compared to PLD2
- PLD1 KO mice show deficits in object recognition and social exploration
- PLD1 ablation disrupts DH-VH dendritic arborization differentiation
- PLD1 ablation reduces LTD induction and GluN2A and SNAP-25 levels in the DH

Santa-Marinha et al., 2020, Cell Reports *30*, 4197–4208
March 24, 2020
https://doi.org/10.1016/j.celrep.2020.02.102

CellPress

Cell Reports
Article

Phospholipase D1 Ablation Disrupts Mouse Longitudinal Hippocampal Axis Organization and Functioning

Luísa Santa-Marinha,[1,2,6] Isabel Castanho,[1,2,6,7] Rita Ribeiro Silva,[1,2] Francisca Vaz Bravo,[1,2] André Miguel Miranda,[1,2] Torcato Meira,[1,2] Rafaela Morais-Ribeiro,[1,2] Fernanda Marques,[1,2] Yimeng Xu,[3] Kimberly Point du Jour,[3,4,8] Markus Wenk,[5] Robin Barry Chan,[3,4] Gilbert Di Paolo,[3,4,9] Vítor Pinto,[1,2] and Tiago Gil Oliveira[1,2,10,*]

[1]Life and Health Sciences Research Institute (ICVS), School of Medicine, University of Minho, Campus Gualtar, 4710-057 Braga, Portugal
[2]ICVS/3B's - PT Government Associate Laboratory, Braga/Guimarães, Portugal
[3]Department of Pathology and Cell Biology, Columbia University Medical Center, New York, NY 10032, USA
[4]Taub Institute for Research on Alzheimer's Disease and the Aging Brain, Columbia University Medical Center, New York, NY 10032, USA
[5]Department of Biochemistry, Yong Loo Lin School of Medicine, National University of Singapore, Singapore 117596, Singapore
[6]These authors contributed equally
[7]Present address: Institute of Biomedical and Clinical Sciences, University of Exeter Medical School, University of Exeter, Exeter EX2 5DW, UK
[8]Present address: Emory University School of Medicine, Atlanta, GA 30308, USA
[9]Present address: Denali Therapeutics, South San Francisco, CA 94080, USA
[10]Lead Contact
*Correspondence: tiago@med.uminho.pt
https://doi.org/10.1016/j.celrep.2020.02.102

SUMMARY

Phosphatidic acid (PA) is a signaling lipid involved in the modulation of synaptic structure and functioning. Based on previous work showing a decreasing PA gradient along the longitudinal axis of the rodent hippocampus, we asked whether the dorsal hippocampus (DH) and the ventral hippocampus (VH) are differentially affected by PA modulation. Here, we show that phospholipase D1 (PLD1) is a major hippocampal PA source, compared to PLD2, and that PLD1 ablation affects predominantly the lipidome of the DH. Moreover, *Pld1* knockout (KO) mice show specific deficits in novel object recognition and social interaction and disruption in the DH-VH dendritic arborization differentiation in CA1/CA3 pyramidal neurons. Also, *Pld1* KO animals present reduced long-term depression (LTD) induction and reduced GluN2A and SNAP-25 protein levels in the DH. Overall, we observe that PLD1-derived PA reduction leads to differential lipid signatures along the longitudinal hippocampal axis, predominantly affecting DH organization and functioning.

INTRODUCTION

The hippocampus is a brain temporal lobe structure that is fundamental for learning and memory. Despite maintaining its cross-sectional architecture along its longitudinal axis, anatomical, gene expression, and functional studies overall suggest an organized gradient that segregates in the rodent dorsal hippocampus (DH) and ventral hippocampus (VH) poles, which correspond in primates to posterior and anterior poles (Strange et al., 2014). While a classical dichotomic view mainly implicated the DH in spatial navigation and episodic memory and the VH in affective and stress-related behaviors (Bannerman et al., 2014; Fanselow and Dong, 2010; Kheirbek et al., 2013; McHugh et al., 2011; Strange et al., 2014), addressing the differential functional roles of DH and VH should take into account a gradual biochemical and functional transition between the hippocampal poles (Bienkowski et al., 2018; Maggio and Segal, 2007; Miranda et al., 2019; Pinto et al., 2015; Shah et al., 2017; Thompson et al., 2008).

The development of tools such as mass spectrometry (MS) and the genetic modulation of lipid pathways has expanded the knowledge of the role of lipids in brain physiology and pathology (Chan et al., 2012; Miranda et al., 2019; Oliveira et al., 2016). Recently, the DH and VH were shown to differ in their sphingolipid and glycerophospholipid compositions. In particular, the DH presented increased phosphatidic acid (PA) and decreased phosphatidylcholine (PC) compared to the VH, potentially implicating the phospholipase D (PLD) pathway in DH-VH axis regulation (Miranda et al., 2019). Moreover, PA levels were differently modulated by corticosterone, a known mediator of stress, suggesting differential recruitment of PA-modulating enzymes in pathological conditions (Miranda et al., 2019).

PLD encompasses a family of lipid-modifying enzymes primarily known for catabolizing PC to PA. Six PLD members (PLD1–PLD6) have been described in mammals, but only 2 isoenzymes with proposed canonical PLD activity have been reported, PLD1 and PLD2 (Frohman, 2015; Oliveira et al., 2010). PLD preferentially uses primary alcohols as a substrate, resulting in the formation of a specific phosphatidylalcohol, such as phosphatidylethanol (PEtOH) in the presence of ethanol, and this property has been used to measure PLD activity (Gustavsson, 1995; Oliveira et al., 2010; Scott et al., 2013). Despite PLD1

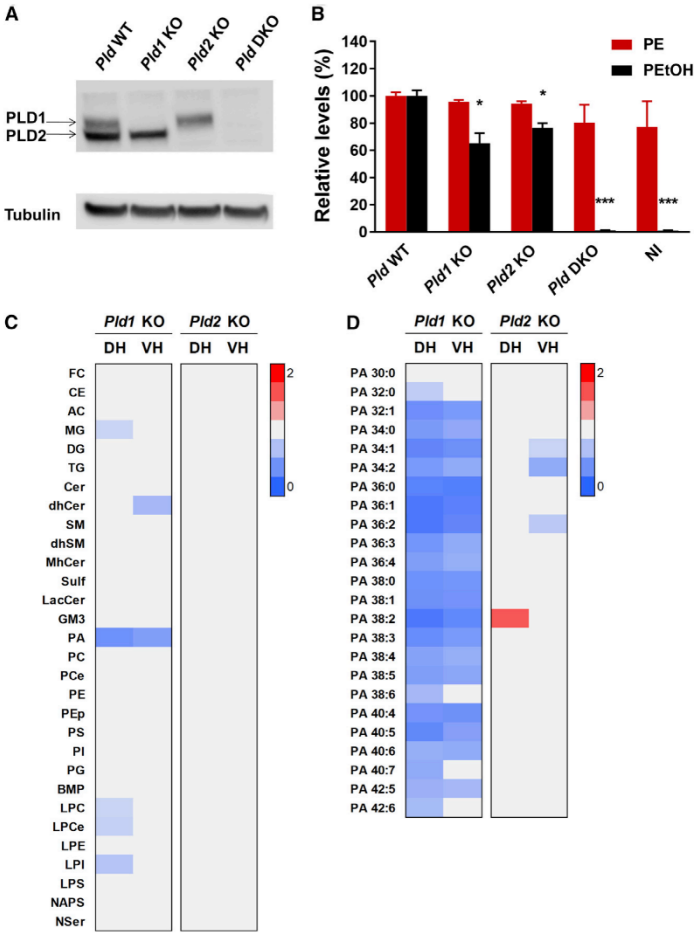

Figure 1. PLD1 Is a Major Contributor to Total Hippocampal PA Levels in Mice, and PLD1 Ablation Has a Major Impact on DH Lipidomics

(A) Forebrains from PLD-ablated mice were processed for western blot analysis. Specific PLD ablation leads to null levels of the corresponding protein.

(B) PLD enzymatic activity assessment. Mice were injected with ethanol, their forebrains were extracted, and the levels of PEtOH were measured by LC-MS analysis and used as an indicator of *in vivo* PLD activity. Individual lipid species were compared with corresponding WT mice (*Pld1* KO: unpaired t test $t(10) = 3.0216$, $p = 0.0129$; *Pld2* KO: unpaired t test $t(10) = 2.4982$, $p = 0.0315$; *Pld* DKO: unpaired t test $t(10) = 23.9625$, $p < 0.0001$; non-injected (NI): unpaired t test $t(9) = 11.9538$, $p < 0.0001$). PE was used as a control lipid. Values denote means ± SEMs ($n_{Pld\ WT} = 6$, $n_{Pld1\ KO} = 6$, $n_{Pld2\ KO} = 6$, $n_{Pld\ DKO} = 6$, $n_{Pld\ WT\ NI} = 5$).

(C) LC-MS analysis of DH and VH from *Pld1* KO and *Pld2* KO animals. In DH, PLD1 ablation decreases the total levels of PA (unpaired t test $t(10) = 7.3291$, $p < 0.0001$), MG (unpaired t test $t(10) = 2.3606$, $p = 0.0399$), LPC (unpaired t test $t(10) = 2.6934$, $p = 0.0226$), LPCe (unpaired t test $t(10) = 3.1084$, $p = 0.0111$), and LPI (unpaired t test $t(10) = 3.8857$, $p = 0.0030$). In VH, PLD1 ablation decreases the levels of PA (unpaired t test $t(10) = 5.4942$, $p = 0.0003$) and dhCer (unpaired t test $t(10) = 3.0964$, $p = 0.0113$).

(D) Impact of PLD1 or PLD2 ablation in specific PA species, analyzed by LC-MS.

Values are represented in gradient color: blue indicates <1 and red indicates above 1-fold change, respectively, normalized to WT mice ($n_{Pld1\ WT} = 5$, $n_{Pld1\ KO} = 7$, $n_{Pld2\ WT} = 8$, $n_{Pld2\ KO} = 8$) (C and D). DKO, *Pld* double-KO; PA, phosphatidic acid; PE, phosphatidylethanolamine; PEtOH, phosphatidylethanol. For other lipid nomenclature see Method Details. $^*p < 0.05$, $^{***}p < 0.001$. See also Figures S1, S2, and S3 and Tables S1 and S2.

and PLD2 having similar enzymatic roles and structure, they differ in their intracellular localization and modulation (Frohman, 2015; Oliveira et al., 2010). Both PLD1 and PLD2 are expressed throughout brain development and postnatal life (Peng and Rhodes, 2000; Zhao et al., 1998), and conflicting results have been reported upon PLD1 or PLD2 ablation in mice behavior, showing either cognitive dysfunction (Burkhardt et al., 2014) or either minor or no major behavioral deficits (Oliveira et al., 2010; Vermeren et al., 2016). The PLD pathway has been implicated in Alzheimer's disease (AD) pathogenesis as being involved in amyloid beta (Aβ) signaling (Bravo et al., 2018; Oliveira et al., 2010) and amyloid precursor protein (APP) processing and trafficking (Cai et al., 2006a, 2006b).

Here, we show that PLD1 is a major source of PA in both rodent DH and VH compared to PLD2, which led us to further test the impact of PLD1 genetic ablation in the mouse hippocampus. We targeted dorsal-ventral hippocampal lipidomic gradient signatures and showed that PLD1 ablation differentially affects hippocampal organization and functioning in a region-specific manner, which has implications for disorders that affect learning and memory.

RESULTS

PLD1 and PLD2 Are the Only Contributors to Total PLD Activity in the Mouse Brain

To confirm the impact on the protein levels of each isoenzyme ablation and validate the genetic ablation of mice, western blot analysis was performed (Figure 1A) using an antibody that recognizes the COOH terminus of both PLD1 and PLD2 isoenzymes. Accordingly, in forebrain extracts, *Pld1* knockout (KO) animals express only PLD2, *Pld2* KO animals express only PLD1 enzyme, and *Pld* double-KO (DKO) animals have no PLD1 or PLD2 expression (Figure 1A). To study the impact of genetic ablation

on enzyme activity, an *in vivo* PLD activity assay was performed, relying on the ability to use primary alcohols—ethanol in this case—as nucleophiles over water in a transphosphatidylation reaction to generate PEtOH. Mice were injected with ethanol; after 1 h, lipid extraction was performed from forebrain tissue and PEtOH was measured by liquid chromatography-mass spectrometry (LC-MS) (Figure 1B). Both *Pld1* and *Pld2* KO mice showed a decrease in total PEtOH levels. Although the decrease in PLD activity was higher in *Pld1* KO animals, no significant differences were observed between *Pld1* and *Pld2* KO animals (Figure 1B). No significant changes were observed in control phospholipid phosphatidylethanolamine (PE) in *Pld1*, *Pld2*, or *Pld* DKO animals (Figure 1B). Also, *Pld* DKO showed almost no detectable PEtOH, which indicates that PEtOH is exclusively produced by PLD1 and PLD2 in the mouse forebrain. In agreement, non-injected animals presented virtually undetectable PEtOH levels (Figure 1B). At the lipid species level, of the 42 PEtOH species evaluated, 15 were significantly reduced in *Pld1* KO and 7 in *Pld2* KO (Figure S1). There were 4 PEtOH minor species, 32:2/16:1, 40:4/20:4, and 40:3/20:3, which were lower in the non-injected group, and 36:1/16:1, which was lower in the DKO. Although these species were significantly lower compared to *Pld* wild type (WT), they did not differ when we compared DKO and the non-injected group (Figure S1). The effect of ablating both PLD isoenzymes in *Pld* DKO on PEtOH levels was of greater magnitude (≈100% decrease) than adding the effects of PLD1 (≈35% decrease) and PLD2 (≈24% decrease) ablation (Figure 1B). Another intriguing observation was that *Pld2* KO forebrain presented increased levels of 4 PEtOH species, 38:4/20:4, 38:2/20:2, 38:2/20:1, and 38:1/20:1 (Figure S1), which was unexpected, considering that these are potential PLD enzymatic products, and indicates that PLD1 is overcompensating in the absence of PLD2. To explore the possibility of an expression compensatory process by either PLD1 or PLD2 upon each isoenzyme ablation, *Pld1*/PLD1 and *Pld2*/PLD2 mRNA and protein levels were measured (Figures S2 and S3). We observed that ablating either of the PLD isoenzymes does not lead to expression upregulation (Figures S2 and S3). These results show that both PLD1 and PLD2 contribute significantly to total PLD activity and that there are no other detectable canonical PLD activity sources in the mouse forebrain.

PLD1 Is a Major PA Source, and Its Ablation Has a Major Impact in the DH Lipidome

Next, we conducted a broad-scale, unbiased lipidomic profiling of DH and VH from both *Pld1* and *Pld2* WT and KO mice. We analyzed the relative abundance of a total of 30 lipid classes, covering the 3 main lipid categories of sterols, sphingolipids, and glycerophospholipids (Figure 1C; Table S1). We found that PLD2 ablation did not have a significant impact on the total levels of the lipid classes analyzed. However, PLD1 ablation led to a dramatic decrease in the total levels of PA in both DH and VH (Figure 1C; Table S1). PLD1 protein levels were higher in the DH when compared to the VH (Figure S3B). Of note, PLD1 ablation significantly decreased the levels of several lipid classes, with a higher impact on the DH compared to VH. The levels of monoacylglycerol (MG), lysophosphatidylcholine (LPC), ether lysophosphatidylcholine (LPCe), and lysophosphatidylinositol (LPI) were reduced in the DH, while levels of dihydroceramide (dhCer) were decreased in the VH (Figure 1C; Table S1). When analyzing the relative abundance of PA species, we found that PLD1 KO animals have decreased levels of nearly all PA species detected in both DH and VH (Figure 1D; Table S2), while PLD2 ablation leads to the decrease in only PA 34:1, 34:2, and 36:2 in the VH and an increase in PA 38:2 in DH (Figure 1D; Table S2). PA 34:1, the PA species with the most relative abundance (Table S2), decreased upon the ablation of either PLD1 or PLD2, and the second and third most abundant species, PA 36:1 and 38:4 (Table S2), only decreased in *Pld1* KO. These results indicate that PLD1 is a major contributor to total PA levels and that PLD1 ablation mainly affects the lipidome of the DH compared to the VH, which is in agreement with the higher PLD1 protein levels in the DH (Figure S3B).

PLD1 Ablation Impairs Object Recognition and Social Exploration in a Hippocampus-Dependent Social Discrimination Task

Knowing that PLD1 was a major contributor to PA total levels compared to PLD2, and since PLD1 ablation was associated with a greater impact in the dorsal-ventral hippocampal lipidome, we explored the impact of PLD1 ablation in hippocampal-associated behaviors. With the open field (OF) (Figure 2A) and elevated plus maze (EPM) (Figure 2B) tests, we observed that *Pld1* KO animals did not demonstrate significant locomotor or anxiety-like impairments. In fear memory evaluation, *Pld1* KO animals did not differ from WT in the average freezing percentage time in contextual or cued memory (Figure 2C, left panel). Also, the extinction of freezing percentage time upon cue exposure was unaltered both in the 5 subsequent days (Figure 2C, right panel) and 30 days later (Figure S4A). To further explore the impact on cognitive functions, the Morris water maze (MWM) was performed to assess spatial learning and reference memory, and *Pld1* KO animals showed preserved spatial learning (Figure 2D, left panel) and memory (Figure 2D, right panel). Moreover, *Pld1* KO animals showed no deficits in reaching a visually cued platform (Figure S4B). We then tested short-term memory, evaluated with the novel object recognition (NOR) test, and *Pld1* KO showed a reduction in the discrimination between familiar and novel objects, mainly at the expense of higher levels of exploration time of the familiar object (Figures 2E and S4C). To understand whether this impairment translated into other animal exploration deficits, the social discrimination, social preference, and preference for social novelty were tested (Figures 2F and S4D–S4F). Although PLD1 ablation did not significantly impair social preference (Figure S4E), the preference for social novelty (Figure S4F), or the ability to recognize a littermate (Figure 2F, left panel, and Figure S4D), *Pld1* KO animals were less social in a hippocampus-dependent task (Meira et al., 2018), since they spent less time exploring compared to WT (Figure 2F, right panel). We show here that PLD1 ablation causes deficits in an NOR task and impairs social behavior in a hippocampus-engaging task.

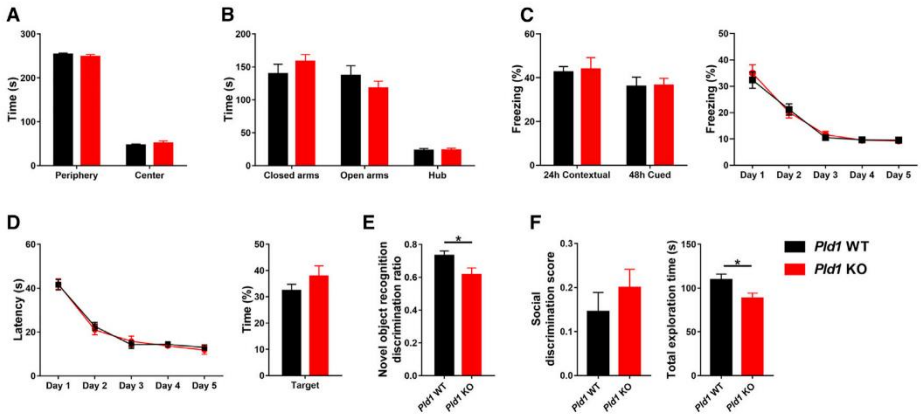

Figure 2. PLD1 Ablation Impairs Object Recognition and Social Exploration during a Social Discrimination Task

(A) The ablation of PLD1 does not have apparent consequences in locomotion, exploratory activity, and anxiety, as assessed by the OF test (n_{WT} = 25, n_{KO} = 23).

(B) *Pld1* KO mice exhibit no alterations in anxiety behavior when compared to WT, assessed by the EPM test (n_{WT} = 23, n_{KO} = 23).

(C) PLD1 ablation has no impact in contextual or cued fear conditioning (left panel) and no impact in the extinction protocol (right panel) (n_{WT} = 8, n_{KO} = 11).

(D) The ablation of PLD1 has no impact in spatial memory, evaluated with the MWM test. No differences were detected concerning spatial learning (left panel) and reference memory (right panel) in *Pld1* KO mice, compared to their WT littermates (n_{WT} = 23, n_{KO} = 20).

(*E*) *Pld1* KO mice deficits in object recognition-related short-term memory, evaluated with the NOR test (unpaired t test $t(29) = 2.315$, $p = 0.0279$). The discrimination ratio was calculated by dividing the time spent exploring the novel object by the time spent exploring both objects (n_{WT} = 16, n_{KO} = 15).

(F) *Pld1* KO mice are able to discriminate between a littermate and a strange mouse (left panel), but they spend less time interacting with conspecifics in a social discrimination task (left panel) (unpaired t test $t(37) = 2.432$, $p = 0.0200$). The social discrimination score was calculated as the difference between the time spent exploring the cups placed on the side chambers, divided by the total time exploring both (n_{WT} = 20, n_{KO} = 19).

Bars represent means ± SEMs. *p < 0.05. See also Figure S4.

PLD1 Ablation Disrupts DH-VH Dendritic Arborization Differentiation

Neuronal dendrites are crucial for information input, signal integration, and neuronal functioning. Since PLD1 has been implicated in dendritic arborization regulation (Ziegler and Tavosanis, 2019), we tested the impact of PLD1 ablation in dendritic branching in CA1 and CA3 pyramidal cells and dentate gyrus (DG) granule cells in both DH and VH. We observed multiple differences when comparing DH to VH in *Pld1* WT, such as decreased VH CA1 basal dendritic length (Figure 3A), decreased VH CA1 apical number of nodes (Figure 3A), increased CA3 VH basal dendritic length of VH (Figure 3B), decreased CA3 VH apical number of nodes (Figure 3B), and increased CA3 VH apical spine density (Figure 3B). These DH-VH differences in CA1–CA3 were not observed upon PLD1 ablation, which suggests that PLD1 is necessary for DH-VH structural differentiation. Also, when directly comparing genotypes, a decrease was observed in the apical dendritic length of CA3 DH of *Pld1* KO mice when compared to *Pld1* WT (Figure 3B). Finally, PLD1 ablation did not have a major impact on DH-VH structural differentiation in the DG (Figure 3C). These observations indicate that PLD1 is necessary for proper dendritic arborization organization and DH-VH structural differentiation, preferentially in both CA1 and CA3.

PLD1 Ablation Reduces LTD Induction in the DH

To further explore the importance of PLD1 in intra-hippocampal circuitry, *ex vivo* hippocampal extracellular electrophysiological recordings were performed upon Schaffer collateral stimulation and recording in CA1 to assess the impact of PLD1 ablation in synaptic plasticity paradigms, such as long-term potentiation (LTP) and long-term depression (LTD), in both the DH and VH (Figure 4). Assessment of LTP showed no major differences between *Pld1* WT and KO animals in either the DH or VH (Figure 4A). However, while there was no impact of PLD1 ablation in LTD in the VH, we observed a reduction in LTD induction in the DH of *Pld1* KO animals (Figure 4B). The input-output recordings and paired pulse facilitation revealed no differences between *Pld1* WT and KO mice in either the DH or VH (Figures 4C and S5). This shows that PLD1 is necessary for synaptic plasticity-associated LTD with a specific regional effect in the DH.

PLD1 Ablation Reduces GluN2A and SNAP-25 Levels in the DH

In light of specific DH-VH alterations at the lipidomic, behavioral, dendritic arborization, and electrophysiological levels, we further evaluated the impact of PLD1 ablation in the levels of proteins involved in synaptic function in both the DH and VH. We found that PLD1 ablation specifically leads to decreased SNAP-25 and GluN2A (also known as NR2A) protein levels in the DH (Figure 5). The levels of another presynaptic protein, synaptophysin, as well as other postsynaptic proteins, PSD95, Homer, GluA1 (also known as GluR1), GluA2 (also known as GluR2), GluN2B (also known as NR2B), and GluN2B-P (phosphorylated at Y1472), were not affected by PLD1 ablation at either the DH or

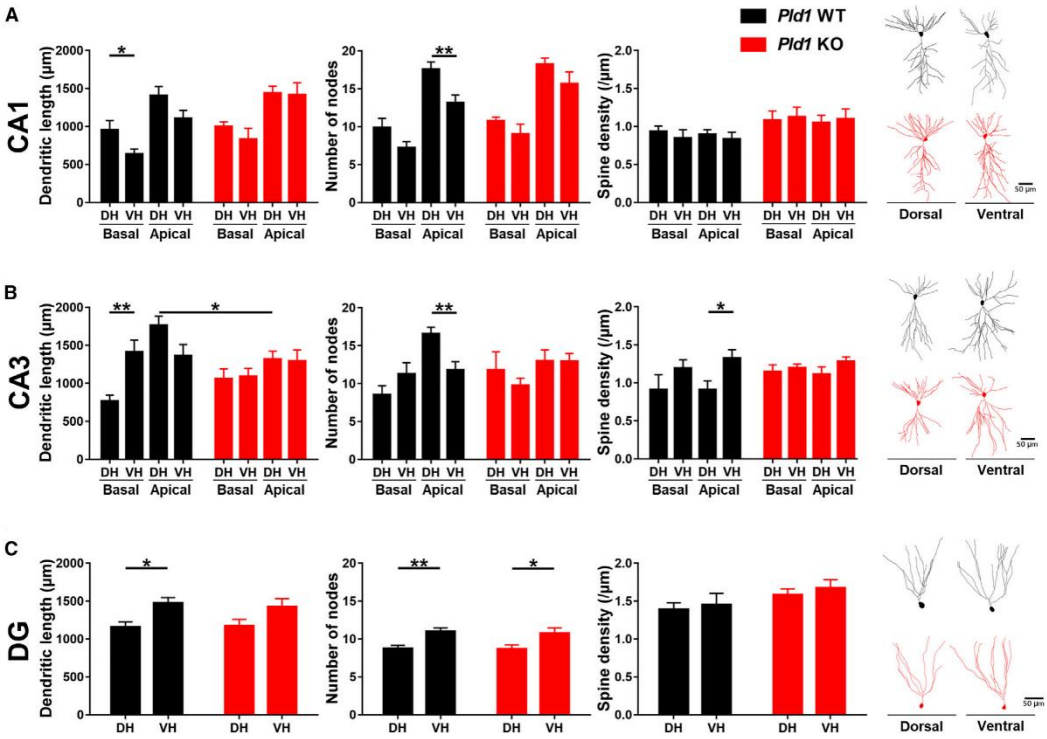

Figure 3. PLD1 Ablation Disrupts DH-VH Dendritic Arborization Differentiation

(A) In CA1 (n_{WT} = 8, n_{KO} = 6–7), there is a significant decrease in the basal dendritic length of VH when compared to DH in *Pld1* WT animals (unpaired t test $t(14)$ = 2.265, p = 0.0399). There is also a significant decrease in the apical number of nodes of VH when compared to DH in *Pld1* WT animals (unpaired t test $t(14)$ = 3.071, p = 0.0083).

(B) In CA3 (n_{WT} = 5–6, n_{KO} = 6), there is a significant increase in the basal dendritic length of VH when compared to DH in *Pld1* WT animals (unpaired t test $t(9)$ = 3.459, p = 0.0072). There is also a significant decrease in the apical number of nodes of VH when compared to DH in *Pld1* WT animals (unpaired t test $t(9)$ = 3.322, p = 0.0089). Moreover, there is a significant increase in the apical spine density of VH when compared to DH in *Pld1* WT animals (unpaired t test $t(9)$ = 2.503, p = 0.0337). Concerning the genotype, a decrease was observed in the apical dendritic length of CA3 DH of *Pld1* KO mice when compared to *Pld1* WT (unpaired t test $t(9)$ = 2.766, p = 0.0219).

(C) In DG (n_{WT} = 6–8, n_{KO} = 6–7), there is a significant increase in the dendritic length of VH when compared to DH in *Pld1* WT animals (unpaired t test $t(13)$ = 3.38, p = 0.0049). There is also a significant increase in the number of nodes of VH when compared to DH in *Pld1* WT animals (unpaired t test $t(13)$ = 3.613, p = 0.0032), which is reproduced when PLD1 is ablated (unpaired t test $t(12)$ = 2.342, p = 0.0372).

Bars represent means ± SEMs. *p < 0.05, **p < 0.01.

VH (Figure 5). Given the observed changes in SNAP-25, we also tested whether other SNARE complex proteins were altered and observed no changes in syntaxin-1A and synaptobrevin-2 protein levels upon PLD1 ablation (Figure 5). GluA1, GluN2A, and GluN2B-P levels were found to be higher in DH compared to VH in *Pld1* WT animals, and while this DH-VH difference persisted for GluA1 upon PLD1 ablation, it was not observed for GluN2A and GluN2B-P (Figure 5). Moreover, the levels of syntaxin-1A were higher in the VH when compared to the DH (Figure 5). Overall, it shows that PLD1 reduction leads to a specific reduction in the DH of SNAP-25 and GluN2A protein levels, which could partially explain the synaptic plasticity changes observed in LTD and disrupted DH-VH segregation.

DISCUSSION

Based on anatomical, gene expression, and functional studies, the hippocampus presents an organized gradient along its longitudinal axis, which highlights the differential contribution of its DH and VH poles to physiological and pathological processes linked to mood regulation, learning, and memory (Strange et al., 2014). In light of recent lipidomic observations suggesting that PA and the PLD pathway could be differentially regulated along the DH-VH axis (Miranda et al., 2019; Pavel et al., 2019), we tested the impact of PLD genetic modulation on the DH-VH axis organization and function. We found that PLD1 is the major contributor for total PA production in the mouse forebrain, when

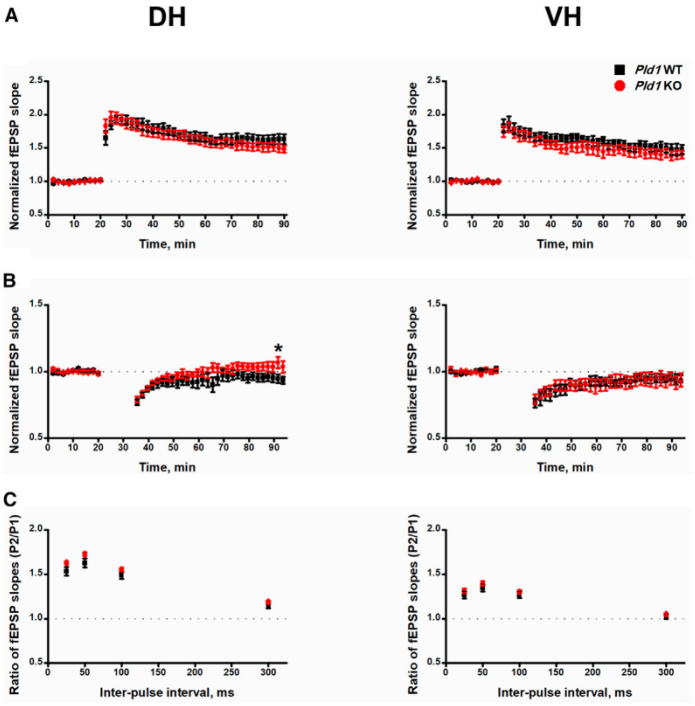

Figure 4. PLD1 Ablation Reduces LTD in the DH

(A) LTP was measured in acute slices of DH (left panel) (n_{WT} = 9, n_{KO} = 8) and VH (right panel) (n_{WT} = 8, n_{KO} = 8).

(B) LTD was measured in acute slices of DH (left panel) (n_{WT} = 9, n_{KO} = 9) and VH (right panel) (n_{WT} = 7, n_{KO} = 8). There was an increase in excitability in the late phase of LTD of DH in *Pld1* KO animals (unpaired t test $t(16) = 2.143$, $p = 0.0478$).

(C) Paired pulse (PP) ratios in acute slices of DH (left panel) (n_{WT} = 18, n_{KO} = 14) and VH (right panel) (n_{WT} = 14, n_{KO} = 14). Within WT animals, 2-way ANOVA showed the PP curves of DH and VH to be different (2-way ANOVA: interaction $F(3,90) = 11.7$, $p < 0.0001$; WT DH/VH $F(1,30) = 16.8$, $p = 0.0003$). The bars represent means ± SEMs. fEPSP, field excitatory postsynaptic potential. *$p < 0.05$.

See also Figure S5.

compared to PLD2, affecting predominantly the DH lipidome. We further showed that PLD1 ablation leads to a CA1/CA3 dendritic arborization reorganization, to behavioral deficits in novelty recognition and social interaction, to deficits in DH LTD, and to specific synaptic protein alterations predominantly in the DH. Thus, we show that PLD1 is necessary for the proper organization and function of the longitudinal hippocampal axis, with a preferential impact in the DH. In this study, we used adult mice, and since *Pld1* expression is high during brain development (Colley et al., 1997), we cannot exclude the possibility that our observations in adult mice could be affected by an early PLD deficit.

To study the impact of modulating the PLD pathway, we measured PLD activity in the forebrains of *Pld1* KO, *Pld2* KO, and *Pld* DKO animals by quantifying PEtOH levels after ethanol injection (Figures 1B and S1). Both *Pld1* and *Pld2* KO show decreased levels of acutely produced forebrain PEtOH (Figures 1B and S1). However, although both PLD1 and PLD2 synthesize PA, PLD1 ablation had a higher-magnitude impact than PLD2 in basal hippocampal PA levels (Figures 1C and 1D), which is in accordance with other recent observations (Liang et al., 2019). The added reducing effect on total PLD activity upon the ablation of either PLD1 (≈35%) and PLD2 (≈24%) does not add up to the near-absence of detectable levels of total PLD activity in *Pld* DKO animals (Figure 1B), which is highly likely due to compensatory mechanisms on both *Pld1* and *Pld2* KO animals. Our data suggest that these compensatory mechanisms do not occur by isoenzyme translation upregulation (Figures S2 and S3); other possibilities are that the activity upregulation could be due to altered localization, post-translational modifications, or differences in co-factor modulation (Selvy et al., 2011). Moreover, the PA and PEtOH species profile analysis suggests that PLD1 and PLD2 modulate different PA pools. While PLD1 affects both shorter and longer fatty acyl carbon length PA species, PLD2 modulates predominantly shorter fatty acyl carbon length PA species (Figures 1D and S1). Overall, these results are somewhat in accordance with previous observations that show no changes in total PA levels upon PLD2 ablation (Oliveira et al., 2010; Vermeren et al., 2016) and a differential effect on various PA species, demonstrating also in some instances an increase in specific PA species (Oliveira et al., 2010; Vermeren et al., 2016), which is likely induced by a compensatory PLD1 response. At the species level, the most consistent change we observed upon PLD2 ablation was the decrease in PA/PEtOH 34:2 (Figures 1 and S1). However, other previously reported decreases in PA 32:1 and 38:4 and increase in PA 32:0 levels (Oliveira et al., 2010) were not observed here, although differences in the analyzed brain regions and mouse age should be accounted for. Increased PLD activity has been proposed to be detrimental and has been implicated in neurodegeneration either by an Aβ-induced overactive state in the context of AD (Oliveira et al., 2010) or by overexpressing PLD in the fly rhabdomere (Raghu et al., 2009), with specific increased levels in PA 34:2 in both cases. In a particular experimental setting with cultured neutrophils, PLD1 or PLD2 ablation only unraveled its PLD-dependent phenotypes upon activating conditions (Norton et al., 2011). Since we observe here compensatory crosstalk between each isoenzyme, it will be relevant in future studies targeting PLD1 or PLD2, by genetic or pharmacological means, to consider the observed phenotypes not only as a loss of

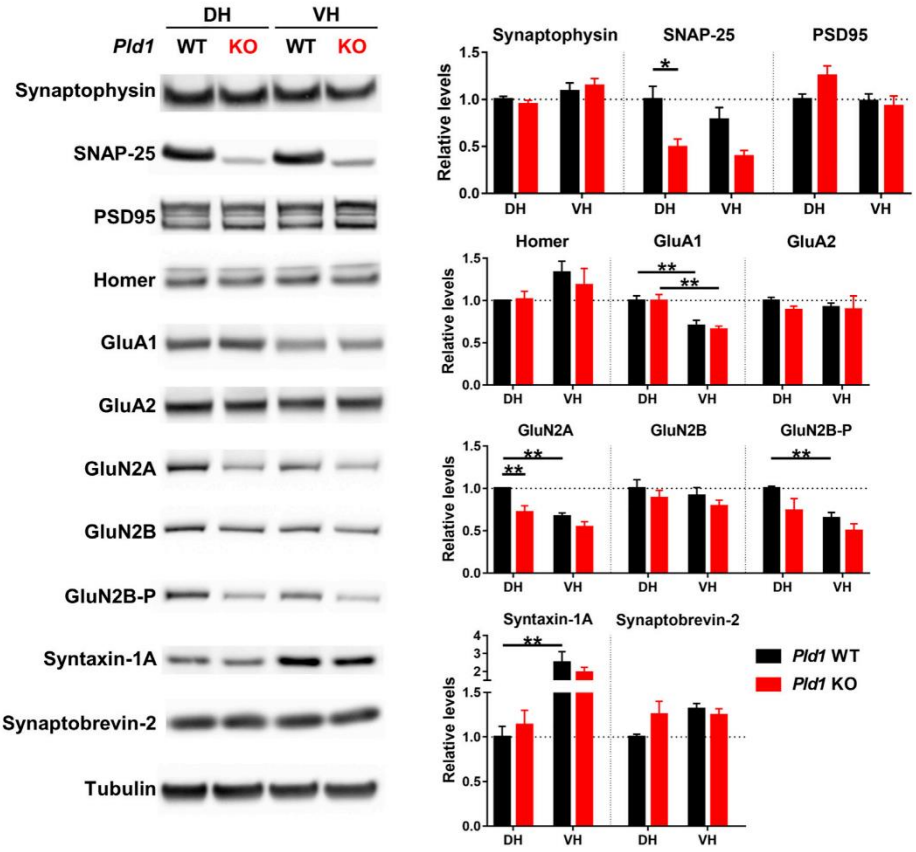

Figure 5. PLD1 Ablation Reduces GluA2 and SNAP-25 Levels in DH

Protein levels of DH and VH were evaluated by western blot analysis and quantified by densitometric analysis (n = 5–9). PLD1 ablation decreased the levels of GluA2 (2-way ANOVA: interaction $F(1,24) = 2.007$, $p = 0.1695$; WT/KO $F(1,24) = 13.73$, $p = 0.0011$; DH WT/KO $p = 0.0070$, Tukey's multiple comparisons test) and SNAP-25 in the DH (2-way ANOVA: interaction $F(1,32) = 0.2838$, $p = 0.5979$; WT/KO $F(1,32) = 16.91$, $p = 0.0003$; DH WT/KO: $p = 0.0126$; Tukey's multiple comparisons test). There was a decrease in GluA1 levels when comparing VH with DH in *Pld1* WT animals. This difference persisted with PLD1 ablation (2-way ANOVA: interaction $F(1,32) = 0.1318$, $p = 0.7190$; DH/VH $F(1,32) = 29.55$, $p < 0.0001$; WT DH/VH $p = 0.0058$; KO DH/VH $p = 0.0014$; Tukey's multiple comparisons test). In *Pld1* WT animals, the levels of GluA2 (2-way ANOVA: interaction $F(1,24) = 2.007$, $p = 0.1695$; DH/VH $F(1,24) = 20.95$, $p = 0.0001$; WT DH/VH $p = 0.0015$; Tukey's multiple comparisons test) and the levels of Glu2B-P (2-way ANOVA: interaction $F(1,28) = 0.3767$, $p = 0.5443$; DH/VH $F(1,28) = 10.79$, $p = 0.0027$; WT DH/VH $p = 0.0472$; Tukey's multiple comparisons test) were decreased in the VH when compared to DH. The levels of syntaxin-1A were increased in the VH when compared to DH in WT animals (2-way ANOVA: interaction $F(1,20) = 1.013$, $p = 0.3261$; DH/VH $F(1,20) = 10.76$, $p = 0.0037$; WT DH/VH $p = 0.0309$; Tukey's multiple comparisons test). Individual protein levels were compared with WT DH. GluN2B-P is phosphorylated at Y1472. Representative blots are shown. The bars represent means ± SEMs. For some points, the error bars are not drawn since they would be shorter than the height of the symbol. *$p < 0.05$, **$p < 0.01$.

function effect but also as a potential gain of function through a compensatory activation of its isoenzyme counterpart. This takes on further importance in light of differential signaling factors that regulate the functioning of either PLD1 or PLD2, or alternatively, that PLD co-factors, such as $PI(4,5)P_2$, could be differentially affected by altered PA synthesis by either PLD1 or PLD2 (Selvy et al., 2011).

Another observation that can be inferred from our PLD activity studies is that PLD1 and PLD2 are likely the only canonical PLD isoenzymes. While the PLD superfamily also includes PLD3–PLD6, which have in common the presence of HKD domains (Barber et al., 2018; Nelson and Frohman, 2015), our data indicate that these other members do not contribute to the production of PEtOH. This is relevant because the PLD pathway has been implicated in AD pathogenesis (Oliveira and Di Paolo, 2010), with reported effects of PLD1 on APP processing and trafficking (Cai et al., 2006a, 2006b) and PLD2 on Aβ downstream pathological signaling (Oliveira et al., 2010). Since human genetic studies implicated PLD3 as a potential risk factor for AD (Cruchaga et al., 2014), the recent understanding of its role in

lysosomal function (Fazzari et al., 2017; Gonzalez et al., 2018) raises the question of whether PLD3 functioning is directly connected to PLD1 or PLD2 AD pathophysiology. Both PLD3 and PLD4 were found to be exonucleases regulating the inflammatory cytokine response (Gavin et al., 2018), which could be linked to the multiple genetic AD risk factors connected to immune system biology (Karch and Goate, 2015).

Concerning the impact of reducing PLD levels on other lipid classes, the ablation of PLD1, but not PLD2, had a significant effect, with greater repercussions in the DH when compared to the VH, mainly affecting lysoglycerophospholipids such as LPC, LPCe, and LPI (Figure 1C). This suggests potential crosstalk between different phospholipases, namely PLA2, which is a main lysoglycerophospholipid source (Burke and Dennis, 2009). Co-expression phospholipase studies showed that PLD2, but not PLD1, augmented PLA2 activity (Ueno et al., 2000), which could in part justify the observed lipidomic alterations in the DH in a hypothetical PLD2 recruitment in a PLD1 ablation condition.

Knowing that PLD1 ablation had a more significant effect on the hippocampal lipidome than did PLD2 ablation, we focused more specifically on studying *Pld1* KO mice. From the multitude of behavioral tests that we covered in *Pld1* KO animals, we observed a deficit only in short-term NOR (Figure 2E) and in the social interaction time in a hippocampal-dependent social discrimination task (Figure 2F). This is partially in accordance with another report in which PLD1 ablation shows a trend toward a deficit in the level of discrimination in long-term NOR and a social recognition deficit (Burkhardt et al., 2014). While the same authors also observed deficits in social and object recognition in *Pld2* KO animals (Burkhardt et al., 2014), others showed that PLD2 ablation had no major behavioral deficits (Oliveira et al., 2010; Vermeren et al., 2016), besides an olfaction deficit in aged mice (Vermeren et al., 2016). Overall, these studies indicate that even though PLD isoenzyme ablation is somewhat manageable by the organism, future approaches should take into account not only the mouse strain used, age, and sex but also the contribution of each isoenzyme specifically in experimental conditions that lead to on-demand PLD activation unraveling specific phenotypes, such as the case of the protective effect observed upon PLD2 ablation in an AD mouse model (Oliveira et al., 2010).

Considering the previously described gradient of PA in the long hippocampal axis with higher PA levels in the DH (Miranda et al., 2019), and since PLD1 is a major PA source (Figure 1), we hypothesized that PLD1 could play an important role in hippocampal dendritic organization. Here, we observed a marked structural DH-VH differentiation of CA1/CA3 dendritic arborization in *Pld1* WT animals, and these differences were essentially absent upon PLD1 ablation (Figures 3A and 3B). Opposing effects on dendritic arborization have been reported upon PLD1 ablation. Some authors showed that *Pld1* KO cultured neurons had decreased dendritic branching (Ammar et al., 2013), while others observed the opposite effect upon reducing PLD1 levels (Zhu et al., 2012). More recently, using mixed neuronal and astrocyte cultures, it was shown that PLD1 reduces PA in astrocytes, reducing protein kinase A activation in neurons and consequently dendritic branching (Zhu et al., 2016). Therefore, the specific role of PLD1 in dendritic arborization and its regulatory factors are still being debated. One plausible possibility is that PA, acting as a fusogenic lipid due to its inverted cone-shaped structure, could differentially contribute to membrane addition in different neurite outgrowth conditions (Tanguy et al., 2019).

At the functional level, we observed that PLD1 ablation reduced LTD induction in the DH CA1 after low-frequency stimulation (LFS) at the Schaffer collaterals, while it had no effects in the VH, unraveling a specific effect along the longitudinal hippocampal axis (Figure 4). Recently, it was shown that PLD1 is necessary for LTD induction in the mouse prefrontal cortex, which phenocopies our observations in the DH (Moran et al., 2019). Along with the observed deficits in NOR in *Pld1* KO animals (Figure 2E), it was previously shown that hippocampal LTD induction was associated with the recognition of novel objects (Kemp and Manahan-Vaughan, 2004). Also, lipid signaling has previously been observed to be involved in LTD mechanisms; aligned with that, not only were arachidonic acid metabolites shown to induce LTD (Feinmark et al., 2003) but also PLA2 inhibition was shown to block LTD in neonatal hippocampal slices (Fitzpatrick and Baudry, 1994). Since we observe here that PLD1 ablation reduces various lysoglycerophospholipid levels in the DH (Figure 1C), it further supports that PLA2 could be in a hypoactive state, partially explaining why LTD induction was reduced upon PLD1 ablation. Another possibility is based on the findings that PA binds and activates phosphatidylinositol 4-phosphate 5-kinase (PIP5K) (Jenkins et al., 1994; Stace et al., 2008), which was shown to be necessary for LFS LTD induction (Unoki et al., 2012). Moreover, since hippocalcin was shown to be necessary for LTD induction (Palmer et al., 2005) and to activate PLD (Hyun et al., 2000; Oh et al., 2006), these observations are coherent with a role for the PLD pathway in LTD-associated plasticity mechanisms, even if the contribution for each PLD isoenzyme should still be addressed. Finally, PLD1 has been shown in *in vitro* neuron culture experiments to be involved in other synaptic plasticity-associated pathways. For instance, it was proposed that PLD1-derived PA activates the mammalian target of rapamycin (mTOR), affecting its synaptic plasticity regulation in a chemical LTP setting with an impact in brain-derived neurotrophic factor (BDNF) dendritic expression levels (Henry et al., 2018). Also, PLD1 was shown to act as a BDNF downstream effector necessary for the phosphorylation of both mTOR and cAMP response element-binding protein (CREB) (Ammar et al., 2013). Overall, these specific pathway regulations could be relevant for other brain regions or could be specific in certain experimental settings, taking into account the complex circuitry and different cell types in an *in vivo-ex vivo* experimental approach.

To gain further insight into the molecular pathways affected by PLD1 ablation, we assessed different synaptic protein levels both in DH and VH (Figure 5). The dendritic DH-VH differences in WT animals occur in parallel with higher protein levels of GluN2A, GluN2B-P (phosphorylated at Y1472), and GluA1 in DH (Figure 5). Accordingly, tyrosine phosphorylation of GluN2B has been reported to regulate the number of dendritic spines and morphological changes (Wang et al., 2018), an autism

spectrum disorder-associated mutation in GluN2B leads to dendritic abnormal development (Sceniak et al., 2019), dendritic branch pruning along maturation is accompanied by an elevation in GluN2A levels (Bustos et al., 2014), GluN2A genetic ablation was shown to reduce dendritic length in dentate granule cells (Kannangara et al., 2014), and GluA1 expression was shown to promote dendritic branching (Zhou et al., 2008). The most intriguing observation was the marked reduction in the target N-ethylmaleimide-sensitive fusion protein attachment protein receptor (t-SNARE) protein SNAP-25 in the DH of *Pld1* KO animals (Figure 5). The SNAP-25 yeast ortholog Spo20p was reported to bind to PA (Liu et al., 2007). Taking advantage of this property, Spo20p is regularly used as a PA probe and was found to co-localize with mammalian SNAP-25 in an experimental context of acutely activated exocytosis (Zeniou-Meyer et al., 2007). Moreover, SNAP-25 was reported to bind to anionic lipids, such as PA, and even though, to our knowledge, PA binding was not specifically tested, SNAP-25 was found to bind to $PI(4,5)P_2$, which PA could still indirectly modulate by PIP5K activation (Jenkins et al., 1994; Stace et al., 2008). Although the reduction of SNAP-25 levels led to deficits in sociability behavior and susceptibility to pharmacologically induced seizures, it partially phenocopied *Pld1* KO animals, which also show deficits in NOR and social interaction in a hippocampus-specific task (Figure 2) and no deficits in spatial learning and memory tasks (Corradini et al., 2014). Moreover, infusion with a C-terminal SNAP-25 fragment, proposed to block its normal functions, reduces CA3-CA1 LTD induction (Zhang et al., 2011), and reduction in SNAP-25 levels also leads to deficits in LTD induction in corticostriatal preparations (Baca et al., 2013). Since the functions of SNAP-25 have been described at both the presynaptic (Bronk et al., 2007) and postsynaptic (Fossati et al., 2015) compartments, both possibilities should be considered when studying the impact of PLD1-derived PA on SNAP-25 functioning. Also, since SNAP-25 is a member of the soluble SNARE complex (Ramakrishnan et al., 2012), we tested the impact on other SNARE complex proteins, such as syntaxin-1A and synaptobrevin-2, and no changes were observed upon PLD1 ablation in either the DH or VH (Figure 5).

In summary, our work shows that lipid signaling modulation differently affects the hippocampus along its longitudinal axis. We show that PLD1 ablation predominantly affects the DH, with implications for disorders that affect learning and memory, such as AD and mood disorders. Moreover, we observe that PLD1 ablation reduces SNAP-25 levels, and since SNAP-25 has been implicated in attention-deficit/hyperactivity disorder (Feng et al., 2005), autism spectrum disorders (Guerini et al., 2011), and schizophrenia (Thompson et al., 2003), it further highlights the potential role of lipid signaling dysregulation in these neuropsychiatric disorders.

STAR★METHODS

Detailed methods are provided in the online version of this paper and include the following:

- KEY RESOURCES TABLE
- LEAD CONTACT AND MATERIALS AVAILABITY
- EXPERIMENTAL MODEL AND SUBJECT DETAILS
- METHOD DETAILS
  - Western Blot
  - *In vivo* PLD activity
  - Lipid Analysis
  - Behavioral testing
  - Dendritic Arborization
  - Electrophysiology
  - Gene expression analysis by qRT-PCR
- QUANTIFICATION AND STATISTICAL ANALYSIS
- DATA AND CODE AVAILABILITY

SUPPLEMENTAL INFORMATION

Supplemental Information can be found online at https://doi.org/10.1016/j.celrep.2020.02.102.

ACKNOWLEDGMENTS

This work was supported by grants from the Portuguese North Regional Operational Program (ON.2, O Novo Norte) under the National Strategic Reference Framework (QREN), through the European Regional Development Fund, European Union (FEDER); the Fundação para a Ciência e Tecnologia, Portugal (PD/BD/105915/2014 to A.M.M.), Norte2020 (UMINHO/BD/52/2017 to L.S.-M.); the Ruth L. Kirschstein National Research Service Award F31 Individual Fellowship (1F31NS073387-01 to K.P.d.J.); and the BIAL Foundation, Portugal (253/14 to T.G.O.). We thank Sung Ho Ryu (Pohang University of Science and Technology, South Korea) for providing the PLD antibody. We appreciate the contributions of João Carlos Gonçalves (University of Minho, Portugal), Inês Xavier Fernandes (University of Minho, Portugal), Sónia Guerra-Gomes (University of Minho, Portugal), and Jorge Da Silva (University of Minho, Portugal) for help with the behavioral analysis. We thank Clarissa Waites (Columbia University, USA), Luís Santos (Mount Sinai Hospital, USA), and Catarina Ferreira (Mount Sinai Hospital, USA) for help in acquiring reagents. We thank Carlos Bandeira Duarte (University of Coimbra, Portugal), Patrícia Monteiro (University of Minho, Portugal), and João Carlos Sousa (University of Minho, Portugal) for scientific discussions and critical input relevant to this project.

AUTHOR CONTRIBUTIONS

T.G.O. conceived the idea. T.G.O. acquired the core funding for the work. L.S.-M., I.C., and T.G.O. designed and planned the experiments. L.S.-M. and I.C. performed the majority of the experiments. V.P. coordinated and supervised the electrophysiological experiments. R.R.S. and F.V.B. contributed to the behavioral analysis and preliminary experiments. T.M. contributed to the planning and the behavioral analysis. R.M.-R. and F.M. contributed to the RT-PCR experiments. L.S.-M., A.M.M., Y.X., K.P.d.J., M.W., R.B.C., G.D.P., and T.G.O. contributed to the lipidomic experiments. L.S.-M. and T.G.O. wrote the paper, and all of the authors reviewed and edited the manuscript.

DECLARATION OF INTERESTS

G.D.P. is a full-time employee of Denali Therapeutics. G.D.P. and T.G.O. are listed as inventors on the patent number WO2010138869A1, "Modulation of Phospholipase D for the Treatment of Neurodegenerative Disorders." R.B.C., G.D.P., and T.G.O. are listed as inventors on the patent number US20120302604A1, "Modulation of Phospholipase D for the Treatment of the Acute and Chronic Effects of Ethanol."

Received: September 17, 2019
Revised: January 29, 2020
Accepted: February 27, 2020
Published: March 24, 2020

REFERENCES

Ammar, M.R., Humeau, Y., Hanauer, A., Nieswandt, B., Bader, M.F., and Vitale, N. (2013). The Coffin-Lowry syndrome-associated protein RSK2 regulates neurite outgrowth through phosphorylation of phospholipase D1 (PLD1) and synthesis of phosphatidic acid. J. Neurosci. *33*, 19470–19479.

Baca, M., Allan, A.M., Partridge, L.D., and Wilson, M.C. (2013). Gene-environment interactions affect long-term depression (LTD) through changes in dopamine receptor affinity in Snap25 deficient mice. Brain Res. *1532*, 85–98.

Bannerman, D.M., Sprengel, R., Sanderson, D.J., McHugh, S.B., Rawlins, J.N., Monyer, H., and Seeburg, P.H. (2014). Hippocampal synaptic plasticity, spatial memory and anxiety. Nat. Rev. Neurosci. *15*, 181–192.

Barber, C.N., Huganir, R.L., and Raben, D.M. (2018). Phosphatidic acid-producing enzymes regulating the synaptic vesicle cycle: role for PLD? Adv. Biol. Regul. *67*, 141–147.

Bienkowski, M.S., Bowman, I., Song, M.Y., Gou, L., Ard, T., Cotter, K., Zhu, M., Benavidez, N.L., Yamashita, S., Abu-Jaber, J., et al. (2018). Integration of gene expression and brain-wide connectivity reveals the multiscale organization of mouse hippocampal networks. Nat. Neurosci. *21*, 1628–1643.

Bligh, E.G., and Dyer, W.J. (1959). A rapid method of total lipid extraction and purification. Can. J. Biochem. Physiol. *37*, 911–917.

Bravo, F.V., Da Silva, J., Chan, R.B., Di Paolo, G., Teixeira-Castro, A., and Oliveira, T.G. (2018). Phospholipase D functional ablation has a protective effect in an Alzheimer's disease Caenorhabditis elegans model. Sci. Rep. *8*, 3540.

Bronk, P., Deák, F., Wilson, M.C., Liu, X., Südhof, T.C., and Kavalali, E.T. (2007). Differential effects of SNAP-25 deletion on Ca2+ -dependent and Ca2+ -independent neurotransmission. J. Neurophysiol. *98*, 794–806.

Burke, J.E., and Dennis, E.A. (2009). Phospholipase A2 biochemistry. Cardiovasc. Drugs Ther. *23*, 49–59.

Burkhardt, U., Stegner, D., Hattingen, E., Beyer, S., Nieswandt, B., and Klein, J. (2014). Impaired brain development and reduced cognitive function in phospholipase D-deficient mice. Neurosci. Lett. *572*, 48–52.

Bustos, F.J., Varela-Nallar, L., Campos, M., Henriquez, B., Phillips, M., Opazo, C., Aguayo, L.G., Montecino, M., Constantine-Paton, M., Inestrosa, N.C., and van Zundert, B. (2014). PSD95 suppresses dendritic arbor development in mature hippocampal neurons by occluding the clustering of NR2B-NMDA receptors. PLoS One *9*, e94037.

Cai, D., Netzer, W.J., Zhong, M., Lin, Y., Du, G., Frohman, M., Foster, D.A., Sisodia, S.S., Xu, H., Gorelick, F.S., and Greengard, P. (2006a). Presenilin-1 uses phospholipase D1 as a negative regulator of beta-amyloid formation. Proc. Natl. Acad. Sci. USA *103*, 1941–1946.

Cai, D., Zhong, M., Wang, R., Netzer, W.J., Shields, D., Zheng, H., Sisodia, S.S., Foster, D.A., Gorelick, F.S., Xu, H., and Greengard, P. (2006b). Phospholipase D1 corrects impaired betaAPP trafficking and neurite outgrowth in familial Alzheimer's disease-linked presenilin-1 mutant neurons. Proc. Natl. Acad. Sci. USA *103*, 1936–1940.

Chan, R.B., Oliveira, T.G., Cortes, E.P., Honig, L.S., Duff, K.E., Small, S.A., Wenk, M.R., Shui, G., and Di Paolo, G. (2012). Comparative lipidomic analysis of mouse and human brain with Alzheimer disease. J. Biol. Chem. *287*, 2678–2688.

Colley, W.C., Altshuller, Y.M., Sue-Ling, C.K., Copeland, N.G., Gilbert, D.J., Jenkins, N.A., Branch, K.D., Tsirka, S.E., Bollag, R.J., Bollag, W.B., and Frohman, M.A. (1997). Cloning and expression analysis of murine phospholipase D1. Biochem. J. *326*, 745–753.

Corradini, I., Donzelli, A., Antonucci, F., Welzl, H., Loos, M., Martucci, R., De Astis, S., Pattini, L., Inverardi, F., Wolfer, D., et al. (2014). Epileptiform activity and cognitive deficits in SNAP-25(+/−) mice are normalized by antiepileptic drugs. Cereb. Cortex *24*, 364–376.

Cruchaga, C., Karch, C.M., Jin, S.C., Benitez, B.A., Cai, Y., Guerreiro, R., Harari, O., Norton, J., Budde, J., Bertelsen, S., et al.; Alzheimer's Research UK (ARUK) Consortium (2014). Rare coding variants in the phospholipase D3 gene confer risk for Alzheimer's disease. Nature *505*, 550–554.

Dall'Armi, C., Hurtado-Lorenzo, A., Tian, H., Morel, E., Nezu, A., Chan, R.B., Yu, W.H., Robinson, K.S., Yeku, O., Small, S.A., et al. (2010). The phospholipase D1 pathway modulates macroautophagy. Nat. Commun. *1*, 142.

Fanselow, M.S., and Dong, H.W. (2010). Are the dorsal and ventral hippocampus functionally distinct structures? Neuron *65*, 7–19.

Fazzari, P., Horre, K., Arranz, A.M., Frigerio, C.S., Saito, T., Saido, T.C., and De Strooper, B. (2017). PLD3 gene and processing of APP. Nature *541*, E1–E2.

Feinmark, S.J., Begum, R., Tsvetkov, E., Goussakov, I., Funk, C.D., Siegelbaum, S.A., and Bolshakov, V.Y. (2003). 12-lipoxygenase metabolites of arachidonic acid mediate metabotropic glutamate receptor-dependent long-term depression at hippocampal CA3-CA1 synapses. J. Neurosci. *23*, 11427–11435.

Feng, Y., Crosbie, J., Wigg, K., Pathare, T., Ickowicz, A., Schachar, R., Tannock, R., Roberts, W., Malone, M., Swanson, J., et al. (2005). The SNAP25 gene as a susceptibility gene contributing to attention-deficit hyperactivity disorder. Mol. Psychiatry *10*, 998–1005, 973.

Fitzpatrick, J.S., and Baudry, M. (1994). Blockade of long-term depression in neonatal hippocampal slices by a phospholipase A2 inhibitor. Brain Res. Dev. Brain Res. *78*, 81–86.

Fossati, G., Morini, R., Corradini, I., Antonucci, F., Trepte, P., Edry, E., Sharma, V., Papale, A., Pozzi, D., Defilippi, P., et al. (2015). Reduced SNAP-25 increases PSD-95 mobility and impairs spine morphogenesis. Cell Death Differ. *22*, 1425–1436.

Frohman, M.A. (2015). The phospholipase D superfamily as therapeutic targets. Trends Pharmacol. Sci. *36*, 137–144.

Gavin, A.L., Huang, D., Huber, C., Mårtensson, A., Tardif, V., Skog, P.D., Blane, T.R., Thinnes, T.C., Osborn, K., Chong, H.S., et al. (2018). PLD3 and PLD4 are single-stranded acid exonucleases that regulate endosomal nucleic-acid sensing. Nat. Immunol. *19*, 942–953.

Gibb, R., and Kolb, B. (1998). A method for vibratome sectioning of Golgi-Cox stained whole rat brain. J. Neurosci. Methods *79*, 1–4.

Gonzalez, A.C., Schweizer, M., Jagdmann, S., Bernreuther, C., Reinheckel, T., Saftig, P., and Damme, M. (2018). Unconventional Trafficking of Mammalian Phospholipase D3 to Lysosomes. Cell Rep. *22*, 1040–1053.

Guerini, F.R., Bolognesi, E., Chiappedi, M., Manca, S., Ghezzo, A., Agliardi, C., Sotgiu, S., Usai, S., Matteoli, M., and Clerici, M. (2011). SNAP-25 single nucleotide polymorphisms are associated with hyperactivity in autism spectrum disorders. Pharmacol. Res. *64*, 283–288.

Gustavsson, L. (1995). ESBRA 1994 Award Lecture. Phosphatidylethanol formation: specific effects of ethanol mediated via phospholipase D. Alcohol Alcohol. *30*, 391–406.

Henry, F.E., Wang, X., Serrano, D., Perez, A.S., Carruthers, C.J.L., Stuenkel, E.L., and Sutton, M.A. (2018). A Unique Homeostatic Signaling Pathway Links Synaptic Inactivity to Postsynaptic mTORC1. J. Neurosci. *38*, 2207–2225.

Hyun, J.K., Yon, C., Kim, Y.S., Noh, D.Y., Lee, K.H., and Han, J.S. (2000). Role of hippocalcin in Ca2+ -induced activation of phospholipase D. Mol. Cells *10*, 669–677.

Jenkins, G.H., Fisette, P.L., and Anderson, R.A. (1994). Type I phosphatidylinositol 4-phosphate 5-kinase isoforms are specifically stimulated by phosphatidic acid. J. Biol. Chem. *269*, 11547–11554.

Kannangara, T.S., Bostrom, C.A., Ratzlaff, A., Thompson, L., Cater, R.M., Gil-Mohapel, J., and Christie, B.R. (2014). Deletion of the NMDA receptor GluN2A subunit significantly decreases dendritic growth in maturing dentate granule neurons. PLoS One *9*, e103155.

Karch, C.M., and Goate, A.M. (2015). Alzheimer's disease risk genes and mechanisms of disease pathogenesis. Biol. Psychiatry *77*, 43–51.

Kemp, A., and Manahan-Vaughan, D. (2004). Hippocampal long-term depression and long-term potentiation encode different aspects of novelty acquisition. Proc. Natl. Acad. Sci. USA *101*, 8192–8197.

Kheirbek, M.A., Drew, L.J., Burghardt, N.S., Costantini, D.O., Tannenholz, L., Ahmari, S.E., Zeng, H., Fenton, A.A., and Hen, R. (2013). Differential control of learning and anxiety along the dorsoventral axis of the dentate gyrus. Neuron *77*, 955–968.

Leger, M., Quiedeville, A., Bouet, V., Haelewyn, B., Boulouard, M., Schumann-Bard, P., and Freret, T. (2013). Object recognition test in mice. Nat. Protoc. *8*, 2531–2537.

Liang, D., Wu, K., Tei, R., Bumpus, T.W., Ye, J., and Baskin, J.M. (2019). A real-time, click chemistry imaging approach reveals stimulus-specific subcellular locations of phospholipase D activity. Proc. Natl. Acad. Sci. USA *116*, 15453–15462.

Liu, S., Wilson, K.A., Rice-Stitt, T., Neiman, A.M., and McNew, J.A. (2007). In vitro fusion catalyzed by the sporulation-specific t-SNARE light-chain Spo20p is stimulated by phosphatidic acid. Traffic *8*, 1630–1643.

Maggio, N., and Segal, M. (2007). Striking variations in corticosteroid modulation of long-term potentiation along the septotemporal axis of the hippocampus. J. Neurosci. *27*, 5757–5765.

McHugh, S.B., Fillenz, M., Lowry, J.P., Rawlins, J.N., and Bannerman, D.M. (2011). Brain tissue oxygen amperometry in behaving rats demonstrates functional dissociation of dorsal and ventral hippocampus during spatial processing and anxiety. Eur. J. Neurosci. *33*, 322–337.

Meira, T., Leroy, F., Buss, E.W., Oliva, A., Park, J., and Siegelbaum, S.A. (2018). A hippocampal circuit linking dorsal CA2 to ventral CA1 critical for social memory dynamics. Nat. Commun. *9*, 4163.

Miranda, A.M., Bravo, F.V., Chan, R.B., Sousa, N., Di Paolo, G., and Oliveira, T.G. (2019). Differential lipid composition and regulation along the hippocampal longitudinal axis. Transl. Psychiatry *9*, 144.

Moran, S.P., Xiang, Z., Doyle, C.A., Maksymetz, J., Lv, X., Faltin, S., Fisher, N.M., Niswender, C.M., Rook, J.M., Lindsley, C.W., and Conn, P.J. (2019). Biased M_1 receptor-positive allosteric modulators reveal role of phospholipase D in M_1-dependent rodent cortical plasticity. Sci. Signal. *12*, eaax2057.

Moy, S.S., Nadler, J.J., Young, N.B., Perez, A., Holloway, L.P., Barbaro, R.P., Barbaro, J.R., Wilson, L.M., Threadgill, D.W., Lauder, J.M., et al. (2007). Mouse behavioral tasks relevant to autism: phenotypes of 10 inbred strains. Behav. Brain Res. *176*, 4–20.

Nelson, R.K., and Frohman, M.A. (2015). Physiological and pathophysiological roles for phospholipase D. J. Lipid Res. *56*, 2229–2237.

Norton, L.J., Zhang, Q., Saqib, K.M., Schrewe, H., Macura, K., Anderson, K.E., Lindsley, C.W., Brown, H.A., Rudge, S.A., and Wakelam, M.J. (2011). PLD1 rather than PLD2 regulates phorbol-ester-, adhesion-dependent and Fcgamma-receptor-stimulated ROS production in neutrophils. J. Cell Sci. *124*, 1973–1983.

Oh, D.Y., Yon, C., Oh, K.J., Lee, K.S., and Han, J.S. (2006). Hippocalcin increases phospholipase D2 expression through extracellular signal-regulated kinase activation and lysophosphatidic acid potentiates the hippocalcin-induced phospholipase D2 expression. J. Cell. Biochem. *97*, 1052–1065.

Oliveira, T.G., and Di Paolo, G. (2010). Phospholipase D in brain function and Alzheimer's disease. Biochim. Biophys. Acta *1801*, 799–805.

Oliveira, T.G., Chan, R.B., Tian, H., Laredo, M., Shui, G., Staniszewski, A., Zhang, H., Wang, L., Kim, T.W., Duff, K.E., et al. (2010). Phospholipase d2 ablation ameliorates Alzheimer's disease-linked synaptic dysfunction and cognitive deficits. J. Neurosci. *30*, 16419–16428.

Oliveira, T.G., Chan, R.B., Bravo, F.V., Miranda, A., Silva, R.R., Zhou, B., Marques, F., Pinto, V., Cerqueira, J.J., Di Paolo, G., and Sousa, N. (2016). The impact of chronic stress on the rat brain lipidome. Mol. Psychiatry *21*, 80–88.

Palmer, C.L., Lim, W., Hastie, P.G., Toward, M., Korolchuk, V.I., Burbidge, S.A., Banting, G., Collingridge, G.L., Isaac, J.T., and Henley, J.M. (2005). Hippocalcin functions as a calcium sensor in hippocampal LTD. Neuron *47*, 487–494.

Pavel, M.A., Petersen, E.N., Wang, H., Lerner, R.A., and Hansen, S.B. (2019). Studies on the mechanism of membrane mediated general anesthesia. bioRxiv. https://doi.org/10.1101/313973.

Peng, J.F., and Rhodes, P.G. (2000). Developmental expression of phospholipase D2 mRNA in rat brain. Int. J. Dev. Neurosci. *18*, 585–589.

Pinto, V., Costa, J.C., Morgado, P., Mota, C., Miranda, A., Bravo, F.V., Oliveira, T.G., Cerqueira, J.J., and Sousa, N. (2015). Differential impact of chronic stress along the hippocampal dorsal-ventral axis. Brain Struct. Funct. *220*, 1205–1212.

Raghu, P., Coessens, E., Manifava, M., Georgiev, P., Pettitt, T., Wood, E., Garcia-Murillas, I., Okkenhaug, H., Trivedi, D., Zhang, Q., et al. (2009). Rhabdomere biogenesis in Drosophila photoreceptors is acutely sensitive to phosphatidic acid levels. J. Cell Biol. *185*, 129–145.

Ramakrishnan, N.A., Drescher, M.J., and Drescher, D.G. (2012). The SNARE complex in neuronal and sensory cells. Mol. Cell. Neurosci. *50*, 58–69.

Sceniak, M.P., Fedder, K.N., Wang, Q., Droubi, S., Babcock, K., Patwardhan, S., Wright-Zornes, J., Pham, L., and Sabo, S.L. (2019). An autism-associated mutation in GluN2B prevents NMDA receptor trafficking and interferes with dendrite growth. J. Cell Sci. *132*, jcs232892.

Scott, S.A., Xiang, Y., Mathews, T.P., Cho, H.P., Myers, D.S., Armstrong, M.D., Tallman, K.A., O'Reilly, M.C., Lindsley, C.W., and Brown, H.A. (2013). Regulation of phospholipase D activity and phosphatidic acid production after purinergic (P2Y6) receptor stimulation. J. Biol. Chem. *288*, 20477–20487.

Selvy, P.E., Lavieri, R.R., Lindsley, C.W., and Brown, H.A. (2011). Phospholipase D: enzymology, functionality, and chemical modulation. Chem. Rev. *111*, 6064–6119.

Shah, S., Lubeck, E., Zhou, W., and Cai, L. (2017). seqFISH Accurately Detects Transcripts in Single Cells and Reveals Robust Spatial Organization in the Hippocampus. Neuron *94*, 752–758.e1.

Stace, C., Manifava, M., Delon, C., Coadwell, J., Cockcroft, S., and Ktistakis, N.T. (2008). PA binding of phosphatidylinositol 4-phosphate 5-kinase. Adv. Enzyme Regul. *48*, 55–72.

Strange, B.A., Witter, M.P., Lein, E.S., and Moser, E.I. (2014). Functional organization of the hippocampal longitudinal axis. Nat. Rev. Neurosci. *15*, 655–669.

Tanguy, E., Wang, Q., Moine, H., and Vitale, N. (2019). Phosphatidic Acid: From Pleiotropic Functions to Neuronal Pathology. Front. Cell. Neurosci. *13*, 2.

Thompson, P.M., Egbufoama, S., and Vawter, M.P. (2003). SNAP-25 reduction in the hippocampus of patients with schizophrenia. Prog. Neuropsychopharmacol. Biol. Psychiatry *27*, 411–417.

Thompson, C.L., Pathak, S.D., Jeromin, A., Ng, L.L., MacPherson, C.R., Mortrud, M.T., Cusick, A., Riley, Z.L., Sunkin, S.M., Bernard, A., et al. (2008). Genomic anatomy of the hippocampus. Neuron *60*, 1010–1021.

Ueno, N., Murakami, M., and Kudo, I. (2000). Functional crosstalk between phospholipase D(2) and signaling phospholipase A(2)/cyclooxygenase-2-mediated prostaglandin biosynthetic pathways. FEBS Lett. *475*, 242–246.

Unoki, T., Matsuda, S., Kakegawa, W., Van, N.T., Kohda, K., Suzuki, A., Funakoshi, Y., Hasegawa, H., Yuzaki, M., and Kanaho, Y. (2012). NMDA receptor-mediated PIP5K activation to produce $PI(4,5)P_2$ is essential for AMPA receptor endocytosis during LTD. Neuron *73*, 135–148.

Vermeren, M.M., Zhang, Q., Smethurst, E., Segonds-Pichon, A., Schrewe, H., and Wakelam, M.J. (2016). The Phospholipase D2 Knock Out Mouse Has Ectopic Purkinje Cells and Suffers from Early Adult-Onset Anosmia. PLoS One *11*, e0162814.

Vorhees, C.V., and Williams, M.T. (2006). Morris water maze: procedures for assessing spatial and related forms of learning and memory. Nat. Protoc. *1*, 848–858.

Walf, A.A., and Frye, C.A. (2007). The use of the elevated plus maze as an assay of anxiety-related behavior in rodents. Nat. Protoc. *2*, 322–328.

Wang, X.Y., Zhou, H.R., Wang, S., Liu, C.Y., Qin, G.C., Fu, Q.Q., Zhou, J.Y., and Chen, L.X. (2018). NR2B-Tyr phosphorylation regulates synaptic plasticity in central sensitization in a chronic migraine rat model. J. Headache Pain *19*, 102.

Zeniou-Meyer, M., Zabari, N., Ashery, U., Chasserot-Golaz, S., Haeberlé, A.M., Demais, V., Bailly, Y., Gottfried, I., Nakanishi, H., Neiman, A.M., et al. (2007). Phospholipase D1 production of phosphatidic acid at the plasma membrane promotes exocytosis of large dense-core granules at a late stage. J. Biol. Chem. *282*, 21746–21757.

Zhang, X.L., Upreti, C., and Stanton, P.K. (2011). $G\beta\gamma$ and the C terminus of SNAP-25 are necessary for long-term depression of transmitter release. PLoS One *6*, e20500.

Zhao, D., Berse, B., Holler, T., Cermak, J.M., and Blusztajn, J.K. (1998). Developmental changes in phospholipase D activity and mRNA levels in rat brain. Brain Res. Dev. Brain Res. *109*, 121–127.

Zhou, W., Zhang, L., Guoxiang, X., Mojsilovic-Petrovic, J., Takamaya, K., Sattler, R., Huganir, R., and Kalb, R. (2008). GluR1 controls dendrite growth through its binding partner, SAP97. J. Neurosci. *28*, 10220–10233.

Zhu, Y.B., Kang, K., Zhang, Y., Qi, C., Li, G., Yin, D.M., and Wang, Y. (2012). PLD1 Negatively Regulates Dendritic Branching. J. Neurosci. *32*, 7960–7969.

Zhu, Y.B., Gao, W., Zhang, Y., Jia, F., Zhang, H.L., Liu, Y.Z., Sun, X.F., Yin, Y., and Yin, D.M. (2016). Astrocyte-derived phosphatidic acid promotes dendritic branching. Sci. Rep. *6*, 21096.

Ziegler, A.B., and Tavosanis, G. (2019). Glycerophospholipids - Emerging players in neuronal dendrite branching and outgrowth. Dev. Biol. *451*, 25–34.

STAR★METHODS

KEY RESOURCES TABLE

REAGENT or RESOURCE	SOURCE	IDENTIFIER
Antibodies		
Alpha-Tubulin (Figure 1)	Sigma-Aldrich	Cat# T5168, RRID:AB_477579
Alpha-Tubulin (Figure 5)	Sigma-Aldrich	Cat#T6074, RRID:AB_477582
GAPDH	Cell Signaling Technology	Cat# 2118, RRID:AB_561053
Phospholipase D	Made in house; Provided by Sung Ho Ryu (Pohang University of Science and Technology)	N/A
Phospholipase D1	Cell Signaling Technology	Cat# 3832, RRID:AB_2172256
Phospholipase D2 (N-term)	Abgent	Cat# AP14669a, RRID:AB_11135353
Synaptophysin 1	Synaptic Systems	Cat# 101 002, RRID:AB_887905
SNAP-25	Abcam	Cat# ab5666, RRID:AB_305033
PSD95	Abcam	Cat# ab2723, RRID:AB_303248
Homer	Abcam	Cat# ab184955, RRID:AB_2744679
GluA1 / GluR1	Millipore	Cat# AB1504, RRID:AB_2113602
GluA2 / GluR2	Abcam	Cat# ab133477, RRID:AB_2620181
GluN2A / NR2A	Millipore	Cat# AB1555P, RRID:AB_90770
GluN2B / NR2B	Abcam	Cat# ab65783, RRID:AB_1658870
pY1472-GluN2B / -NR2B	Abcam	Cat# ab3856, RRID:AB_304114
Syntaxin-1A	Synaptic Systems	Cat# 110 302, RRID:AB_887846
Synaptobrevin-2	Synaptic Systems	Cat# 104 202, RRID:AB_887810
Goat Anti-rabbit IgG	Bio-Rad	Cat# 170-6515, RRID:AB_11125142
Goat Anti-mouse IgG	Bio-Rad	Cat# 170-6516, RRID:AB_11125547
Chemicals, Peptides, and Recombinant Proteins		
cOmplete, Mini, EDTA-free Protease Inhibitor Cocktail	Roche	Cat#11836170001
Phosphatase Inhibitor Cocktail 2	Sigma-Aldrich	Cat#P5726
Phosphatase Inhibitor Cocktail 3	Sigma-Aldrich	Cat#P0044
NuPAGE Sample Reducing Agent	Invitrogen	Cat#NP0009
NuPAGE LDS Sample Buffer	Invitrogen	Cat#NP0007
NuPAGE 4-12% Bis-Tris Protein Gels	Invitrogen	Cat#NP0322
NuPAGE MES SDS Running Buffer	Invitrogen	Cat#NP0002
Amersham Protran Premium 0.45 NC nitrocellulose western blotting membranes	GE Healthcare Life Sciences	Cat# GE10600008
Clarity Western ECL Substrate	Bio-Rad	Cat#1705060
SuperSignal West Femto Maximum Sensitivity Substrate	ThermoFisher Scientific	Cat#34095
TRIzol reagent	Life Technologies, Thermo Fisher Scientific	Cat# 15596018
Critical Commercial Assays		
Pierce BCA protein assay	ThermoFisher Scientific	Cat#23225
iScript cDNA Synthesis Kit	Bio-Rad	Cat#1708891
HOT FIREPol EvaGreen qPCR Mix Plus (ROX) Kit	Solys Biodine	Cat# 08-24-00020
Experimental Models: Organisms/Strains		
Mouse: Pld1$^{tm1.1Gdp}$/J	Provided by Gilbert Di Paolo (Columbia University)	Available at Jackson laboratory Cat#028665; RRID:IMSR_JAX:028665
Mouse: B6.Cg-$^{Pld2tm1.1Gdp}$/J	Provided by Gilbert Di Paolo (Columbia University)	Available at Jackson laboratory Cat#028668; RRID:IMSR_JAX:028668

(*Continued on next page*)

Continued

REAGENT or RESOURCE	SOURCE	IDENTIFIER
Oligonucleotides		
Primer for qRT-PCR: Phospholipase D1 (*PLD1*) - Forward (5′→3′): CATCGACAGCACCTCCAAC	Stab Vida	N/A
Primer for qRT-PCR: Phospholipase D1 (*PLD1*) - Reverse (5′→3′): GAGTTCTCCCACTCCGGTCT	Stab Vida	N/A
Primer for qRT-PCR: Phospholipase D2 (*PLD2*) - Forward (5′→3′): TGGGTGACCCCTCTGAACCTGT	Stab Vida	N/A
Primer for qRT-PCR: Phospholipase D2 (*PLD2*) - Reverse (5′→3′): GTCCAGCTGCACCCAGTCCTT	Stab Vida	N/A
Primer for qRT-PCR: Heat Shock Protein 90 alpha family class B member 1 (*Hsp90ab1*) - Forward (5′→3′): GCTGGCTGAGGACAAGGAGA	Stab Vida	N/A
Primer for qRT-PCR: Heat Shock Protein 90 alpha family class B member 1 (*Hsp90ab1*) - Reverse (5′→3′): CGTCGGTTAGTGGAATCTTCATG	Stab Vida	N/A
Software and Algorithms		
ImageJ	NIH	RRID:SCR_003070
Prism	Graphpad	RRID:SCR_002798
MED-PC IV	Med Associates Inc.	N/A
Neurolucida software	MBF Bioscience	RRID:SCR_001775
NeuroExplorer software	MBF Bioscience	N/A
WinLTP software	WinLTP Ltd. and The University of Bristol	RRID:SCR_008590
Primer Blast	NCBI	RRID:SCR_003095
7500 Real-Time PCR Software	Applied Biosystems	RRID:SCR_014596

LEAD CONTACT AND MATERIALS AVAILABILITY

Further information and requests for resources and reagents should be directed to and will be fulfilled by the Lead Contact, Tiago Gil Oliveira (tiago@med.uminho.pt). This study did not generate new unique reagents.

EXPERIMENTAL MODEL AND SUBJECT DETAILS

Pld1$^{-/-}$ mice were originally generated through the removal of exons 13 (that codes for the first HKD motif for PLD1) and 14, using a Cre-lox/FLP-FRT recombination system, as previously described (Dall'Armi et al., 2010). Using the same system, *Pld2*$^{-/-}$ mice were produced as a result of the elimination of exons 13-15, including exon 14 (that encodes for the first HKD motif of PLD2 as well), as shown before (Oliveira et al., 2010). The animals had C57BL/6 background with exception of the animals used in the experiments of Figures 1A and 1B that had mixed background (C57BL/6-129svj). Littermate mice were used in all experiments, except for experiments of Figures 1A and 1B. For the generation of *Pld1*$^{-/-}$ / *Pld2*$^{-/-}$ (DKO) mice, *Pld1*$^{-/-}$ animals were crossed with *Pld2*$^{-/-}$ animals. All experimental procedures were performed in compliance with the Portuguese authority for animal experimentation, *Direção Geral de Alimentação e Veterinária* (DGAV), the Directive 2010/63/EU guidelines and approved by the local committee. All mice had *ad libitum* access to water and food and maintained on a 12h light/dark cycle. All the procedures were performed during daytime, except for the social discrimination, sociability and preference for social novelty behavioral tests. Before all behavioral tests, animals were placed in the testing room one hour prior to testing, so they could acclimatize. The arenas and apparatus were cleaned with a 10% ethanol solution between testing subjects. 3-4 months male and female mice were used in all tests, except for western blot analysis (3-6 months), fear conditioning (males 3-7 months old) and social discrimination, sociability and preference for social novelty tests (males 3-6 months).

METHOD DETAILS

Western Blot

Animals were sacrificed by cervical dislocation and forebrain or the hippocampus were dissected. Hippocampi were divided in approximately three equal dorsal, intermediate and ventral parts. Samples were diluted in radioimmunoprecipitation assay buffer

(RIPA) containing 150 nM NaCl, 1.0% Triton X-100, 0.5% sodium deoxycholate, 0.1% SDS, 50 mM TrisBase pH = 8 and supplemented with protease (Roche) and phosphatase inhibitor cocktails (Sigma-Aldrich). After homogenization, samples were mixed in a rotator at 4°C for 2 hours at 40rpm and then centrifuged at 4°C for 20 minutes at 14000rpm. Supernatants were quantified (BCA, Pierce) and samples diluted to equal concentration in RIPA. Samples were prepared with NuPAGE LDS sample buffer and NuPAGE reducing reagent and loaded in NuPAGE 4%–12% Bis–Tris gels. MES SDS running buffer (NuPAGE) was used for separation. Wet transfer used 50% running buffer, 20% methanol and 30% deionized water and was made on 0.45μm nitrocellulose membranes (Amersham) for 2 hours at 100V. Membrane blockage was performed with 5% dried milk (Nestle) for 1 hour at room temperature. Incubation with primary antibodies, diluted in 2.5% dried milk or bovine serum albumin (BSA), was performed overnight at 4°C and incubation with HRP-conjugated secondary antibodies, diluted in 2.5% dried milk or BSA, was performed for 1 hour at room temperature. Chemiluminescence signal was detected with ChemiDoc XRS+ (Bio-Rad) and membrane development was achieved with Clarity Western ECL Substrate (Bio-Rad) or SuperSignal West Femto Maximum Sensitivity Substrate (ThermoScientific). Quantification was performed with ImageJ software. Primary antibodies used were: α-Tubulin (T5168, Sigma-Aldrich 1:10000) – Figure 1A; α-Tubulin (T6074, Sigma-Aldrich, 1:10000); GAPDH (Cell Signaling Technology, 1:3000); Antibody to the COOH terminus of PLD (kind gift of Dr. Sung Ho Ryu, Pohang University of Science and Technology; 1:200); PLD1 (Cell Signaling Technology, 1:500); PLD2 (Abgent, 1:500), Synaptophysin (Synaptic Systems, 1:5000); SNAP-25 (Abcam, 1:5000); PSD95 (Abcam, 1:5000); Homer (Abcam, 1:3000); GluA1/GluR1 (Millipore, 1:1000); GluA2/GluR2 (Abcam, 1:1000); GluN2A/NR2A (Millipore, 1:1000); GluN2B/NR2B (Abcam, 1:1000), pY1472-GluN2B/NR2B (Abcam, 1:1000), Syntaxin-1A (Synaptic Systems, 1:1000) and Synaptobrevin-2 (Synaptic Systems, 1:4000). HRP-conjugated secondary antibodies used were: Goat Anti-rabbit IgG (BioRad) and Goat Anti-mouse IgG (BioRad).

In vivo PLD activity

In the presence of primary alcohols, PLD utilizes preferentially short-chain alcohols as substrates resulting in the formation of the corresponding phosphatidylalcohol. This property was used to measure PLD activity. Mice were injected intraperitoneally with 3g/kg ethanol and sacrificed 1 hour postinjection, as previously described (Oliveira et al., 2010). Briefly, lipid extracts were prepared from mice whole forebrain using a modified Bligh and Dyer method (described below). The levels of PEtOH produced via a PLD-specific transphosphatidylation reaction were measured by LC-MS analysis (described below) and used as an indicator of *in vivo* PLD activity. Individual lipid species from *Pld1* KO, *Pld2* KO and *Pld* DKO mice were compared with wild-type (WT) mice. Phosphatydilethanolamine (PE) measurements were used as reference levels.

Lipid Analysis

Lipids were extracted using a modified Bligh and Dyer method (Bligh and Dyer, 1959) and lipid analysis performed as previously described (Chan et al., 2012; Miranda et al., 2019). Briefly, samples were homogenenized in a solution of methanol:chloroform (2:1) and lipids extracted with a solution of chloroform:KCl (3:2, 1 M). Samples were centrifuged at 4°C for 2 minutes at 9000rpm and the bottom phase (organic) was dried under vacuum nitrogen and stored at −80°C. Lipid extracts of purified microsome were spiked with a cocktail of internal standards and analyzed using a 6490 Triple Quadrupole LC/MS system (Agilent Technologies). Glycerophospholipids and sphingolipids were separated with normal-phase HPLC as described before (Chan et al., 2012), with a few modifications. An Agilent Zorbax Rx-Sil column (inner diameter 2.1 × 100 mm) was used under the following conditions: mobile phase A (chloroform:methanol:1 M ammonium hydroxide, 89.9:10:0.1, v/v) and mobile phase B (chloroform:methanol:water:ammonium hydroxide, 55:39.9:5:0.1, v/v); 95% A for 2 min, linear gradient to 30% A over 18 min and held for 3 min, and linear gradient to 95% A over 2 min and held for 6 min. Quantification of lipid species was accomplished using multiple reaction monitoring (MRM) transitions and instrument settings that were determined in earlier studies (Chan et al., 2012) in conjunction with referencing of known amounts of internal standards: PA 14:0/14:0, PC 14:0/14:0, PE 14:0/14:0, PI 12:0/13:0, PS 14:0/14:0, SM d18:1/12:0, (Avanti Polar Lipids). Nomenclature abbreviations are FC, free cholesterol; CE, cholesteryl ester; AC, acyl carnitine; MG, monoacylglycerol; DG, diacylglycerol; TG, triacylglycerol; Cer, ceramide; dhCer, dihydroceramide; SM, sphingomyelin; dhSM, dihydrosphingomyelin; MhCer, monohexosylceramide; Sulf, sulfatides; LacCer, lactosylceramide; GM3, monosialodihexosylganglioside; PA, phosphatidic acid; PC, phosphatidylcholine; PCe, ether phosphatidylcholine; PE, phosphatidylethanolamine; PEp, plasmalogen phosphatidylethanolamine; PS, phosphatidylserine; PI, phosphatidylinositol; PG, phosphatidylglycerol; BMP, bis (monoacylglycero)phosphate; LPC, lysophosphatidylcholine; LPCe, ether lysophosphatidylcholine; LPE, lysophosphatidylethanolamine; LPI, lysophosphatidylinositol; LPS, lysophosphatidylserine; NAPS, N-acyl phosphatidylserine; NSer, N-acyl serine.

Behavioral testing

Open Field

The OF test was used to measure motor and exploratory activity, as well as anxious-like behaviors. A square arena, delimited by transparent high walls (43.2 × 43.2 × 30.5 cm) was used, associated to an infrared detection system and a computer interface (ENV-515; MedAssociates). Mice were individually placed in the center of the arena and freely explored it for 5 minutes. The central area was defined as 25% of the total arena and the time spent in the center and periphery was calculated.

Elevated Plus Maze

Anxious behavior was specifically evaluated through the EPM test, as previously described (Walf and Frye, 2007). The plus shape apparatus was elevated 72.4 cm above the floor and consisted of two opposite open arms and two enclosed arms (50.8 cm × 10.2 cm each) (ENV-560; MedAssociates). Mice were placed individually in the center of the maze and allowed to explore for 5 minutes. An infrared detection system connected to a computer interface was used to record and automatically quantify time on each arm. The test was performed under bright light (in a dim lighted room).

Fear Conditioning

The FC protocol was performed to test contextual and cued memory. Standard operant chambers (Med Associates Inc.) (22 × 19 × 12.5 cm) with a grid on the bottom where shocks were transmitted was used, except for day 3. On the first day (fear acquisition) the subject mice was placed in the arena and allowed to explore for 5 minutes. Then a tone (80 dB) was presented for 30 s and in the last second a mild shock (0.5 mA for 1 s) was given. This was repeated for 5 blocks, with an interval of 30 s between then. On the second day the subject mice was only placed in the arena and allowed to explore for 5 minutes in order to evaluate the contextual fear conditioning. On the third day the subject mice was placed in a different arena (24 × 32 × 18.5 cm) and allowed to explore for 5 minutes. Then 5 blocks of 30 s of tone and 30 s of interval were given. This allowed cued fear conditioning evaluation. For the next 5 days an extinction protocol was performed by placing the animal in the arena and giving 15 blocks of 30 s of tone followed by 30 s of interval. 30 days after the last day of extinction spontaneous recovery was evaluated. Mice were placed in the arena and allowed to explore for 5 minutes. Then 5 blocks of 30 s of tone followed by 30 s of interval were presented. Animals were video-recorded and the percentage of freezing behavior was analyzed. All stimulation procedures were done through Med-PC IV (Med Associates Inc.) software, except for the shock that was manually given.

Morris Water Maze

The MWM test was performed to assess spatial learning and reference memory as previously described (Vorhees and Williams, 2006). A circular pool (116 cm of diameter) containing tap water was used (22 ± 1°C; 25 cm of depth) and made opaque by adding titanium oxide powder (Sigma Aldrich). The pool was divided into four imaginary quadrants and a transparent escape platform (11 cm of diameter; 24 cm high), invisible to the animals (submerged 1-2 cm below the water surface), was placed in the center of one of the quadrants. The test consisted of 5 days of acquisition plus one day for reference memory assessment, and 2 days of visual cueing. In the first 5 days mice learned to find the platform, kept in a constant position. A total of 4 trials (of a maximum of 60 s) were achieved per day, and animals were placed in different starting positions everyday. Mice had to locate the hidden platform based on distant cues distributed along the testing room walls. Animals that failed to find the platform within the trial period were gently guided to the platform and an escape latency of 60 s was registered. All mice were allowed to stay in the platform for 30 s on the first 2 days and 15 s on the subsequent 3 days during the inter-trial interval. On the 6th day a probe trial was performed (for 30 s) in which the platform was removed and the entry point was set to the quadrant opposite to the target quadrant. Visual cueing, used to detect the presence of visual and/or motivational impairments, was assessed for 2 days for which the platform was made visible by the addition of a flag and changed in location for the different trials. Time spent in each quadrant and escape latency were monitored and recorded using a video-tracking system connected to a computer (Viewpoint, Champagne-au-Mont-d'Or), to be used as readouts of task performance. Testing was conducted under dim light.

Novel Object Recognition

Since rodents are naturally exploratory and prefer to explore novelty, the NOR test was performed to evaluate recognition memory as previously described (Leger et al., 2013). The test was performed in a 30 × 30 × 30 cm arena under dimmed light and consisted of 3 days of habituation (where the animals were placed in the arena for 20 minutes) and 1 day of testing. The test was divided in two stages. First, the animal was presented with two equal objects for 10 minutes (training) and in the second phase was exposed for 5 minutes to a novel object and one of the previously examined objects. We used 1-hour interval between the two phases to assess short-term memory, in which the subject returned to its original cage. Behavior was video-recorded and time spent exploring each object was posteriorly manually scored. The discrimination ratio was calculated by dividing the time spent exploring the novel object by time spent exploring both objects.

Three-chamber Social Discrimination and Three-chamber Sociability and Preference for Social Novelty

These tests were adapted from previously described protocols (Meira et al., 2018; Moy et al., 2007) and performed on a transparent rectangular arena (56 cm long x 50 cm wide x 39 cm high) divided in three equal chambers with openings that allowed access into each chamber. The tests consisted of 10-minute trials, where the subject mice were allowed to explore the arena. After this time, when the animal stopped in the center arena, the access to the other chambers was blocked with two doors to switch trials.

The social discrimination test consisted of three trials. In the first habituation trial, mice were individually placed in the center of the arena and freely explore. In the second habituation trial, two empty round wire cups (9.8 cm high, with a bottom diameter of 8 cm and several horizontal opened bars spaced 3.7 × 0.5 cm apart which allowed nose contact between the bars) were placed on the side chambers and the subject mice freely explored the arena. In the third trial, a co-housed littermate and an unfamiliar male stranger with no prior contact with the tested mouse were each placed inside one of the wire cups. The location of the stranger and the littermate mouse was systematically alternated between mice.

The sociability and preference for social novelty test consisted of four trials. The first and second trials were similar to the ones previously described. In the third trial, an unfamiliar male mice (stranger 1), which had no prior contact with the subject mice, was placed inside one of the cups to test sociability of the subject mice. In the fourth trial, a second stranger male mice (stranger 2)

was enclosed in the previously empty cup and preference for social novelty was assessed. The location of the strangers was systematically alternated between mice. Measures were taken of the amount of time spent interacting with each cup were manually scored. Social discrimination, social preference and preference for social novelty scores were calculated as the difference between the time spent exploring the cups placed on the side chambers, divided by the total time exploring both. Testing was conducted under red light.

Dendritic Arborization

To evaluate the morphological reconstruction of hippocampal CA1 and CA3 pyramidal neurons and DG granular cells, Golgi-Cox impregnation was used according to a protocol proposed by others (Gibb and Kolb, 1998), with slight modifications. Briefly, after cervical dislocation, brains were immersed in Golgi-Cox solution (1:1 solution of 5% $K_2C_{r2}O_7$ and 5% $HgCl_2$ diluted 4:10 with 5% K_2CrO_4) and stored in the dark for 14 days, with daily agitation. Brains were then transferred to a 30% sucrose solution and stored in the dark at 4°C for at least 5 days. Coronal sections (200 μm) were obtained using a vibratome and mounted in slides that were submerged in a 28% ammonia solution, developed and fixed using Kodak Fixer (Sigma Aldrich), dehydrated and subsequently embedded in a solution containing absolute ethanol (1:3), chloroform (1:3) and xylene (1:3). Finally, samples were cleared in xylene, mounted and coverslipped. Neuronal three-dimensional reconstructions were achieved at 600x magnification using a motorized microscope (BX51, Olympus), attached to a camera (MicroBrightField Bioscience), and Neurolucida software (MicroBrightField Bioscience). 5-6 neurons were analyzed per sub-region and for each animal. The three-dimensional evaluation of the reconstructed neurons was performed using NeuroExplorer software (MicroBrightField Bioscience), and the parameters assessed included total dendritic length, total number of nodes and spine density (total spines divided by dendritic length).

Electrophysiology

Electrophysiological recordings were performed as described elsewhere (Pinto et al., 2015). The animals were anesthetized by intraperitoneal injection of Na^+-pentobarbital (40mg/kg) and decapitated. The brain was rapidly removed and placed in ice-cold sucrose-based solution containing the following (in mM): 2.5 KCl, 7 $MgCl_2$, 1.25 NaH_2PO_4, 110 sucrose, 26 $NaHCO_3$, 10 glucose, bubbled with carbogen gas (95% O_2, 5% CO_2). Slices (300 μm) transverse to the axis of the hippocampus were cut using a tissue slicer (Leica VT 1200s) and placed in a container with artificial cerebrospinal fluid (ACSF) containing (in mM): 124 NaCl, 2.5 KCl, 1 $MgSO_4$, 2 $CaCl_2$, 1.25 NaH_2PO_4, 26 $NaHCO_3$, 10 glucose, bubbled with carbogen gas and maintained at 33°C for 30 minutes. Slices were then stored at room temperature for a minimum of 30 minutes before recording. Extracellular recordings were performed in a submerge-type chamber bathed with ACSF at 31°C. A custom-made bipolar tungsten stimulation electrode was placed in the transition between CA1 and CA3, at the Schaffer collaterals, and a recording borosilicate glass pipette filled with ACSF (3-5 MΩ) was positioned in the middle of the stratum radiatum of CA1 at a predetermined fixed distance of approximately 1mm apart the stimulation electrode. Recordings were digitized with a Multiclamp 700B amplifier (Axon Instruments). Signals were low-pass filtered at 3 kHz and sampled at 10 kHz. Stimulation strength was adjusted to 30%–50% of the maximum field excitatory post synaptic potential (fEPSP) slope, after a fixed protocol of 4 increasing stimulus (2000-8000mV) was applied (input-output relationship). Before baseline acquisition, a series of paired pulse stimuli of varying interpulse interval (25, 50, 100 and 300ms) were given. The paired pulse (PP) ratio was calculated by dividing the slope of fEPSP2 by fEPSP1. A minimum of 10 minute stable baseline recordings were acquired at 0.03 Hz. LTD was elicited by delivering a low-frequency stimulation protocol consisting of 15 min 1 Hz stimulation. LTP was elicited by delivering 3 θ-burst stimuli (θ-burst: 100 Hz burst of four pulses repeated at 5 Hz with each tetanus including 10-burst trains) separated by 15 s intervals. All stored curves were an average of four consecutive recordings. Maximum EPSP slopes were calculated offline using the WinLTP software. For LTP and LTD analysis, all individual slopes were normalized to the average slope of baseline recordings. Averages of the slopes of the last 4 min recordings were used for comparison in LTP and LTD.

Gene expression analysis by qRT-PCR

Total RNA was extracted from the hippocampus using TRIzol reagent (Life Technologies, Thermo Fisher Scientific) according to the manufacturer's instructions. Then, after quantification in the NanoDrop (Thermo Fisher Scientific), 500 ng of total RNA from each sample was reverse transcribed into cDNA using the iScript cDNA Synthesis Kit (Bio-Rad) following the manufacturer's instructions. Primers used to measure the expression levels of selected mRNA transcripts by qRT-PCR were designed using the Primer-BLAST tool of the National Center for Biotechnology Information (Bethesda, MD) on the basis of the respective GenBank accession numbers. Primer DNA sequences are provided in STAR Methods. qRT-PCR was performed on a 7500 Real-Time PCR system thermocycler (Applied biosystems) and quantifications were performed in a Fast Real-Time PCR software (Applied Biosystems), with the commercial kit HOT FIREPol EvaGreen qPCR Mix Plus (ROX) (Solis Biodyne), according to the manufacturer's instructions, using equal amounts of cDNA from each sample. The cycling parameters were 1 cycle at 95°C, for 1 min, followed by 40 cycles at 95°C for 15 s, annealing temperature (primer specific) for 20 s and 72°C for 20 s, finishing with 1 cycle at 65°C to 95°C for 5 s (melting curve). Product fluorescence was detected at the end of the elongation cycle. All melting curves exhibited a single sharp peak at the expected temperature. Heat Shock Protein 90 alpha family class B member 1 (*Hsp90ab1*) was used as reference gene.

QUANTIFICATION AND STATISTICAL ANALYSIS

Western blot analysis was performed using ImageJ (NIH). The statistical analysis was performed using GraphPad Prism 7.00 software. Statistical significance was assessed by one-way ANOVA, two-way ANOVA and Student's t test, and referenced in figure legends whenever used. Values were accepted as significant when $p < 0.05$. *$p < 0.05$, **$p < 0.01$, ***$p < 0.001$. Number of mice for all statistical analyses is indicated in each legend. Values are expressed as mean ± SEM.

DATA AND CODE AVAILABILITY

This study did not generate any unique datasets or code.

CHAPTER 2 – Supplementary Information

Phospholipase D1 Ablation Disrupts Mouse Longitudinal Hippocampal Axis Organization and Functioning

Cell Reports, Volume *30*

Supplemental Information

Phospholipase D1 Ablation Disrupts Mouse Longitudinal Hippocampal Axis Organization and Functioning

Luísa Santa-Marinha, Isabel Castanho, Rita Ribeiro Silva, Francisca Vaz Bravo, André Miguel Miranda, Torcato Meira, Rafaela Morais-Ribeiro, Fernanda Marques, Yimeng Xu, Kimberly Point du Jour, Markus Wenk, Robin Barry Chan, Gilbert Di Paolo, Vítor Pinto, and Tiago Gil Oliveira

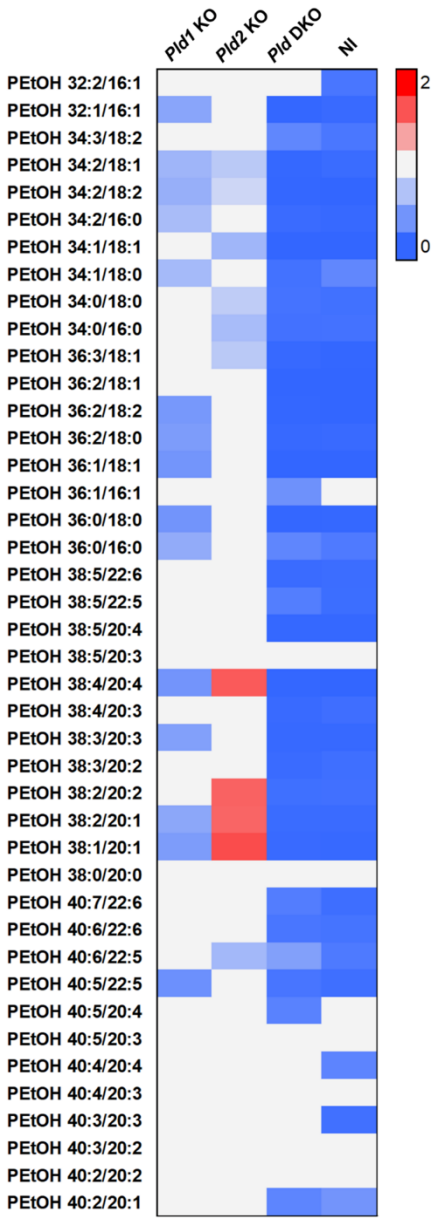

Figure S1. PEtOH species in PLD enzymatic activity assessment. Related to Figure 1.

Mice were injected with ethanol. Their forebrains were extracted and the levels of PEtOH were measured by LC-MS analysis and used as an indicator of *in vivo* PLD activity. Individual lipid species were compared with corresponding WT mice ($n_{Pld\ WT}$=6, $n_{Pld1\ KO}$=6, $n_{Pld2\ KO}$=6, $n_{Pld\ DKO}$=6, $n_{Pld\ WT\ NI}$=5). Values are represented in gradient color, blue indicates below one and red indicates above onefold-change, respectively, normalized to WT mice. dKO – *Pld* double KO; NI – WT non injected; PEtOH – Phosphatidylethanol.

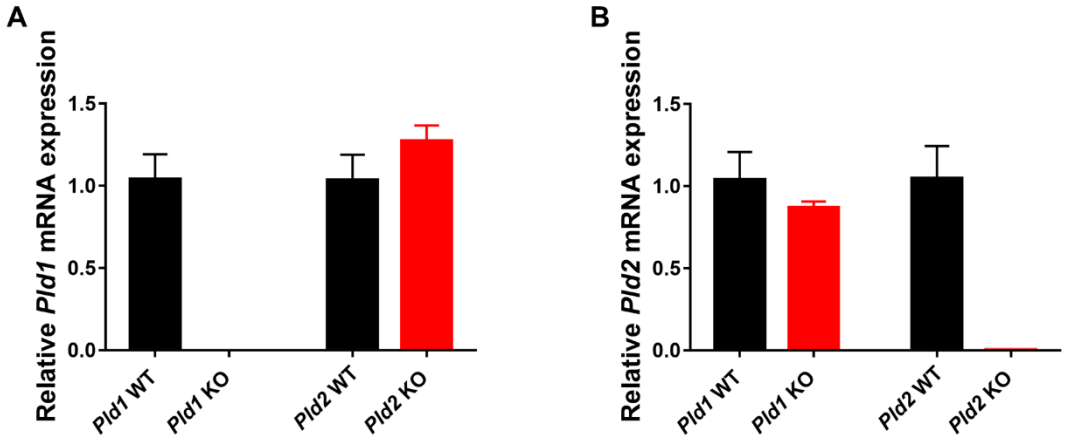

Figure S2. No compensation at mRNA levels upon PLD1 or PLD2 ablation. Related to Figure 1.

Relative mRNA expression of *Pld1* (A) and *Pld2* (B) in *Pld1* and *Pld2* WT and KO mice total hippocampus ($n_{Pld1\ WT}$=4, $n_{Pld1\ KO}$=4, $n_{Pld2\ WT}$=4, $n_{Pld2\ KO}$=4). The ablation of one isoenzyme has no impact on the mRNA levels of the other isoenzyme. The relative abundance of each gene of interest was calculated on the basis of the Delta Delta Ct method and the results normalized to one housekeeping gene (*Hsp90ab1*). The bars represent mean ± SEM.

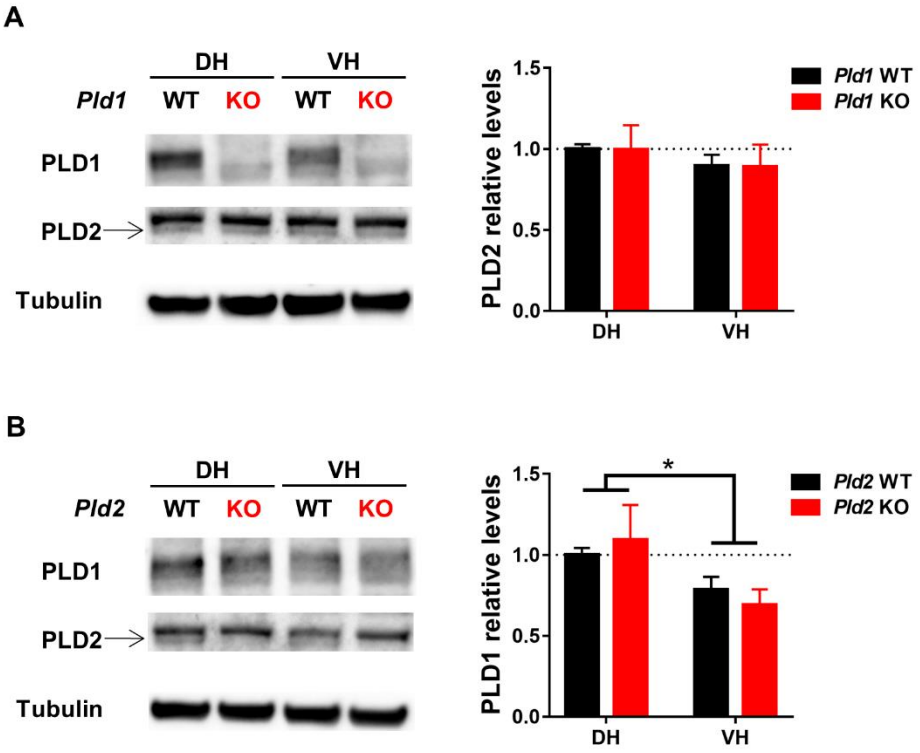

Figure S3. No compensation at protein levels upon PLD1 or PLD2 ablation. Related to Figure 1.

Protein levels of DH and VH in *Pld1* (A) and *Pld2* (B) WT and KO animals were evaluated by Western blot analysis and quantified by densitometric analysis (n =4-5). The ablation of one isoenzyme has no impact on the protein levels of the other isoenzyme. Moreover, the levels of PLD1 are higher in the DH when compared to the VH (B) (two-way ANOVA: Interaction $F(1, 16) = 0.5613$, $p = 0.4646$; DH/VH $F(1, 16) = 5.921$, $p = 0.0271$). The bars represent mean ± SEM.

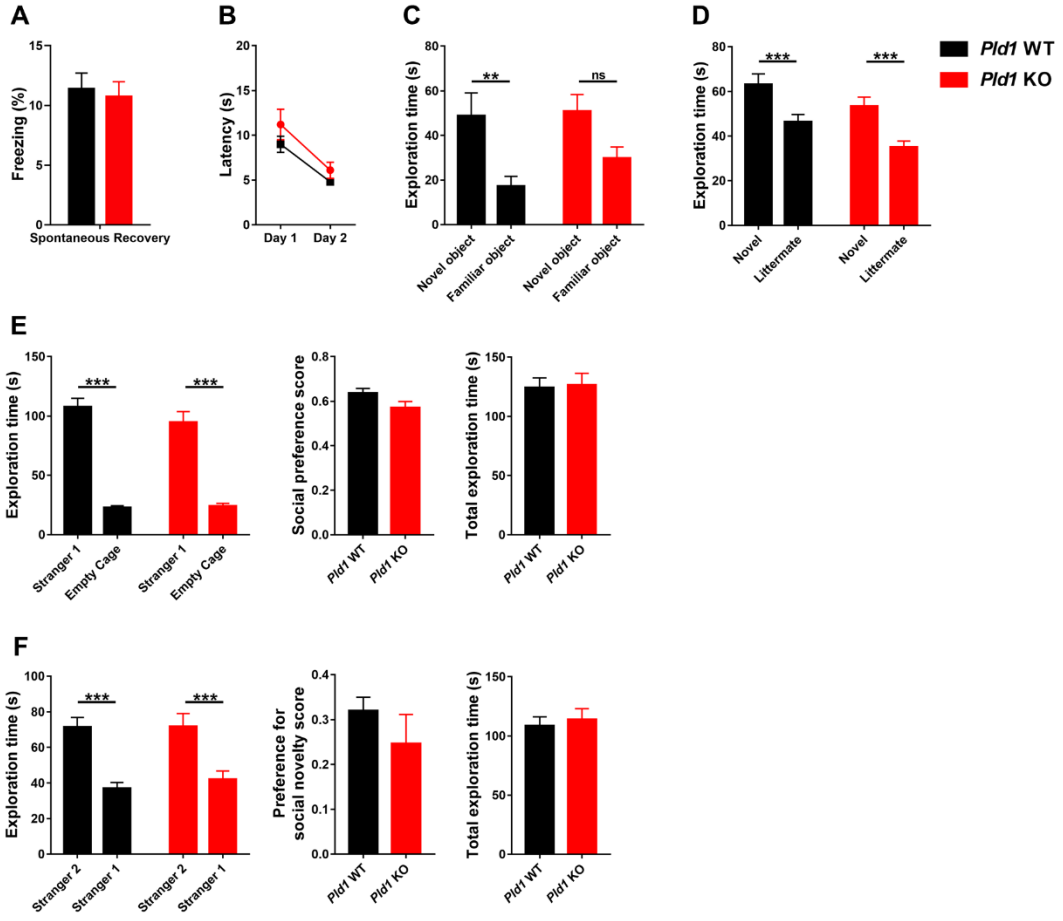

Figure S4. Supplementar behavior analysis. Related to Figure 2.

(A) PLD1 ablation does not impair spontaneous recovery 30 days after FC protocol (n_{WT}=8, n_{KO}=11).

(B) PLD1 ablation has no impact in cued learning evaluated with MWM test (n_{WT}=23, n_{KO}=20).

(C) PLD1 ablation leads to a deficit in object-recognition related short-term memory (two-way ANOVA: Interaction $F(1, 58) = 0.5313$, $p = 0.4690$; familiar/novel $F(1, 58) = 13.09$, $p = 0.0006$; WT: $p = 0.0056$; KO: $p = 0.0957$, Sidak's multiple comparisons test) (n_{WT}=16, n_{KO}=15).

(D) PLD1 ablation does not affect the ability to distinguish between a littermate and a stranger mice (two-way ANOVA: Interaction $F(1, 37) = 0.0659$, $p = 0.7988$; Exploration time $F(1, 37) = 31.7$, $p < 0.0001$; littermate/stranger WT: $p = 0.0009$; KO: $p = 0.0004$, Sidak's multiple comparisons test).

(E) PLD1 ablation has no impact on social preference (two-way ANOVA: Interaction $F(1, 43) = 1.912$, $p = 0.1739$; Exploration time $F(1, 43) = 223$, $p < 0.0001$; stranger 1/empty cage WT: $p < 0.0001$; KO: $p < 0.0001$, Sidak's multiple comparisons test).

(F) PLD1 ablation has no impact on preference for social novelty (two-way ANOVA: Interaction $F(1, 43) = 0.2841$, $p = 0.5967$; Exploration time $F(1, 43) = 51.88$, $p < 0.0001$; stranger 2/stranger 1 WT: $p < 0.0001$; KO: $p < 0.0001$, Sidak's multiple comparisons test) (n_{WT}=23, n_{KO}=22). Social preference and preference for social novelty scores were calculated as the difference between the time spent exploring the cups placed on the side chambers, divided by the total time exploring both. Bars represent mean ± SEM. (*$p < 0.05$, **$p < 0.01$, and ***$p < 0.001$).

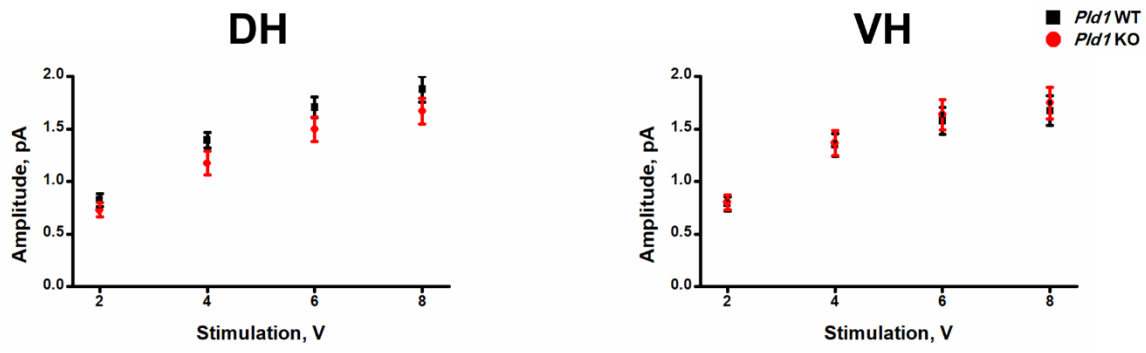

Figure S5. PLD1 ablation has no effect in input-output recordings. Related to Figure 4.

Crescent stimuli were given in acute slides of DH (n_{WT}=18, n_{KO}=17) and VH (n_{WT}=15, n_{KO}=16). The bars represent mean ± SEM.

Table S1. Descriptive statistics of LC-MS analysis of lipid classes of DH and VH from *Pld1* KO and *Pld2* KO animals, related to Figure 1.

	Average mol% ± SEM							
	Dorsal		Ventral		Dorsal		Ventral	
	PLD1 WT	PLD1 KO	PLD1 WT	PLD1 KO	PLD2 WT	PLD2 KO	PLD2 WT	PLD2 KO
FC	41.011 ± 2.98	43.981 ± 1.06	34.082 ± 3.82	39.803 ± 1.20	39.980 ± 1.75	43.479 ± 1.92	36.502 ± 1.74	36.959 ± 2.55
CE	0.094 ± 0.01	0.090 ± 0.01	0.106 ± 0.01	0.105 ± 0.01	0.095 ± 0.01	0.102 ± 0.01	0.092 ± 0.01	0.096 ± 0.01
AC	0.070 ± 0.01	0.071 ± 0.01	0.070 ± 0.00	0.071 ± 0.01	0.088 ± 0.01	0.094 ± 0.01	0.067 ± 0.01	0.063 ± 0.00
MG	2.177 ± 0.19	1.748 ± 0.07	1.939 ± 0.31	1.805 ± 0.11	0.222 ± 0.03	0.281 ± 0.08	0.198 ± 0.02	0.183 ± 0.03
DG	0.300 ± 0.03	0.240 ± 0.01	0.338 ± 0.05	0.263 ± 0.02	0.110 ± 0.01	0.094 ± 0.01	0.103 ± 0.01	0.102 ± 0.02
TG	0.058 ± 0.01	0.057 ± 0.00	0.075 ± 0.00	0.068 ± 0.00	0.056 ± 0.00	0.057 ± 0.01	0.062 ± 0.01	0.069 ± 0.01
Cer	0.098 ± 0.01	0.105 ± 0.01	0.160 ± 0.02	0.123 ± 0.01	0.123 ± 0.01	0.137 ± 0.01	0.130 ± 0.01	0.145 ± 0.01
dhCer	0.002 ± 0.00	0.002 ± 0.00	0.004 ± 0.00	0.003 ± 0.00	0.004 ± 0.00	0.003 ± 0.00	0.003 ± 0.00	0.004 ± 0.00
SM	2.746 ± 0.25	2.120 ± 0.17	2.783 ± 0.75	2.750 ± 0.28	2.634 ± 0.18	2.593 ± 0.11	2.710 ± 0.16	2.868 ± 0.15
dhSM	0.299 ± 0.05	0.225 ± 0.04	0.276 ± 0.04	0.225 ± 0.02	0.246 ± 0.02	0.314 ± 0.03	0.337 ± 0.02	0.376 ± 0.04
MhCer	1.821 ± 0.28	1.464 ± 0.15	0.936 ± 0.09	0.833 ± 0.12	1.166 ± 0.15	1.434 ± 0.06	0.779 ± 0.05	0.587 ± 0.09
Sulf	0.328 ± 0.06	0.296 ± 0.03	0.220 ± 0.04	0.189 ± 0.02	0.328 ± 0.03	0.310 ± 0.03	0.199 ± 0.03	0.152 ± 0.02
LacCer	0.008 ± 0.00	0.008 ± 0.00	0.006 ± 0.00	0.006 ± 0.00	0.001 ± 0.00	0.001 ± 0.00	0.001 ± 0.00	0.001 ± 0.00
GM3	0.037 ± 0.00	0.034 ± 0.00	0.070 ± 0.02	0.042 ± 0.01	0.065 ± 0.01	0.043 ± 0.01	0.034 ± 0.01	0.032 ± 0.01
PA	0.024 ± 0.00	0.008 ± 0.00	0.020 ± 0.00	0.009 ± 0.00	0.025 ± 0.00	0.023 ± 0.00	0.020 ± 0.00	0.017 ± 0.00
PC	17.166 ± 1.58	17.951 ± 0.80	21.049 ± 1.37	19.697 ± 1.06	15.912 ± 0.80	15.233 ± 0.57	16.458 ± 0.42	15.729 ± 1.17
PCe	0.488 ± 0.03	0.504 ± 0.03	0.573 ± 0.06	0.521 ± 0.02	0.719 ± 0.05	0.707 ± 0.04	0.663 ± 0.03	0.645 ± 0.07
PE	13.419 ± 0.71	12.067 ± 0.20	15.578 ± 1.36	13.492 ± 0.29	13.715 ± 1.13	11.887 ± 0.70	14.832 ± 1.33	14.653 ± 1.28
PEp	12.153 ± 0.47	11.412 ± 0.31	12.161 ± 0.93	11.421 ± 0.31	12.312 ± 0.74	11.159 ± 0.68	12.943 ± 1.00	12.217 ± 0.98
PS	5.196 ± 0.50	5.323 ± 0.61	6.900 ± 1.09	5.979 ± 0.46	9.258 ± 1.23	9.391 ± 1.42	10.781 ± 0.94	12.413 ± 1.38
PI	2.158 ± 0.24	2.001 ± 0.22	2.330 ± 0.22	2.302 ± 0.11	2.507 ± 0.27	2.226 ± 0.15	2.703 ± 0.27	2.319 ± 0.18
PG	0.035 ± 0.00	0.031 ± 0.00	0.048 ± 0.01	0.037 ± 0.00	0.031 ± 0.00	0.030 ± 0.00	0.042 ± 0.01	0.037 ± 0.00
BMP	0.011 ± 0.00	0.010 ± 0.00	0.008 ± 0.00	0.009 ± 0.00	0.011 ± 0.00	0.011 ± 0.00	0.009 ± 0.00	0.009 ± 0.00
LPC	0.142 ± 0.01	0.114 ± 0.01	0.123 ± 0.01	0.115 ± 0.01	0.126 ± 0.01	0.120 ± 0.00	0.107 ± 0.00	0.107 ± 0.01
LPCe	0.002 ± 0.00	0.002 ± 0.00	0.002 ± 0.00	0.001 ± 0.00	0.002 ± 0.00	0.002 ± 0.00	0.001 ± 0.00	0.001 ± 0.00
LPE	0.003 ± 0.00	0.003 ± 0.00	0.004 ± 0.00	0.003 ± 0.00	0.004 ± 0.00	0.004 ± 0.00	0.003 ± 0.00	0.004 ± 0.00
LPI	0.008 ± 0.00	0.006 ± 0.00	0.009 ± 0.00	0.006 ± 0.00	0.010 ± 0.00	0.010 ± 0.00	0.010 ± 0.00	0.010 ± 0.00
LPS	0.130 ± 0.00	0.111 ± 0.01	0.120 ± 0.01	0.111 ± 0.01	0.228 ± 0.01	0.234 ± 0.03	0.201 ± 0.03	0.192 ± 0.02
NAPS	0.006 ± 0.00	0.007 ± 0.00	0.003 ± 0.00	0.004 ± 0.00	0.005 ± 0.00	0.009 ± 0.00	0.003 ± 0.00	0.003 ± 0.00
NSer	0.011 ± 0.00	0.007 ± 0.00	0.008 ± 0.00	0.007 ± 0.00	0.017 ± 0.00	0.014 ± 0.00	0.008 ± 0.00	0.008 ± 0.00

p < 0.05
p < 0.01
p < 0.001

Table S2. Descriptive statistics of LC-MS analysis of PA species of DH and VH from *Pld1* KO and *Pld2* KO animals, related to Figure 1.

Average mol% ± SEM

	Dorsal		Ventral		Dorsal		Ventral	
	PLD1 WT	PLD1 KO	PLD1 WT	PLD1 KO	PLD2 WT	PLD2 KO	PLD2 WT	PLD2 KO
PA 30:0	0.000529 ± 0.000058	0.000470 ± 0.000042	0.000572 ± 0.000040	0.000463 ± 0.000046	0.000804 ± 0.000044	0.001123 ± 0.000379	0.000766 ± 0.000058	0.000703 ± 0.000082
PA 32:0	0.000489 ± 0.000046	0.000362 ± 0.000012	0.000516 ± 0.000072	0.000385 ± 0.000027	0.000571 ± 0.000076	0.000471 ± 0.000085	0.000541 ± 0.000061	0.000507 ± 0.000058
PA 32:1	0.000287 ± 0.000027	0.000088 ± 0.000012	0.000197 ± 0.000036	0.000077 ± 0.000010	0.000301 ± 0.000023	0.000240 ± 0.000044	0.000268 ± 0.000041	0.000217 ± 0.000042
PA 34:0	0.000677 ± 0.000087	0.000268 ± 0.000025	0.000577 ± 0.000083	0.000283 ± 0.000027	0.000566 ± 0.000041	0.000491 ± 0.000064	0.000406 ± 0.000048	0.000440 ± 0.000046
PA 34:1	0.005214 ± 0.000735	0.001287 ± 0.000070	0.003744 ± 0.000479	0.001158 ± 0.000091	0.005596 ± 0.000663	0.004613 ± 0.000467	0.004140 ± 0.000247	0.003255 ± 0.000269
PA 34:2	0.000413 ± 0.000052	0.000159 ± 0.000022	0.000347 ± 0.000068	0.000172 ± 0.000016	0.000387 ± 0.000036	0.000344 ± 0.000015	0.000327 ± 0.000041	0.000165 ± 0.000037
PA 36:0	0.000435 ± 0.000060	0.000098 ± 0.000024	0.000303 ± 0.000048	0.000060 ± 0.000015	0.000559 ± 0.000068	0.000406 ± 0.000092	0.000297 ± 0.000048	0.000248 ± 0.000038
PA 36:1	0.004633 ± 0.000750	0.000758 ± 0.000080	0.002806 ± 0.000431	0.000620 ± 0.000065	0.005091 ± 0.000642	0.004507 ± 0.000543	0.003414 ± 0.000245	0.002489 ± 0.000428
PA 36:2	0.001796 ± 0.000304	0.000258 ± 0.000018	0.001064 ± 0.000150	0.000264 ± 0.000028	0.001751 ± 0.000187	0.001811 ± 0.000138	0.001403 ± 0.000114	0.001019 ± 0.000094
PA 36:3	0.000217 ± 0.000046	0.000076 ± 0.000014	0.000237 ± 0.000035	0.000117 ± 0.000027	0.000233 ± 0.000042	0.000337 ± 0.000055	0.000266 ± 0.000032	0.000240 ± 0.000028
PA 36:4	0.001018 ± 0.000134	0.000422 ± 0.000043	0.001106 ± 0.000122	0.000577 ± 0.000059	0.001129 ± 0.000221	0.001016 ± 0.000115	0.000991 ± 0.000093	0.000943 ± 0.000095
PA 38:0	0.000550 ± 0.000068	0.000179 ± 0.000018	0.000427 ± 0.000065	0.000157 ± 0.000030	0.000521 ± 0.000102	0.000499 ± 0.000066	0.000394 ± 0.000069	0.000303 ± 0.000051
PA 38:1	0.000580 ± 0.000103	0.000184 ± 0.000025	0.000407 ± 0.000077	0.000138 ± 0.000016	0.000594 ± 0.000112	0.000698 ± 0.000112	0.000450 ± 0.000065	0.000354 ± 0.000055
PA 38:2	0.000446 ± 0.000043	0.000073 ± 0.000010	0.000318 ± 0.000042	0.000086 ± 0.000012	0.000412 ± 0.000064	0.000677 ± 0.000092	0.000351 ± 0.000052	0.000270 ± 0.000029
PA 38:3	0.000539 ± 0.000065	0.000159 ± 0.000025	0.000424 ± 0.000093	0.000164 ± 0.000022	0.000680 ± 0.000158	0.000481 ± 0.000066	0.000523 ± 0.000067	0.000479 ± 0.000046
PA 38:4	0.003068 ± 0.000336	0.001410 ± 0.000143	0.003814 ± 0.000582	0.001990 ± 0.000276	0.002554 ± 0.000385	0.002314 ± 0.000391	0.003081 ± 0.000254	0.002737 ± 0.000270
PA 38:5	0.000720 ± 0.000068	0.000304 ± 0.000031	0.000656 ± 0.000096	0.000310 ± 0.000038	0.000568 ± 0.000068	0.000662 ± 0.000054	0.000583 ± 0.000073	0.000484 ± 0.000050
PA 38:6	0.000396 ± 0.000045	0.000239 ± 0.000022	0.000347 ± 0.000035	0.000270 ± 0.000029	0.000342 ± 0.000025	0.000307 ± 0.000043	0.000379 ± 0.000057	0.000314 ± 0.000033
PA 40:4	0.000453 ± 0.000107	0.000155 ± 0.000021	0.000404 ± 0.000053	0.000133 ± 0.000014	0.000530 ± 0.000088	0.000410 ± 0.000077	0.000379 ± 0.000034	0.000310 ± 0.000017
PA 40:5	0.000256 ± 0.000020	0.000068 ± 0.000010	0.000217 ± 0.000026	0.000094 ± 0.000017	0.000323 ± 0.000066	0.000260 ± 0.000063	0.000254 ± 0.000036	0.000201 ± 0.000026
PA 40:6	0.000471 ± 0.000059	0.000250 ± 0.000040	0.000571 ± 0.000040	0.000290 ± 0.000035	0.000700 ± 0.000107	0.000763 ± 0.000098	0.000729 ± 0.000079	0.000783 ± 0.000133
PA 40:7	0.000181 ± 0.000028	0.000090 ± 0.000019	0.000172 ± 0.000028	0.000101 ± 0.000026	0.000123 ± 0.000027	0.000198 ± 0.000028	0.000096 ± 0.000020	0.000104 ± 0.000028
PA 42:5	0.000330 ± 0.000025	0.000181 ± 0.000014	0.000343 ± 0.000050	0.000206 ± 0.000013	0.000273 ± 0.000091	0.000246 ± 0.000046	0.000188 ± 0.000025	0.000223 ± 0.000059
PA 42:6	0.000661 ± 0.000071	0.000414 ± 0.000038	0.000658 ± 0.000081	0.000495 ± 0.000053	0.000252 ± 0.000047	0.000434 ± 0.000113	0.000204 ± 0.000059	0.000344 ± 0.000112

p < 0.05
p < 0.01
p < 0.001

CHAPTER 3

Phospholipase D2 ablation leads to deficits in social memory

(Manuscript to be submitted)

Luísa Santa-Marinha,[1,2] Francisca Vaz Bravo,[1,2] André Miguel Miranda[1,2], Torcato Meira,[1,2] Vítor Pinto,[1,2] and Tiago Gil Oliveira [1,2]

[1]Life and Health Sciences Research Institute (ICVS), School of Medicine, University of Minho, Campus Gualtar, 4710-057 Braga, Portugal

[2]ICVS/3B's - PT Government Associate Laboratory, Braga/Guimarães, Portugal

Abstract

The hippocampus is a temporal brain region crucial for learning and memory organized along a longitudinal dorsal-ventral axis in mice. Classically, the dorsal hippocampus (DH) is preferentially associated with spatial navigation and episodic memory and the ventral hippocampus (VH) with emotional stress-related behaviors. Its cross-sectional architecture is constituted by the dentate gyrus and *Cornu Ammonis* subfields, CA1, CA2 and CA3. Previous work showed a decreasing phosphatidic acid (PA) gradient along the longitudinal axis of the rodent hippocampus, suggesting the phospholipase D (PLD) pathway could be involved in DH-VH axis regulation. Even though the PLD superfamily includes six members (PLD1-PLD6), only two of them, PLD1 and PLD2, are shown to hydrolyze phosphatidylcholine into PA. We previously showed PLD1 as a major contributor for total PA production in the mouse hippocampus compared to PLD2, and that PLD1 ablation leads to behavioral deficits in novelty recognition and social interaction, to deficits in long-term depression and changes in specific synaptic protein in the DH.

Here, we expand the observations on the role of the PLD pathway in DH-VH organization and functioning. We show that PLD2 ablation leads to littermate recognition impairment and decreases social exploration in a CA2-dependent task. We also performed a complete electrophysiological characterization studying the effect of PLD2 ablation in the DH and VH, and we observed that it specifically reduces long-term potentiation (LTP) in the VH CA1. Finally, we found no major impact on synaptic protein levels upon ablation of PLD2 in either the DH or VH.

Since PLD2 is highly expressed in CA2, and since it was previously shown that CA2 impacts social memory in a circuit that depends on VH CA1, our results suggest a potential role for PLD2 in “dorsal CA2” – “ventral CA1” circuit regulation with an impact in social memory recall, and potential implications for the pathophysiology of neuropsychiatric disorders.

Introduction

The hippocampus is a temporal brain region crucial for learning and memory. Its transversal organization is preserved along the longitudinal axis and is constituted by the dentate gyrus (DG) and Cornu Ammonis (CA) subfields, consisting of CA1, CA2 and CA3 (Strange et al., 2014). Despite this intrinsic circuitry being preserved throughout the longitudinal axis and across species, anatomical features (such as cortical and subcortical connections), electrophysiological, gene expression and functional studies segregate a longitudinal dorsal-ventral (DH-VH) axis in rodents, which correspond in primates to posterior-anterior poles (Strange et al., 2014). Classically, the DH is preferentially associated with spatial navigation and episodic memory and the VH with emotional stress-related behaviors (Bannerman et al., 2014; Fanselow and Dong, 2010; Kheirbek et al., 2013; McHugh et al., 2011; Strange et al., 2014) although a gradual biochemical and functional transition between the two poles has been approached (Bienkowski et al., 2018; Maggio and Segal, 2007; Miranda et al., 2019; Pinto et al., 2015; Shah et al., 2017; Thompson et al., 2008).

The importance of hippocampal subregions has been extensively addressed by inhibition or genetic manipulations of these structures. CA1 has been shown to be necessary for spatial memory (Tsien et al., 1996). Specifically, dorsal CA1 was shown to be involved in contextual memory, remote memory recall and spatial and object memory (Goshen et al., 2011; Roy et al., 2017; Stackman et al., 2016) and ventral CA1 (and its projections to the nucleus accumbens) was implicated in the storage of social memory (Okuyama et al., 2016). CA3 is important for rapid one-trial contextual learning and for pattern completion recall (Nakashiba et al., 2008) and for social memory (Chiang et al., 2018). Regarding the DG, where neurogenesis persists into adulthood, it was shown that pattern separation depends on adult-born young granule cells, while recall by pattern completion relies on older granule cells (Nakashiba et al., 2012). CA2 is a morphological, molecular and electrophysiological region with distinct synaptic connectivity and gene expression profile (Dudek et al., 2016). Importantly, genetically targeted inactivation of dorsal CA2 pyramidal neurons causes lack of social memory (ability of an animal to remember a conspecific) but no alterations in sociability or other hippocampus dependent behaviors (Hitti and Siegelbaum, 2014). A recent study showed that dorsal CA2 plays an active role in social memory encoding, consolidation, and recall and that dorsal CA2 projections to ventral CA1 are necessary for social memory (Meira et al., 2018).

Glycerophospholipids can be remodeled in order to generate products that can serve as second messengers by different classes of phospholipases that act on different positions of the phosphodiester bond (Panda et al., 2018). In mammals, the phospholipase D (PLD) superfamily includes six members (PLD1-PLD6), but only two of them, PLD1 and PLD2, are able to hydrolyze the membrane phospholipid phosphatidylcholine (PC) into the metabolically active phosphatidic acid (PA) (Frohman, 2015; Oliveira et al., 2010; Yao et al., 2020). Curiously, there is a distinctive lipid composition along the hippocampal longitudinal axis, mainly in the relative abundance of sphingolipids and phospholipids. Particularly, the DH presents increased PA and decreased PC when compared to VH, potentially implicating the PLD pathway in DH-VH axis regulation (Miranda et al., 2019). Previous studies showed that PLD1 and PLD2 are the only contributors to total PLD activity in the mouse brain, although PLD1 is a major source of PA in both rodent DH and VH when compared to PLD2 (see chapter 2) (Santa-Marinha et al., 2020). PLD1 ablation affects predominantly the lipidome of the DH and *Pld1* knockout (KO) mice present specific deficits in novel object recognition and social interaction, disruption in the DH-VH dendritic arborization differentiation in CA1/CA3 pyramidal neurons, reduced long-term depression (LTD) induction and reduced GluN2A and SNAP-25 protein levels in the DH.

Here we expand the observations on the role of PLD1 in DH-VH organization and show that PLD2 ablation leads to social discrimination deficits, namely littermate recognition impairment, decreases social exploration and reduces long-term potentiation (LTP) in the VH, showing that, although PLD1 and PLD2 catalyze the same reaction, their specific ablation promotes different phenotypes.

Materials and Methods

Animals

Pld2-/- mice were generated through the elimination of exons 13-15, including exon 14 (that encodes for the first HKD motif of PLD2), using a Cre-lox/FLP-FRT recombination system, as previously described (Oliveira et al., 2010). *Pld2*+/- mice (C57BL/6 background) were crossed so littermate mice could be used for the procedures. All experimental procedures were performed in agreement with the Portuguese authority for animal experimentation, Direção Geral de Alimentação e Veterinária (DGAV), the Directive 2010/63/EU guidelines and approved by the local committee. All mice had ad libitum access to water and food and were maintained on a 12h light/dark cycle. All the procedures were performed during daytime, except for the social discrimination, sociability and preference for social novelty behavioral tests. Prior to all behavioral tests, animals were placed in the testing room for one hour in order to acclimatize. All apparatus were cleaned with 10% ethanol solution between testing subjects.

Animal Behavior

Fear Conditioning (FC)

The Fear Conditioning (FC) protocol aimed to test contextual and cued memory. 3.5-7.5 months male mice were tested. Standard operant chambers (Med Associates Inc.) (22 x 19 x 12.5 cm) with a grid on the bottom where shocks were transmitted was used, except on day 3. On the first day mice were placed in the arena and allowed to explore for 5 minutes. Then a tone (80 dB) was presented for 30 seconds and in the last second a mild shock (0.5 mA for 1 second) was given for fear acquisition. This was repeated for 5 blocks, with an interval of 30 seconds between then. To evaluate the contextual fear conditioning on the second day, mice were only placed in the arena and allowed to explore for 5 minutes. On the third day mice were placed in a different arena (24 x 32 x 18.5 cm) and allowed to explore for 5 minutes. Then 5 blocks of 30 seconds of tone and 30 seconds of interval were given in order to evaluate cued fear conditioning. For the next 5 days mice were placed in the arena and give 15 blocks of 30 seconds of tone followed by 30 seconds of interval, to evaluate the extinction of the freezing response. 30 days after the last day of extinction protocol, mice were placed in the arena and allowed to explore for 5 minutes. Then 5 blocks of 30 seconds of tone followed by 30 seconds of interval were presented to

evaluate spontaneous recovery. Animals were video-recorded and the percentage of freezing behavior was analyzed. All stimulation procedures were done through Med-PC IV (Med Associates Inc.) software, except for the shock that was manually given.

Three-chamber Social Discrimination and Three-chamber Sociability and Preference for Social Novelty

These tests were adapted from previously described protocols (Meira et al., 2018; Moy et al., 2007). 3-6 months male mice were used for the social tests. A transparent rectangular arena (56 cm long x 50 cm wide x 39 cm high) was divided in three equal chambers with openings that allowed access into each chamber. Trials consisted of 10-minute period each, where the subject mice were allowed to explore the arena. When the trial ended and the animal stopped in the center arena, the access to the other chambers was blocked with two doors to switch trials.

The social discrimination test consisted of three trials. In the first habituation trial, mice were individually placed in the center of the arena and freely explore. In the second habituation trial, two empty round wire cups (9.8 cm high, with a bottom diameter of 8 cm and several horizontal opened bars spaced 3.7 x 0.5 cm apart which allowed nose contact between the bars) were placed on the side chambers and the subject mice freely explored the arena. In the third trial, a co-housed littermate and an unfamiliar male stranger with no prior contact with the tested mouse were each placed inside one of the wire cups. The location of the stranger and the littermate mouse was systematically alternated between the tested mice.

The sociability and preference for social novelty test consisted of four trials. The first and second trials were equal to the ones previously described. In the third trial, an unfamiliar male mice (stranger 1), which had no prior contact with the subject mice, was placed inside one of the cups to test sociability of the subject mice. In the fourth trial, a second stranger male mice (stranger 2) was enclosed in the previously empty cup and preference for social novelty was assessed. The location of the strangers was systematically alternated between the tested mice. Behavior was video-recorded and the amount of time spent interacting with each cup was manually scored. Social discrimination, social preference and preference for social novelty scores were calculated as the difference between the time spent exploring the cups placed on the side chambers, divided by the total time exploring both. Testing was conducted under red light.

Electrophysiology

Electrophysiological recordings were performed according to a protocol described elsewhere (Pinto et al., 2015). Slices from 2-3 months male and female mice were used. Briefly, after intraperitoneal injection of Na+-pentobarbital (40mg/kg) anesthesia and decapitation, the brain was rapidly removed and placed in ice-cold sucrose-based solution containing the following (in mM): 2.5 KCl, 7 $MgCl_2$, 1.25 NaH_2PO_4, 110 sucrose, 26 $NaHCO_3$, 10 glucose, bubbled with carbogen gas (95% O_2, 5% CO_2). Slices of 300 μm were cut transverse to the axis of the hippocampus using a tissue slicer (Leica VT 1200s) and placed in a container with artificial cerebrospinal fluid (ACSF) containing (in mM): 124 NaCl, 2.5 KCl, 1 $MgSO_4$, 2 $CaCl_2$, 1.25 NaH_2PO_4, 26 $NaHCO_3$, 10 glucose, bubbled with carbogen gas and maintained at 33°C for 30 minutes. Before recording, the slices were then stored at room temperature for a minimum of 30 minutes. Extracellular recordings were performed in a submerge-type chamber bathed with ACSF at 31°C. A custom-made bipolar tungsten stimulation electrode was placed in the transition between CA1 and CA3, at the Schaffer collaterals, and a recording borosilicate glass pipette filled with ACSF (3-5 MΩ) was positioned in the middle of the stratum radiatum of CA1 at a predetermined fixed distance of approximately 1mm apart the stimulation electrode. Recordings were digitized with a Multiclamp 700B amplifier (Axon Instruments) Signals were low-pass filtered at 3 kHz and sampled at 10 kHz. Stimulation strength was adjusted to 30–50 % of the maximum field excitatory post synaptic potential (fEPSP) slope, after a fixed protocol of 4 increasing stimulus (2000-8000mV) was applied (input-output relationship). Before baseline acquisition, a series of paired pulse stimuli of varying interpulse interval (25, 50, 100 and 300ms) were given. The paired pulse (PP) ratio was calculated by dividing the slope of fEPSP2 by fEPSP1. A minimum of 10 minute stable baseline recordings were acquired at 0.03 Hz. LTD was elicited by delivering a low-frequency stimulation protocol consisting of 15 min 1 Hz stimulation. LTP was elicited by delivering 3 θ-burst stimuli (θ-burst: 100 Hz burst of four pulses repeated at 5 Hz with each tetanus including 10-burst trains) separated by 15 s intervals. All stored curves were an average of four consecutive recordings. Maximum EPSP slopes were calculated off-line using the WinLTP software. For LTP and LTD analysis, all individual slopes were normalized to the average slope of baseline recordings.

Western Blot

After cervical dislocation and hippocampi dissection, they were divided in approximately three equal dorsal, intermediate and ventral parts. Brains from 3.5-7 months male and female mice were used. Samples were diluted in radioimmunoprecipitation assay buffer (RIPA) containing 150 nM NaCl, 1.0% triton X-100, 0.5% sodium deoxycholate, 0.1% SDS, 50 mM TrisBase pH=8 and supplemented with protease (Roche) and phosphatase inhibitor cocktails (Sigma-Aldrich). After homogenization, samples were mixed in a rotator at 4°C for 2 hours at 40rpm and then centrifuged at 4°C for 20 minutes at 14000rpm. Supernatants were quantified (BCA, Pierce) and diluted to equal concentration in RIPA. Samples were prepared with NuPAGE LDS sample buffer and NuPAGE reducing reagent and loaded in NuPAGE 4–12% Bis–Tris gels. MES SDS running buffer (NuPAGE) was used for separation. Wet transfer used 50% running buffer, 20% methanol and 30% deionized water and was made on 0.45µm nitrocellulose membranes (Amersham) for 2 hours at 100V. Membrane blockage was performed with 5% dried milk (Nestle) for 1 hour at room temperature. Incubation with primary antibodies, diluted in 2.5% dried milk or bovine serum albumin (BSA), was performed overnight at 4°C and incubation with HRP-conjugated secondary antibodies, diluted in 2.5% dried milk or BSA, was performed for 1 hour at room temperature. Chemiluminescence signal was detected with ChemiDoc XRS+ (Bio-Rad) and membrane development was achieved with Clarity Western ECL Substrate (Bio-Rad) or SuperSignal West Femto Maximum Sensitivity Substrate (ThermoScientific). ImageJ software was used for quantification. Primary antibodies used were: α-Tubulin (T6074, Sigma-Aldrich, 1:10000); GAPDH (Cell Signaling Technology, 1:3000); Synaptophysin (Synaptic Systems, 1:5000); SNAP-25 (Abcam, 1:5000); PSD95 (Abcam, 1:5000); Homer (Abcam, 1:3000); GluA1/GluR1 (Millipore, 1:1000); GluA2/GluR2 (Abcam, 1:1000); GluN2A/NR2A (Millipore, 1:1000); GluN2B/NR2B (Abcam, 1:1000) and pY1472-GluN2B/NR2B (Abcam, 1:1000). HRP-conjugated secondary antibodies used were: Goat Anti-rabbit IgG (BioRad) and Goat Anti-mouse IgG (BioRad).

Quantification and Statistical Analysis

Western blot analysis was performed using ImageJ (NIH). The statistical analysis was performed using GraphPad Prism 7.00 software. Statistical significance was assessed by two-way ANOVA and Student's t test, and referenced in figure legends whenever used. Values were accepted as

significant when $p<0.05$. *$p<0.05$, **$p< 0.01$, ***$p<0.001$. Number of mice for all statistical analyses is indicated in each legend. Values are expressed as mean±SEM.

Results

PLD2 ablation impairs social discrimination and decreases social exploration in a hippocampus-dependent social discrimination task

In order to evaluate the impact of PLD2 ablation on hippocampal functioning, we performed hippocampal-associated behaviors. First, when performing the FC test, we observe that *Pld2* KO animals had similar freezing responses when comparing to wild-type (WT) mice when contextual and cued memories were evaluated (Figure 1A, left panel), and in the 5 subsequent days in the extinction freezing upon a cue protocol (Figure 1A, middle panel). Curiously, 30 days later, KO animals tend to freeze less when exposed to the context and cue (Figure 1A, right panel). Then, we performed social tests, in order to evaluate social preference and preference for social novelty and social discrimination. The ablation of PLD2 does not impair the social preference (Figure 1B and S1A) neither the preference for social novelty (Figure 1C and S1B) but impairs social discrimination by reducing the ability to recognize a littermate (Figure 1D, left panel, and S1C). Moreover, *Pld2* KO mice were less social in a hippocampus-dependent task, considering that they spent less time exploring (Figure 1D, right panel).

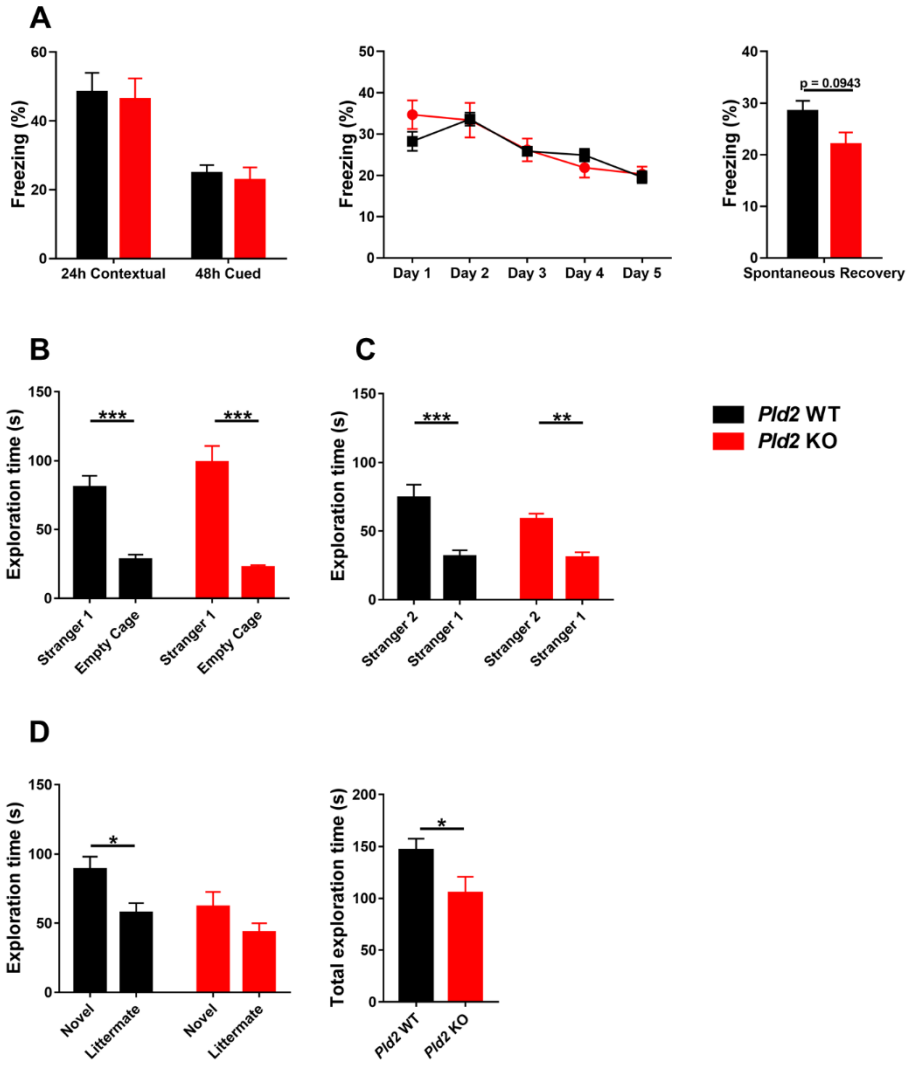

Figure 1. PLD2 ablation impairs the ability to recognize a littermate and decreases social exploration.

(A) PLD2 ablation has no impact in contextual or cued fear conditioning (left panel), neither in the extinction protocol (middle panel). There is a tendency for KO animals to freeze less than WT animals in spontaneous recovery 30 days after FC protocol (unpaired t test $t(19) = 1.761$, $p = 0.0943$) (right panel) ($n_{WT} = 11$, $n_{KO} = 11$).

(B) PLD2 ablation has no impact on social preference (2-way ANOVA: Interaction $F(1, 20) = 2.364$, $p = 0.1398$; Exploration time $F(1, 20) = 68.92$, $p < 0.0001$; stranger 1/empty cage WT: $p = 0.0004$; KO: $p < 0.0001$, Sidak's multiple comparisons test) ($n_{WT} = 10$, $n_{KO} = 12$).

(C) PLD2 ablation has no impact on preference for social novelty (2-way ANOVA: Interaction $F(1, 20) = 1.833$, $p = 0.1909$; Exploration time $F(1, 20) = 41.52$, $p < 0.0001$; stranger 2/stranger 1 WT: $p < 0.0001$; KO: $p = 0.0024$, Sidak's multiple comparisons test) ($n_{WT} = 10$, $n_{KO} = 12$).

(D) PLD2 ablation impairs the ability to discriminate between a littermate and a strange mouse (2-way ANOVA: Interaction $F(1, 24) = 0.8038$, $p = 0.3789$; Exploration time $F(1, 24) = 11.21$, $p = 0.0027$; littermate/novel WT: $p = 0.0123$; KO: $p = 0.1824$, Sidak's multiple comparisons test). *Pld2* KO mice spend less time interacting with conspecifics in a social discrimination task (unpaired t test $t(24) = 2.151$, $p = 0.0418$) ($n_{WT} = 13$, $n_{KO} = 13$).

The bars represent mean±SEMs. *p < 0.05, **p < 0.01, ***p < 0.001. See also Figure S1.

PLD2 ablation reduces LTP in the VH

Ex vivo extracellular electrophysiological recordings were performed by stimulating Schaffer collaterals and recording in CA1. The lack of PLD2 led to a decrease in all phases of LTP in the VH (Figure 2A, right panel), but not in DH (Figure 2A, left panel). There was not an apparent significant impact in the curves of PP facilitation (Figure 2C), although when comparing only the 100ms in VH there is a difference in the PP between WT and KO animals (Figure 2C, right panel). Moreover, there was no impact in LTD in DH and VH (Figure 2B), neither in the input-output relationship (Figure S2). Within WT animals, PP curves are different between DH and VH, which highlight the intrinsic functional difference between these two regions (Figure 2C).

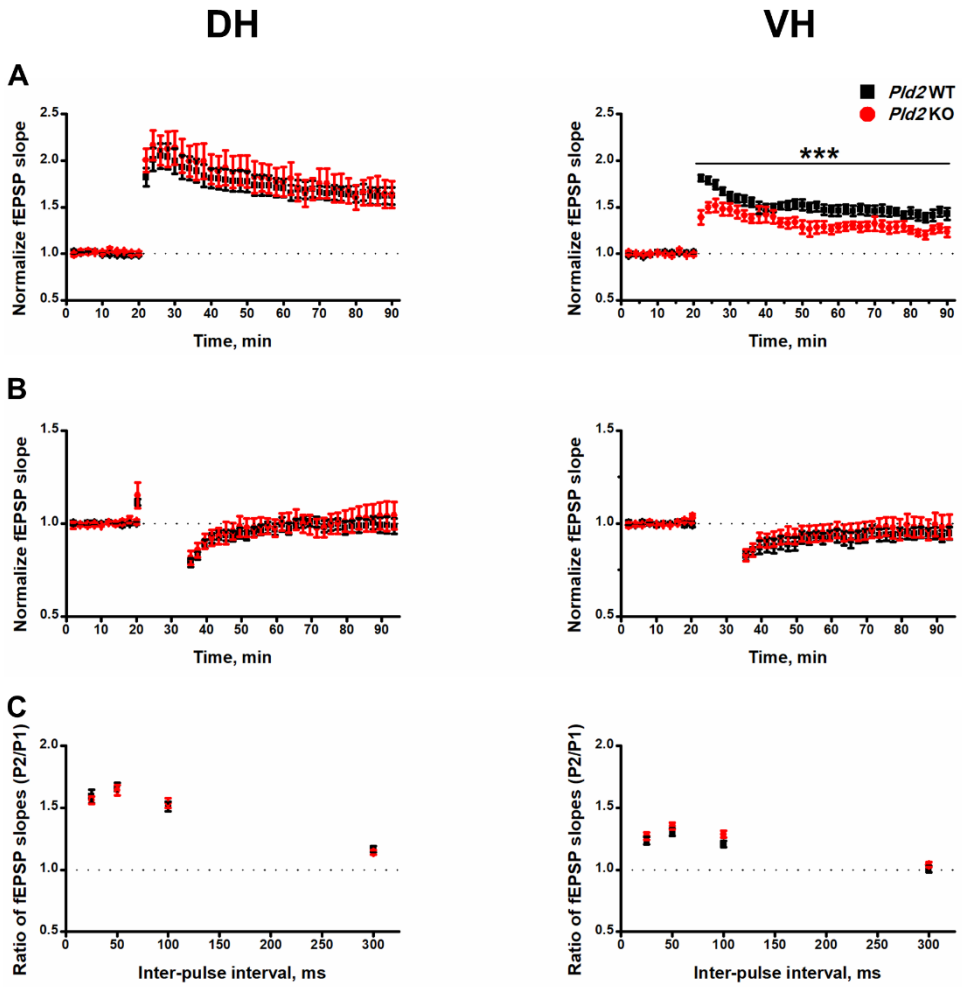

Figure 2. PLD2 ablation impairs the ability to generate LTP in VH.

(A) LTP was measured in acute slices of DH (left panel) (n_{WT} = 10, n_{KO} = 7) and VH (right panel) (n_{WT} = 7, n_{KO} = 7). PLD2 ablation impairs the ability to generate LTP in VH - the curves of LTP were different between WT and KO animals (2-way ANOVA: Interaction $F(34, 408) = 2.254$, $p = 0.0001$; WT/KO $F(1, 12) = 7.166$, $p = 0.0202$). Particularly, there was a decrease in excitability in the early phase (first 6 minutes) (unpaired t test $t(12) = 5.255$, $p = 0.0002$) and late phase (last 4 minutes) (unpaired t test $t(12) = 2.48$, $p = 0.0289$) of LTP in the VH of *Pld2* KO animals.

(B) LTD was measured in acute slices of DH (left panel) (n_{WT} = 10, n_{KO} = 8) and VH (right panel) (n_{WT} = 9, n_{KO} = 9).

(C) Paired pulse (PP) ratios in acute slices of DH (left panel) (n_{WT} = 20, n_{KO} = 14) and VH (right panel) (n_{WT} = 15, n_{KO} = 15). At 100ms in VH there is a difference in the PP between WT and KO animals (unpaired t test $t(30) = 2.06$, $p = 0.0482$). Within WT animals, 2-way ANOVA showed the PP curves of DH and DH to be different (2-way ANOVA: Interaction $F(3, 99) = 12.96$, $p < 0.0001$;

WT DH/VH $F(1, 33) = 31.93$, $p < 0.0001$). The bars represent mean±SEM. ***$p < 0.001$. See also Figure S2.

PLD2 ablation has no apparent impact on synaptic proteins levels

We evaluated the levels of proteins involved in synaptic function, in both the DH and VH (Figure 3). There were no apparent differences between WT and KO animals in the levels of the synaptic proteins evaluated: synaptophysin, SNAP-25, PSD95, Homer, GluA1, GluA2, GluN2A, GluN2B and GluN2B-P (phosphorylated at Y1472). Interestingly, although there is a differentiation between DH and VH GluA1 levels in WT animals, this differentiation is lost when PLD2 is ablated. Globally, we also observe a decrease in the VH of the levels of GluN2A and GluN2B-P when compared to WT.

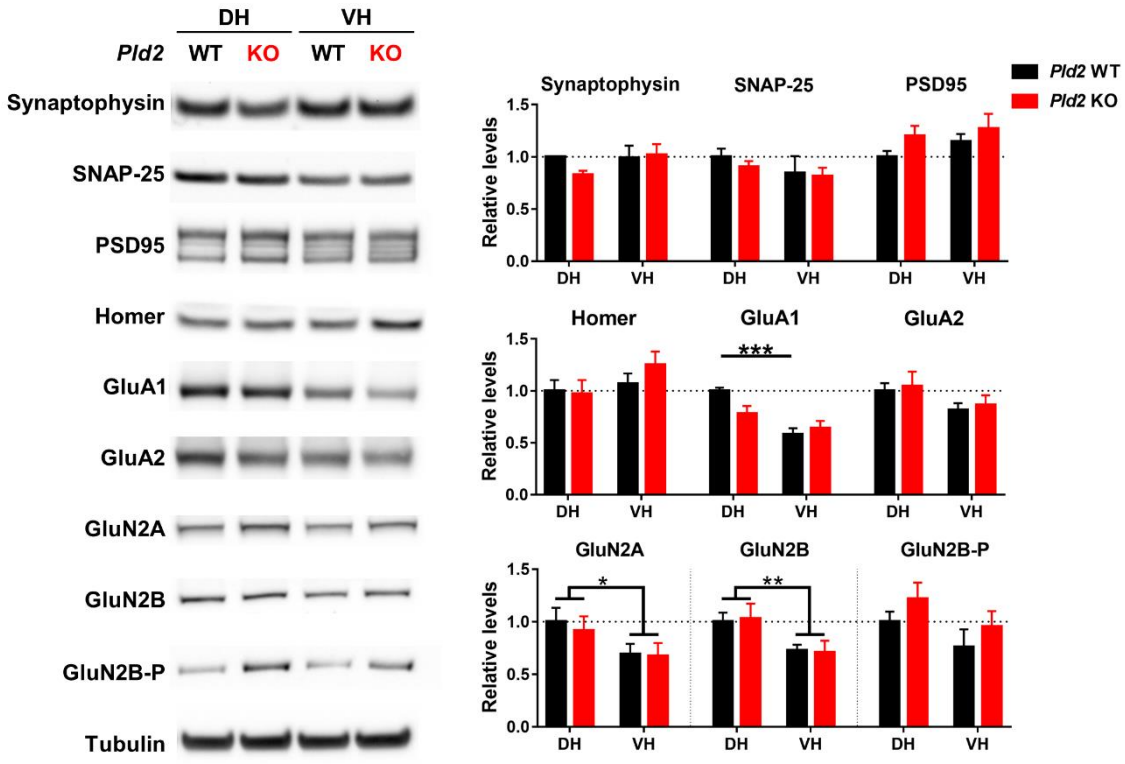

Figure 3. PLD2 ablation has no greater impact on synaptic proteins.

DH and VH proteins were evaluated by western blot analysis and quantified by densitometric analysis (n = 6–8). There was a decrease in GluA1 levels in VH when compared with DH in *Pld2* WT animals (2-way ANOVA: interaction $F(1,28) = 5.353$, $p = 0.0282$; DH/VH $F(1,28) = 22.31$, p

< 0.0001; WT DH/VH p = 0.0002; Tukey's multiple comparisons test). This difference did not persist upon PLD2 ablation. Globally, the levels of GluN2A were higher in the DH when compared to the VH (2-way ANOVA: Interaction $F(1,20) = 0.0682$, p = 0.7967; DH/VH $F(1,20) = 5.038$, p=0.0363). Also, the levels of GluN2B were globally higher in the DH when compared to the VH (2-way ANOVA: Interaction $F(1,20) = 0.0580$, p = 0.8121; DH/VH $F(1,20) = 8.407$, p = 0.0089). The bars represent mean±SEM. *p < 0.05, **p < 0.01, ***p < 0.001.

Discussion

The hippocampus is a brain temporal lobe structure essential for learning and memory. It runs along a longitudinal axis with an anatomical, genomic and functional organized gradient, segregating into its DH and VH poles, with different physiological and pathological importance (Strange et al., 2014). Previous work addressing the role of PLD1 in DH-VH axis organization showed that PLD1 is a major contributor for total PA production in the mouse forebrain compared to PLD2, and that PLD1 ablation leads to a CA1/CA3 dendritic arborization reorganization, to behavioral deficits in novel object recognition and social interaction, to deficits in LTD and specific synaptic protein alterations predominantly in the DH (Santa-Marinha et al., 2020). Here we show that PLD2 ablation leads to social discrimination deficits, with littermate recognition impairment, decreases social exploration and reduces LTP in the VH.

Unpublished work from our group showed that PLD2 ablation has no impact in the performance of cognitive and memory tests as Open Field, Elevated Plus Maze, Morris Water Maze and Novel Object Recognition (in contrast to PLD1 ablation). Taking this into account, we performed social and contextual and cued memory tests. The lack of PLD2 did not interfere with sociability and preference for social novelty, since *Pld2* KO animals preferred to interact with an animal rather than with an empty cage and with a novel animal rather than a familiar mouse, respectively (see Figure 1B, 1C, S1A and S1B). On the other hand, *Pld2* KO mice lost the ability to discriminate between a littermate and a strange mouse. In addition, *Pld2* KO mice spent less time interacting with conspecifics in this social discrimination task (see Figure 1D and S1C).

Genetically targeted inactivation of dorsal CA2 pyramidal neurons in a mouse line induces loss of social memory (which means the ability of an animal to remember a conspecific), with no other impact on sociability or several hippocampal-dependent behaviors, including spatial memory, contextual memory, and novel object recognition (Hitti and Siegelbaum, 2014). In addition, ventral CA3 is necessary for the encoding of a social memory (Chiang et al., 2018) and ventral CA1 (and its projections to the nucleus accumbens) is implicated in the storage of social memory (Okuyama et al., 2016). A recent study implicated dorsal CA2 in social memory encoding, consolidation, and recall (Meira et al., 2018). Acute silencing of dorsal CA2 impairs recall of social memory, since it impairs the discrimination between a littermate and a novel subject (Meira et al., 2018), identical to the phenotype described upon PLD2 ablation. Previous work with *in situ* hybridization revealed that most functional regions of the brain express PLD2 mRNA

to varying degrees, depending on neuron types. Within the hippocampus, CA2 has noticeably more signal than CA1 and CA3 regions, which, in turn, express far more than the DG, where PLD2 is almost undetected (Vermeren et al., 2016). Moreover, dorsal CA2 provides an excitatory input to the same ventral CA1 subregion that projects to the nucleus accumbens shell, implicated in social memory (Meira et al., 2018). Curiously, mice lacking PLD2, highly expressed in CA2, have reduced LTP when Schaffer collaterals are stimulated in VH (see figure 2A, right panel). Based on these behavioral observations, one possibility is that PLD2 specifically affects the dorsal CA2 – ventral CA1 circuit, which could explain the connection with social memory.

CA2 region has features that distinguish it from CA1 and CA3, from synaptic connectivity and electrophysiological characteristics to gene expression profile and relative resistance to cell death (Dudek et al., 2016). CA2 has high resistance to damage from injury (Nadler et al., 1978; Sloviter and Damiano, 1981) and resistance to synaptic plasticity, namely failure to display LTP and LTD compared with other CA regions (Zhao et al., 2007). Several classes of proteins are particularly enriched in CA2, such as calcium regulators, extracellular matrix components, proteins involved in growth factor- and G protein-coupled receptor (GPCR)-mediated signaling, and intracellular signal transduction proteins (Dudek et al., 2016). Arginine vasopressin (AVP) receptor 1b (AVPR1b) and oxytocin (OXT) receptor (OXTR) are also highly expressed in CA2 pyramidal neurons (Hammock and Levitt, 2013; Hidema et al., 2016; Mitre et al., 2016; Yoshida et al., 2009; Young et al., 2006). OXT and AVP are two hypothalamic produced neuropeptides. OXT is first known as a regulator of parturition and lactation and AVP is a regulator of extracellular fluid volume and a vasoconstrictor, but they have also been study for their ability to modulate social behaviors. Decreased levels of OXT and OXTR, either in full KO (Takayanagi et al., 2005) or conditional KO mice, lead to social deficits and poor social recognition (Lee et al., 2008). Recent studies showed that OXTR in the anterior DG and anterior CA2/CA3 are essential for discrimination of social stimuli (and not non-social) (Raam et al., 2017) and for long-term social recognition memory, without any effect on sociability and preference for social novelty (Lin et al., 2018). Regarding AVPR1b, it was shown that AVPR1b KO mice have impairment of sociability (DeVito et al., 2009) and social memory (DeVito et al., 2009; Wersinger et al., 2002; Wersinger et al., 2008). Partial replacement of this receptor through lentiviral delivery into the dorsal CA2 is able to restore the probability of socially motivated attack behavior in AVPR1b KO mice (Pagani et al., 2015) and optogenetic release of AVP in CA2 enhances social memory encoding, but not social recall (Smith et al., 2016).

Association between PLD and AVP/OXT has already been described. In cultured rat glomerular mesangial cells, AVP increases the phosphatidylethanol (PEtOH) formation (indicating PLD activity) and inhibition of PLD decreases AVP produced PEtOH (Kusaka et al., 1996). Other studies implicate PLD activation by AVP in myogenesis (Komati et al., 2005; Naro et al., 1997) and PLD in AVP-stimulated Ca^{2+} spiking in vascular smooth muscle cells (Li et al., 2001). In fact, PLD activation by AVP in myogenic cells increases exocytosis and vesicle traffic (Coletti et al., 2000). PLD activity in cultured amnion cells is activated by the addition of AVP and OXT (Inamori et al., 1995) and OXT also activates PLD in cultured human pregnant myometrial cells (Morrison et al., 1996). We can speculate that the connections between PLD2 and OXT/AVP are dysregulated in *Pld2* KO animals, thus leading to social deficits. Another interesting feature is that OXT transiently reduces synaptic inhibition in multiple brain regions and enables long-term synaptic plasticity in the auditory cortex (Mitre et al., 2016) and selective activation of AVPR1b or OXTR agonists induces significant potentiation in excitatory synaptic responses in CA2, despite its resistance to LTP (Pagani et al., 2015). This enhances the possibility that PLD2 could be responsible for synaptic electrophysiological responses with impact on social behavior, since its ablation causes deficits in LTP (see Figure2, right panel).

Another possibility is that TWIK-related K+ channel (TREK), a subfamily of K2P channels lipid-regulated membrane proteins, could be involved in PLD2 ablation associated phenotypes. TREK channels include TREK1, TREK2, and TWIK-related arachidonic acid stimulated K+ channel (TRAAK) (Comoglio et al., 2014). Importantly, Comoglio et al. showed that TREK1 and TREK2 are potentiated by PLD2 and that none of these channels is modulated by PLD1, since PLD2, but not PLD1, directly binds to the C terminus of TREK1 and TREK2 (and not to TRAAK). Coexpression of TREK1/TREK2 and PLD2 increases TREK1/TREK2 current (Comoglio et al., 2014). This selective binding allows a local PA production that tonically activates the channel and contributes to resting membrane potential (Comoglio et al., 2014). Remarkably, TREK1, is also highly expressed in CA2 (Talley et al., 2001) and TREK1 ablation in mice leads to decreased LTP in CA1 region, similarly to the alterations seen in the VH of *Pld2* KO mice (Wang et al., 2020). Human 22q11.2 deletion syndrome (22q11.2DS) mouse model (Df(16)$A^{+/-}$), also known as DiGeorge syndrome (the greatest molecular genetic risk factor for schizophrenia) display impaired social memory, that phenocopies a silent CA2 (Piskorowski et al., 2016). These mice have intrinsic decreased action potential in CA2 pyramidal neurons, with a hyperpolarized resting membrane potential. This hyperpolarization relates to the upregulated current of TREK1 channel

in CA2 (Piskorowski et al., 2016). One could hypothesize that the ablation of PLD2 could have an impact in the regulation of TREK1, leading to social deficits in these animals.

Of note, although social deficits were already described in mice lacking PLD2 (Burkhardt et al., 2014), our careful *Pld2* KO studies did not reveal impaired preference for social novelty. In agreement to previous work, PLD2 ablation did not impact the percentage of freezing in contextual FC (Figure 1A, left panel) (Oliveira et al., 2010). *Pld2* KO also performed as WT in cued fear conditioning (Figure 1A, left panel) and in the extinction protocol (Figure 1A, middle panel). Despite this, there was a tendency for KO animals to freeze less than WT animals in spontaneous recovery 30 days after FC protocol (Figure 1A, tight panel).

There is a great amount of evidence involving the VH in acquisition of conditioned fear, many of them focusing on the reciprocal connections of VH with the amygdala (Bast et al., 2001; Chaaya et al., 2018; Cox et al., 2013; Hobin et al., 2006; Izquierdo et al., 2016; Silva et al., 2019; Zhang et al., 2001). Interestingly, a study used a foot shock associated with optogenetic stimulation of auditory inputs targeting the amygdala for animal conditioning and then delivered optogenetical LTD and LTP conditioning to the auditory input (Nabavi et al., 2014). Curiously, LTD inactivates and LTP reactivates the memory of the shock (Nabavi et al., 2014). Since *Pld2* KO mice lack the ability to induce LTP, this impairment might justify the tendency to freeze less when recalling the contextual fear memory.

PLD2 has a documented role in the pathophysiology of Alzheimer's disease (AD). In primary cortical neurons, Aβ oligomers induce total PLD activity, which is abolished in mouse cultured neurons without PLD2 (Oliveira et al., 2010). Moreover, genetic ablation of PLD2 leads to attenuation of AD pathogenesis by increasing resistance to Aβ oligomer insult. Behavioral tests with SwAPP mouse model showed that ablating PLD2 improves learning in memory in contextual FC and radial arm water maze test, thus leading to memory deficit protection (Oliveira et al., 2010). The hippocampus is an early target of AD pathology and CA2 is highly affected. Immunohistochemistry of human AD brain revealed a decrease in parvalbumin interneuron density in CA2, similar to what is found in CA1 and DG (Brady and Mufson, 1997), in agreement with findings in mouse models (Cattaud et al., 2018). The record of the activity of hippocampal place cells in Tg-F344 AD model (with human genetic mutations APPSwe and PS1ΔE9) showed that spiking activity of place cells in the CA2 and CA3 pyramidal regions in AD rats have sharply reduced spatial fidelity (Galloway et al., 2018).

With this work we expose PLD2 as essential for social behavior and hippocampal synaptic potentiation, enhancing a possible dysregulation of AVPR1b/OXT/TREK1 and of the connectivity from dorsal CA2 to ventral CA1, whose impairment also leads to social deficits and potentiation in excitatory synaptic. Further studies should tackle this relationship, either by colocalization studies, protein quantification or acute inhibition of PLD2. It is also mandatory to tackle the possible role of PLD2 in the pathophysiology of AD and the implications on CA2 region.

References

Bannerman, D.M., Sprengel, R., Sanderson, D.J., McHugh, S.B., Rawlins, J.N., Monyer, H., and Seeburg, P.H. (2014). Hippocampal synaptic plasticity, spatial memory and anxiety. Nature reviews Neuroscience *15*, 181-192.

Bast, T., Zhang, W.N., and Feldon, J. (2001). The ventral hippocampus and fear conditioning in rats. Different anterograde amnesias of fear after tetrodotoxin inactivation and infusion of the GABA(A) agonist muscimol. Experimental brain research *139*, 39-52.

Bienkowski, M.S., Bowman, I., Song, M.Y., Gou, L., Ard, T., Cotter, K., Zhu, M., Benavidez, N.L., Yamashita, S., Abu-Jaber, J.*, et al.* (2018). Integration of gene expression and brain-wide connectivity reveals the multiscale organization of mouse hippocampal networks. Nature neuroscience *21*, 1628-1643.

Brady, D.R., and Mufson, E.J. (1997). Parvalbumin-immunoreactive neurons in the hippocampal formation of Alzheimer's diseased brain. Neuroscience *80*, 1113-1125.

Burkhardt, U., Stegner, D., Hattingen, E., Beyer, S., Nieswandt, B., and Klein, J. (2014). Impaired brain development and reduced cognitive function in phospholipase D-deficient mice. Neuroscience letters *572*, 48-52.

Cattaud, V., Bezzina, C., Rey, C.C., Lejards, C., Dahan, L., and Verret, L. (2018). Early disruption of parvalbumin expression and perineuronal nets in the hippocampus of the Tg2576 mouse model of Alzheimer's disease can be rescued by enriched environment. Neurobiology of aging *72*, 147-158.

Chaaya, N., Battle, A.R., and Johnson, L.R. (2018). An update on contextual fear memory mechanisms: Transition between Amygdala and Hippocampus. Neuroscience and biobehavioral reviews *92*, 43-54.

Chiang, M.C., Huang, A.J.Y., Wintzer, M.E., Ohshima, T., and McHugh, T.J. (2018). A role for CA3 in social recognition memory. Behavioural brain research *354*, 22-30.

Coletti, D., Silvestroni, L., Naro, F., Molinaro, M., Adamo, S., and Palleschi, S. (2000). Vesicle-mediated phosphatidylcholine reapposition to the plasma membrane following hormone-induced phospholipase D activation. Experimental cell research *256*, 94-104.

Comoglio, Y., Levitz, J., Kienzler, M.A., Lesage, F., Isacoff, E.Y., and Sandoz, G. (2014). Phospholipase D2 specifically regulates TREK potassium channels via direct interaction and local production of phosphatidic acid. Proceedings of the National Academy of Sciences of the United States of America *111*, 13547-13552.

Cox, D., Czerniawski, J., Ree, F., and Otto, T. (2013). Time course of dorsal and ventral hippocampal involvement in the expression of trace fear conditioning. Neurobiology of learning and memory *106*, 316-323.

DeVito, L.M., Konigsberg, R., Lykken, C., Sauvage, M., Young, W.S., 3rd, and Eichenbaum, H. (2009). Vasopressin 1b receptor knock-out impairs memory for temporal order. The Journal of neuroscience : the official journal of the Society for Neuroscience *29*, 2676-2683.

Dudek, S.M., Alexander, G.M., and Farris, S. (2016). Rediscovering area CA2: unique properties and functions. Nature reviews Neuroscience *17*, 89-102.

Fanselow, M.S., and Dong, H.W. (2010). Are the dorsal and ventral hippocampus functionally distinct structures? Neuron *65*, 7-19.

Frohman, M.A. (2015). The phospholipase D superfamily as therapeutic targets. Trends Pharmacol Sci *36*, 137-144.

Galloway, C.R., Ravipati, K., Singh, S., Lebois, E.P., Cohen, R.M., Levey, A.I., and Manns, J.R. (2018). Hippocampal place cell dysfunction and the effects of muscarinic M(1) receptor agonism in a rat model of Alzheimer's disease. Hippocampus *28*, 568-585.

Goshen, I., Brodsky, M., Prakash, R., Wallace, J., Gradinaru, V., Ramakrishnan, C., and Deisseroth, K. (2011). Dynamics of retrieval strategies for remote memories. Cell *147*, 678-689.

Hammock, E.A., and Levitt, P. (2013). Oxytocin receptor ligand binding in embryonic tissue and postnatal brain development of the C57BL/6J mouse. Frontiers in behavioral neuroscience *7*, 195.

Hidema, S., Fukuda, T., Hiraoka, Y., Mizukami, H., Hayashi, R., Otsuka, A., Suzuki, S., Miyazaki, S., and Nishimori, K. (2016). Generation of Oxtr cDNA(HA)-Ires-Cre Mice for Gene Expression in an Oxytocin Receptor Specific Manner. Journal of cellular biochemistry *117*, 1099-1111.

Hitti, F.L., and Siegelbaum, S.A. (2014). The hippocampal CA2 region is essential for social memory. Nature *508*, 88-92.

Hobin, J.A., Ji, J., and Maren, S. (2006). Ventral hippocampal muscimol disrupts context-specific fear memory retrieval after extinction in rats. Hippocampus *16*, 174-182.

Inamori, K., Sagawa, N., Hasegawa, M., Itoh, H., Yano, J., and Mori, T. (1995). Activation of phospholipase D in cultured human amnion cells. Reproduction, fertility, and development *7*, 1591-1594.

Izquierdo, I., Furini, C.R., and Myskiw, J.C. (2016). Fear Memory. Physiological reviews *96*, 695-750.

Kheirbek, M.A., Drew, L.J., Burghardt, N.S., Costantini, D.O., Tannenholz, L., Ahmari, S.E., Zeng, H., Fenton, A.A., and Hen, R. (2013). Differential control of learning and anxiety along the dorsoventral axis of the dentate gyrus. Neuron *77*, 955-968.

Komati, H., Naro, F., Mebarek, S., De Arcangelis, V., Adamo, S., Lagarde, M., Prigent, A.F., and Némoz, G. (2005). Phospholipase D is involved in myogenic differentiation through remodeling of actin cytoskeleton. Molecular biology of the cell *16*, 1232-1244.

Kusaka, I., Ishikawa, S.E., Higashiyama, M., Saito, T., Nagasaka, S., and Saito, T. (1996). The activation of phospholipase D participates in the mitogenic action of arginine vasopressin in cultured rat glomerular mesangial cells. Endocrinology *137*, 5421-5428.

Lee, H.J., Caldwell, H.K., Macbeth, A.H., Tolu, S.G., and Young, W.S., 3rd (2008). A conditional knockout mouse line of the oxytocin receptor. Endocrinology *149*, 3256-3263.

Li, Y., Shiels, A.J., Maszak, G., and Byron, K.L. (2001). Vasopressin-stimulated Ca2+ spiking in vascular smooth muscle cells involves phospholipase D. American journal of physiology Heart and circulatory physiology *280*, H2658-2664.

Lin, Y.T., Hsieh, T.Y., Tsai, T.C., Chen, C.C., Huang, C.C., and Hsu, K.S. (2018). Conditional Deletion of Hippocampal CA2/CA3a Oxytocin Receptors Impairs the Persistence of Long-Term Social Recognition Memory in Mice. The Journal of neuroscience : the official journal of the Society for Neuroscience *38*, 1218-1231.

Maggio, N., and Segal, M. (2007). Striking variations in corticosteroid modulation of long-term potentiation along the septotemporal axis of the hippocampus. The Journal of neuroscience : the official journal of the Society for Neuroscience *27*, 5757-5765.

McHugh, S.B., Fillenz, M., Lowry, J.P., Rawlins, J.N., and Bannerman, D.M. (2011). Brain tissue oxygen amperometry in behaving rats demonstrates functional dissociation of dorsal and ventral hippocampus during spatial processing and anxiety. The European journal of neuroscience *33*, 322-337.

Meira, T., Leroy, F., Buss, E.W., Oliva, A., Park, J., and Siegelbaum, S.A. (2018). A hippocampal circuit linking dorsal CA2 to ventral CA1 critical for social memory dynamics. Nature communications *9*, 4163.

Miranda, A.M., Bravo, F.V., Chan, R.B., Sousa, N., Di Paolo, G., and Oliveira, T.G. (2019). Differential lipid composition and regulation along the hippocampal longitudinal axis. Transl Psychiatry *9*, 144.

Mitre, M., Marlin, B.J., Schiavo, J.K., Morina, E., Norden, S.E., Hackett, T.A., Aoki, C.J., Chao, M.V., and Froemke, R.C. (2016). A Distributed Network for Social Cognition Enriched for Oxytocin Receptors. The Journal of neuroscience : the official journal of the Society for Neuroscience *36*, 2517-2535.

Morrison, J.J., Dearn, S.R., Smith, S.K., and Ahmed, A. (1996). Activation of protein kinase C is required for oxytocin-induced contractility in human pregnant myometrium. Human reproduction (Oxford, England) *11*, 2285-2290.

Moy, S.S., Nadler, J.J., Young, N.B., Perez, A., Holloway, L.P., Barbaro, R.P., Barbaro, J.R., Wilson, L.M., Threadgill, D.W., Lauder, J.M.*, et al.* (2007). Mouse behavioral tasks relevant to autism: phenotypes of 10 inbred strains. Behavioural brain research *176*, 4-20.

Nabavi, S., Fox, R., Proulx, C.D., Lin, J.Y., Tsien, R.Y., and Malinow, R. (2014). Engineering a memory with LTD and LTP. Nature *511*, 348-352.

Nadler, J.V., Perry, B.W., and Cotman, C.W. (1978). Intraventricular kainic acid preferentially destroys hippocampal pyramidal cells. Nature *271*, 676-677.

Nakashiba, T., Cushman, J.D., Pelkey, K.A., Renaudineau, S., Buhl, D.L., McHugh, T.J., Rodriguez Barrera, V., Chittajallu, R., Iwamoto, K.S., McBain, C.J.*, et al.* (2012). Young dentate

granule cells mediate pattern separation, whereas old granule cells facilitate pattern completion. Cell *149*, 188-201.

Nakashiba, T., Young, J.Z., McHugh, T.J., Buhl, D.L., and Tonegawa, S. (2008). Transgenic inhibition of synaptic transmission reveals role of CA3 output in hippocampal learning. Science (New York, NY) *319*, 1260-1264.

Naro, F., Donchenko, V., Minotti, S., Zolla, L., Molinaro, M., and Adamo, S. (1997). Role of phospholipase C and D signalling pathways in vasopressin-dependent myogenic differentiation. Journal of cellular physiology *171*, 34-42.

Okuyama, T., Kitamura, T., Roy, D.S., Itohara, S., and Tonegawa, S. (2016). Ventral CA1 neurons store social memory. Science (New York, NY) *353*, 1536-1541.

Oliveira, T.G., Chan, R.B., Tian, H., Laredo, M., Shui, G., Staniszewski, A., Zhang, H., Wang, L., Kim, T.W., Duff, K.E.*, et al.* (2010). Phospholipase d2 ablation ameliorates Alzheimer's disease-linked synaptic dysfunction and cognitive deficits. The Journal of neuroscience : the official journal of the Society for Neuroscience *30*, 16419-16428.

Pagani, J.H., Zhao, M., Cui, Z., Avram, S.K., Caruana, D.A., Dudek, S.M., and Young, W.S. (2015). Role of the vasopressin 1b receptor in rodent aggressive behavior and synaptic plasticity in hippocampal area CA2. Mol Psychiatry *20*, 490-499.

Panda, A., Thakur, R., Krishnan, H., Naik, A., Shinde, D., and Raghu, P. (2018). Functional analysis of mammalian phospholipase D enzymes. Bioscience reports *38*.

Pinto, V., Costa, J.C., Morgado, P., Mota, C., Miranda, A., Bravo, F.V., Oliveira, T.G., Cerqueira, J.J., and Sousa, N. (2015). Differential impact of chronic stress along the hippocampal dorsal-ventral axis. Brain structure & function *220*, 1205-1212.

Piskorowski, R.A., Nasrallah, K., Diamantopoulou, A., Mukai, J., Hassan, S.I., Siegelbaum, S.A., Gogos, J.A., and Chevaleyre, V. (2016). Age-Dependent Specific Changes in Area CA2 of the Hippocampus and Social Memory Deficit in a Mouse Model of the 22q11.2 Deletion Syndrome. Neuron *89*, 163-176.

Raam, T., McAvoy, K.M., Besnard, A., Veenema, A.H., and Sahay, A. (2017). Hippocampal oxytocin receptors are necessary for discrimination of social stimuli. Nature communications *8*, 2001.

Roy, D.S., Kitamura, T., Okuyama, T., Ogawa, S.K., Sun, C., Obata, Y., Yoshiki, A., and Tonegawa, S. (2017). Distinct Neural Circuits for the Formation and Retrieval of Episodic Memories. Cell *170*, 1000-1012.e1019.

Santa-Marinha, L., Castanho, I., Silva, R.R., Bravo, F.V., Miranda, A.M., Meira, T., Morais-Ribeiro, R., Marques, F., Xu, Y., Point du Jour, K.*, et al.* (2020). Phospholipase D1 Ablation Disrupts Mouse Longitudinal Hippocampal Axis Organization and Functioning. Cell reports *30*, 4197-4208.e4196.

Shah, S., Lubeck, E., Zhou, W., and Cai, L. (2017). seqFISH Accurately Detects Transcripts in Single Cells and Reveals Robust Spatial Organization in the Hippocampus. Neuron *94*, 752-758.e751.

Silva, B.A., Burns, A.M., and Gräff, J. (2019). A cFos activation map of remote fear memory attenuation. Psychopharmacology *236*, 369-381.

Sloviter, R.S., and Damiano, B.P. (1981). Sustained electrical stimulation of the perforant path duplicates kainate-induced electrophysiological effects and hippocampal damage in rats. Neuroscience letters *24*, 279-284.

Smith, A.S., Williams Avram, S.K., Cymerblit-Sabba, A., Song, J., and Young, W.S. (2016). Targeted activation of the hippocampal CA2 area strongly enhances social memory. Mol Psychiatry *21*, 1137-1144.

Stackman, R.W., Jr., Cohen, S.J., Lora, J.C., and Rios, L.M. (2016). Temporary inactivation reveals that the CA1 region of the mouse dorsal hippocampus plays an equivalent role in the retrieval of long-term object memory and spatial memory. Neurobiology of learning and memory *133*, 118-128.

Strange, B.A., Witter, M.P., Lein, E.S., and Moser, E.I. (2014). Functional organization of the hippocampal longitudinal axis. Nature reviews Neuroscience *15*, 655-669.

Takayanagi, Y., Yoshida, M., Bielsky, I.F., Ross, H.E., Kawamata, M., Onaka, T., Yanagisawa, T., Kimura, T., Matzuk, M.M., Young, L.J.*, et al.* (2005). Pervasive social deficits, but normal parturition, in oxytocin receptor-deficient mice. Proceedings of the National Academy of Sciences of the United States of America *102*, 16096-16101.

Talley, E.M., Solorzano, G., Lei, Q., Kim, D., and Bayliss, D.A. (2001). Cns distribution of members of the two-pore-domain (KCNK) potassium channel family. The Journal of neuroscience : the official journal of the Society for Neuroscience *21*, 7491-7505.

Thompson, C.L., Pathak, S.D., Jeromin, A., Ng, L.L., MacPherson, C.R., Mortrud, M.T., Cusick, A., Riley, Z.L., Sunkin, S.M., Bernard, A.*, et al.* (2008). Genomic anatomy of the hippocampus. Neuron *60*, 1010-1021.

Tsien, J.Z., Huerta, P.T., and Tonegawa, S. (1996). The essential role of hippocampal CA1 NMDA receptor-dependent synaptic plasticity in spatial memory. Cell *87*, 1327-1338.

Vermeren, M.M., Zhang, Q., Smethurst, E., Segonds-Pichon, A., Schrewe, H., and Wakelam, M.J. (2016). The Phospholipase D2 Knock Out Mouse Has Ectopic Purkinje Cells and Suffers from Early Adult-Onset Anosmia. PloS one *11*, e0162814.

Wang, W., Kiyoshi, C.M., Du, Y., Taylor, A.T., Sheehan, E.R., Wu, X., and Zhou, M. (2020). TREK-1 Null Impairs Neuronal Excitability, Synaptic Plasticity, and Cognitive Function. Molecular neurobiology *57*, 1332-1346.

Wersinger, S.R., Ginns, E.I., O'Carroll, A.M., Lolait, S.J., and Young, W.S., 3rd (2002). Vasopressin V1b receptor knockout reduces aggressive behavior in male mice. Mol Psychiatry *7*, 975-984.

Wersinger, S.R., Temple, J.L., Caldwell, H.K., and Young, W.S., 3rd (2008). Inactivation of the oxytocin and the vasopressin (Avp) 1b receptor genes, but not the Avp 1a receptor gene, differentially impairs the Bruce effect in laboratory mice (Mus musculus). Endocrinology *149*, 116-121.

Yao, Y., Wang, X., Li, H., Fan, J., Qian, X., Li, H., and Xu, Y. (2020). Phospholipase D as a key modulator of cancer progression. Biological reviews of the Cambridge Philosophical Society.

Yoshida, M., Takayanagi, Y., Inoue, K., Kimura, T., Young, L.J., Onaka, T., and Nishimori, K. (2009). Evidence that oxytocin exerts anxiolytic effects via oxytocin receptor expressed in serotonergic neurons in mice. The Journal of neuroscience : the official journal of the Society for Neuroscience *29*, 2259-2271.

Young, W.S., Li, J., Wersinger, S.R., and Palkovits, M. (2006). The vasopressin 1b receptor is prominent in the hippocampal area CA2 where it is unaffected by restraint stress or adrenalectomy. Neuroscience *143*, 1031-1039.

Zhang, W.N., Bast, T., and Feldon, J. (2001). The ventral hippocampus and fear conditioning in rats: different anterograde amnesias of fear after infusion of N-methyl-D-aspartate or its noncompetitive antagonist MK-801 into the ventral hippocampus. Behavioural brain research *126*, 159-174.

Zhao, M., Choi, Y.S., Obrietan, K., and Dudek, S.M. (2007). Synaptic plasticity (and the lack thereof) in hippocampal CA2 neurons. The Journal of neuroscience : the official journal of the Society for Neuroscience *27*, 12025-12032.

CHAPTER 3 – Supplementary Information

Phospholipase D2 ablation leads to deficits in social memory

(Manuscript to be submitted)

Luísa Santa-Marinha,[1,2] Francisca Vaz Bravo,[1,2] André Miguel Miranda[1,2], Torcato Meira,[1,2] Vítor Pinto,[1,2] and Tiago Gil Oliveira [1,2]

[1]Life and Health Sciences Research Institute (ICVS), School of Medicine, University of Minho, Campus Gualtar, 4710-057 Braga, Portugal

[2]ICVS/3B's - PT Government Associate Laboratory, Braga/Guimarães, Portugal

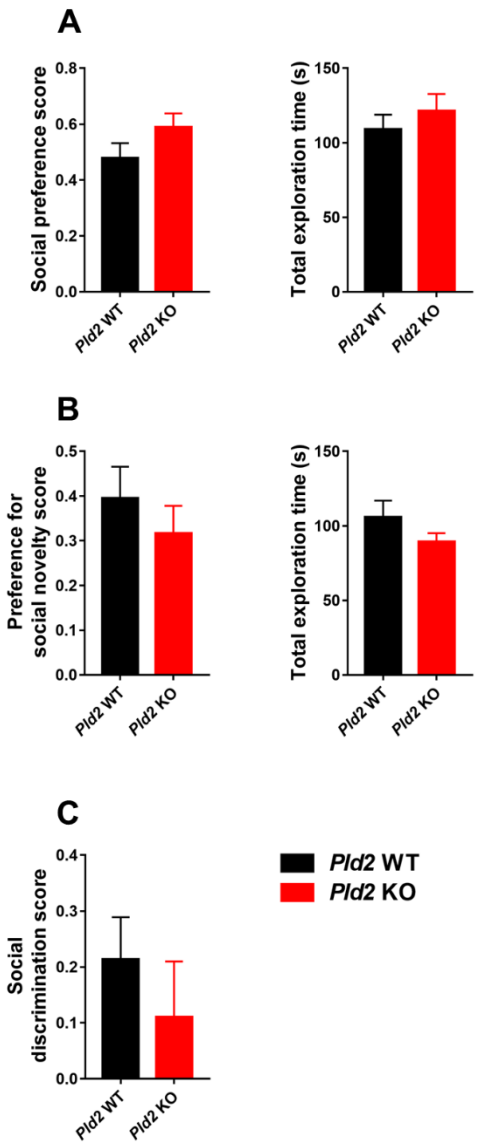

Figure S1 – Supplementary behavior analysis. Related to Figure 1

(A) Three-chamber sociability test social preference score and total exploration time.

(B) Three-chamber preference for social novelty test preference for social novelty scored and total exploration time. Social preference and preference for social novelty scores were calculated as the difference between the time spent exploring the cups placed on the side chambers, divided by the total time exploring both (n_{WT} = 10, n_{KO} = 12).

(C) Three-chamber social discrimination test social discrimination score. Social discrimination score was calculated as the difference between the time spent exploring the cups placed on the side chambers, divided by the total time exploring both (n_{WT} = 13, n_{KO} = 13).

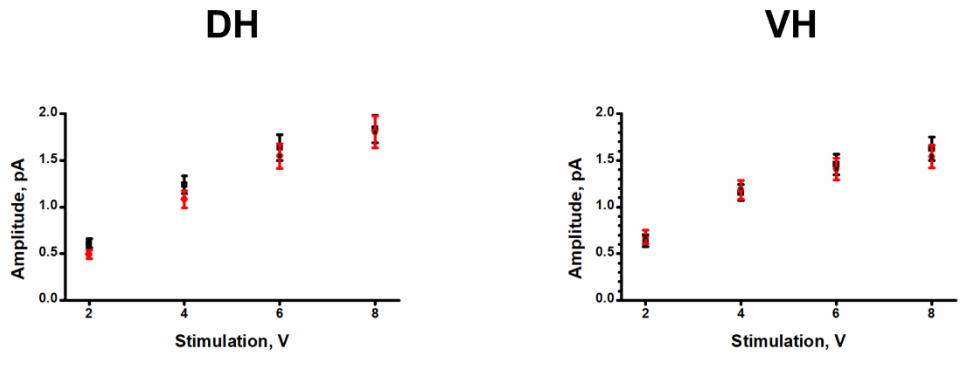

Figure S2 – PLD2 ablation has no effect in input-output recordings. Related to Figure 2.

Input-output recordings. Crescent stimuli were given in acute slices of DH (left panel) (n_{WT} = 20, n_{KO} = 14) and VH (right panel) (n_{WT} = 16, n_{KO} = 17). The bars represent mean±SEM.

CHAPTER 4

General Discussion

The hippocampus is a brain temporal lobe structure present in all mammals, fundamental for learning, memory and spatial navigation (Strange et al., 2014). Taking into account anatomical, gene expression and functional studies, it is now known that the hippocampus has an organized gradient along its longitudinal axis, segregating into its dorsal (DH) and ventral (VH) poles, with different physiological and pathological importance (Strange et al., 2014). Despite running along this DH-VH axis, its cross-sectional architecture, which consists of the dentate gyrus (DG) and the hippocampus proper – Cornu Ammonis (CA) - CA1, CA2 and CA3, is preserved.

The great advances in genomics, proteomics and lipidomics allow us to expand our knowledge regarding life molecular composition. In particular, with the emergence of tools such as nuclear magnetic resonance, chromatographic tools and mass spectrometry (MS)-based lipidomics, it was possible to broaden our knowledge regarding lipids (Wenk, 2005). Lipids are essential for all aspects of life, with an important role in the pathology of neurodegeneration, neuroinflammation, psychiatric, infectious and metabolic diseases, cancer, among many other disorders. In the brain, lipids are major constituents, since half of the human brain dry weight is represented by lipids (Piomelli et al., 2007).

Phospholipases are lipid-modulator enzymes that can remodel the structure of glycerophospholipids and generate second messengers. Specifically, phospholipase D (PLD) is mainly known for hydrolyzing the phosphodiester bond, in the presence of water, of phosphatodylcholine (PC) and generate phosphatidic acid (PA) , a second messenger signaling lipid, and free choline (Jenkins and Frohman, 2005; Oliveira et al., 2010b). However, in the presence of primary alcohols, PLD preferentially uses these as a substrate, leading to the formation of a specific phosphatidylalcohol, such as phosphatidylethanol (PEtOH) in the presence of ethanol and this property has been used to measure PLD activity (Gustavsson, 1995; Oliveira et al., 2010b; Scott et al., 2013).

Lipidomic studies have been unveiling the importance of how lipid modulation can impact brain functioning in physiological and pathological conditions, namely stress and Alzheimer's disease (AD) (Chan et al., 2012; Miranda et al., 2019; Oliveira et al., 2016; Oliveira et al., 2010b). A recent study topographically characterized the differential lipid composition and regulation along the hippocampal longitudinal axis, making use of an unbiased MS approach to characterize the lipid composition of distinct hippocampal subregions (Miranda et al., 2019). It was observed greater similarity between the different hippocampal subregions when compared to other brain

regions (Miranda et al., 2019). Within the hippocampus, there was a continuous molecular gradient along the longitudinal axis, with the DH and VH extremities differing significantly from each other, mostly in the relative abundance of sphingolipids and phospholipids, making lipid composition a molecular marker of the different sections of the hippocampus (Miranda et al., 2019). In particular, the DH presented increased PA and decreased PC when compared to the VH, potentially implicating the PLD pathway in DH-VH axis regulation (Miranda et al., 2019). In the same study, chronic corticosterone administration (used in this study as a model of chronic stress) led to differential DH-VH modulation of PA levels, also suggesting differential recruitment of PA-modulating enzymes, such as PLD, in DH-VH dysfunction (Miranda et al., 2019). With all the previously exposed, our main goal was to study the impact of PLD genetic modulation on the DH-VH axis organization and function.

PLD exists in virus, bacteria, plants and lower and higher eukaryotes. While in invertebrates there is only one *Pld* gene, in chordates there is an evident evolutionary burden, with other *Pld* superfamily genes arising (Panda et al., 2018). In budding yeast, PLD (spo14) is essential for meiosis and sporulation (Rose et al., 1995). In the nematode *Caenorhabditis elegans* (*C. elegans*) there is only one *Pld* gene, important for longevity and biometry (Bravo et al., 2018). In *Drosophila melanogaster* there is also only a single *Pld* gene (d*Pld*), functioning as photoreceptor and acting on phototransduction (Raghu et al., 2009a; Thakur et al., 2016). When looking into higher eukaryotes, it is known that mammals have six PLD isoforms (PLD1-PLD6), which have in common the presence of HxKxxxxD (HKD) domains (Barber et al., 2018; Frohman, 2015). Despite this, only PLD1 and PLD2 fulfill the canonical PLD activity (hydrolyzing PC into PA) (Nelson and Frohman, 2015), but they still present differences in their structure, cellular localization and regulators of their catalytic activities (Colley et al., 1997; Hiroyama and Exton, 2005; Jenkins and Frohman, 2005; Liscovitch et al., 1999; Oliveira et al., 2010b; Selvy et al., 2011).

Panda et. al recently performed a phylogenetic analysis that revealed that PLD1 sequences of chordates are evolutionarily closer to insect PLD sequences than the PLD2 subcluster (Panda et al., 2018). In fact, overexpression of hPLD1 in *Drosophila* led to light-dependent retinal degeneration, which phenocopied the overexpression of dPLD and this was not reproduced with overexpression of hPLD2, suggesting that PLD1 and PLD2 have different functions in this process (Panda et al., 2018). Moreover, transgenic overexpression of the mammalian hPLD1 was able to rescue the retinal degeneration of a *Drosophila* PLD loss of function model (*dPLD*$^{3.1}$), that has no

residual PLD activity, better than the reconstitution with hPLD2 (Panda et al., 2018). Another interesting fact was that, when comparing the localization of dPLD, hPLD1, and hPLD2 in photoreceptors, dPLD and hPLD1 are uniquely distributed in the subplasma membrane region (Panda et al., 2018).

PLD deficiency leads to apparent normal development of organisms (Bravo et al., 2018; Oliveira et al., 2010b; Panda et al., 2018). One possibility is that other sources of PA, such as diacylglycerol (DAG) kinases (DGK) and lyso-PA (LPA) acyltransferase (LPAAT), can compensate the lack of PLD (Oliveira and Di Paolo, 2010). But when we look closely to anatomical and physiological features, animal behavior and functioning under stress and disease, we observe relevant phenotypes upon PLD ablation. For example, yeast lacking the heterologous *Pld* gene do not exhibit any phenotype during vegetative growth, only during meiosis and sporulation (Rose et al., 1995). In the *C. elegans*, the lack of *pld* results in decreased levels of PA and PLD activity (Bravo et al., 2018) and PLD downregulation shortens longevity and induces age-related biomarkers through reactive oxygen species accumulation (Park et al., 2018). There are two PLD genes in zebrafish *Danio rerio* (*pld1* and *pld2*) (Raghu et al., 2009b) and manipulation of PLD1 in zebrafish results in intersegmental vascular pattern defects (Zeng et al., 2009). In *Drosophila melanogaster* the loss of function of the only *Pld* gene results in reduced PA levels (Panda et al., 2018) and in defects in vesicular transport that lead to collapse of the photoreceptor plasma membrane (Thakur et al., 2016). In mice, PLD ablation is responsible for behavior impairment (as discussed below) (Burkhardt et al., 2014). On the other hand, PLD overexpression also produces relevant phenotypes. It alters vesicular transport in cultured mammalian cells (Cai et al., 2006b; Choi et al., 2002; Huang et al., 2005; Vitale et al., 2001) and overexpression of dPLD in *Drosophila* results in a progressive collapse of the apical domain of these cells (retinal degeneration) (Panda et al., 2018). Also, overexpression of PLD1 decreases the levels of amyloid beta (Aβ) (Cai et al., 2006a) and promotes the formation of amyloid precursor protein (APP)-containing secretory vesicles from trans-Golgi network and inhibition of PLD1 activity decreases APP trafficking (Cai et al., 2006b), in the context of AD, as discussed below.

In order to study the impact of PLD ablation, namely in the modulation of the longitudinal hippocampal axis, we made use of adult mice knock-out (KO) for *Pld1* and/or *Pld2* genes (we should have in mind that we cannot exclude the possibility that our results could be affected by an early developmental PLD deficits). We confirmed the lack of the corresponding isoenzyme in

these mice by western blot analysis, using an antibody that recognizes the COOH terminus of both PLD1 and PLD2 isoenzymes. *Pld1* KO animals express only PLD2, *Pld2* KO animals express only PLD1 enzyme, and *Pld* double-KO (DKO) animals have no PLD1 or PLD2 expression (see Chapter 2, figure 1A). As an approach to understand the differences between the two canonical mammalian PLD isoenzymes we used a method to study *in vivo* PLD activity performed by Oliveira et al (Oliveira et al., 2010b). By making use of the ability of PLD1 and PLD2 to use primary alcohols as nucleophiles over water in a transphosphatidylation, we injected mice with ethanol and then sacrificed to measure the levels of PEtOH with liquid chromatography-MS in the forebrain, in order to measure PLD activity (see Chapter 2, figures 1B and S1). With this experiment we confirmed that PLD1 and PLD2 are likely the only canonical PLD isoenzymes, since *Pld* DKO had almost no detectable PEtOH, indicating that PEtOH is exclusively produced by PLD1 and PLD2 and that the other PLD superfamily members (PLD3-6) do not contribute to the production of PEtOH (see Chapter 2, figures 1B and S1).

Then, we conducted a broad-scale lipidomic profiling of DH and VH from both *Pld1* and *Pld2* WT and KO mice and analyzed the relative abundance of a total of 30 lipid classes, covering the 3 main lipid categories of sterols, sphingolipids, and glycerophospholipids (see Chapter 2, Figure 1C and Table S1). Once more we observed that PLD1 ablation creates a higher burden than PLD2 ablation, since PLD2 ablation did not have a significant impact on the total levels of the lipid classes analyzed (see Chapter 2, Figure 1C and Table S1) and PLD1 ablation significantly decreased the levels of several lipid classes (see Chapter 2, Figure 1C and Table S1), with a higher impact on the DH compared to VH, which is relatable with PLD1 protein levels being higher in the DH when compared to the VH (see Chapter 2, Figure S3B). The lack of PLD1 decreased the levels of PA, monoacylglycerol (MG) and lysoglycerophospholipids such as lysophosphatidylcholine (LPC), ether lysophosphatidylcholine (LPCe), and lysophosphatidylinositol (LPI) in the DH and the levels of PA and dihydroceramide (dhCer) in the VH (see Chapter 2, Figure 1C and Table S1). We should consider potential crosstalk between different phospholipases, that cleave the various bonds in phospholipids, namely phospholipase A (PLA_2) superfamily that catalyze the hydrolysis of the sn-2 ester bond in a variety of different phospholipids, producing free fatty acids, such as arachidonic acid (AA), and lysophospholipids (Burke and Dennis, 2009), phospholipase C (PLC) that cleave the phosphodiester bond on the glycerol side forming diacylglycerols and a phospho-base, and PLD (Farooqui et al., 2000). Crosstalk between PLA_2, PLC and PLD isozymes is crucial for maintaining normal homeostasis.

PLA_2 reactions, resulting in free fatty acids, PLC reactions, resulting in DAG, and PLD catalyzed reactions, synergistically stimulate PKC activity (Farooqui and Horrocks, 2005). PLD and DAG generated by PLC stimulate various isoforms of protein kinase C (PKC), which activates both PLA_2 and PLD (Clark et al., 1995; Farooqui and Horrocks, 2005). In addition, AA and eicosanoids produced by PLA_2 activate isoforms of PLC, PLD, and PKC (Klein et al., 1995). In fact, co-expression of cytosolic ($cPLA_2$) or type IIA secretory ($sPLA_2$-IIA) PLA_2 and PLD2, but not PLD1, augmented stimulus-induced arachidonate acid release (indicative of PLA_2 activity) (Ueno et al., 2000). This justifies the observed lipidomic alterations in upon PLD1 ablation.

While PLD2 ablation did not affect the levels of total PA in both DH and VH, PLD1 ablation led to a great decrease in the total levels of PA (see Chapter 2, Figure 1C and Table S1), in accordance with the observation of *Pld1* KO animals having a greater decrease in PLD activity when compared to *Pld2* KO animals (see Chapter 2, figure 1B) and in agreement with previous studies (Vermeren et al., 2016). The analysis of PA species upon ablation of either PLD1 or PLD2 revealed that *Pld1* KO animals have decreased levels of nearly all PA species detected in both DH and VH, while PLD2 ablation leads to the decrease in only 3 PA species in the VH and an increase in 1 in DH, proving once more that PLD1 is a major contributor to total PA levels when compared to PLD2 (see Chapter 2, Figure 1D and Table S2). These findings indicate that PLD1 and PLD2 modulate different PA pools, which might account for or contribute to the differential functions of PLD1 and PLD2. Curiously, work from Panda et al. with overexpression of human PLD in a *Drosophila* model with dPLD loss of function ($dPLD^{3.1}$) also showed that hPLD1 and hPLD2 produce distinct molecular species of PA (Panda et al., 2018). They found that most of the PA species that were lower in $dPLD^{3.1}$ were mostly reconstituted by dPLD (Panda et al., 2018). When reconstituted with human PLD, the pattern of species restored by PLD1 expression was substantially more similar to the observed in wild-type (WT) than that observed with overexpression of PLD2 (Panda et al., 2018). Different PA species exhibit different structure, which is related to the acyl chain length and unsaturation of the fatty acyl chain at sn-1 and sn-2 positions, leading to distinct repercussion on membrane structure, for example membrane curvature (van Meer, 2005). It was shown recently that PA saturation level influences its functions in neurosecretory pathway. While mono-unsaturated PA regulates the number of exocytotic events, poly-unsaturated PA regulates fusion pore stability and expansion (Tanguy et al., 2020a). Another interesting finding was that PLD1 affects both shorter and longer fatty acyl carbon length PA species, while PLD2 modulates predominantly shorter fatty acyl carbon length

PA species (see Chapter 2, Figures 1D and Table S2). It is known that shorter chain PA may promote membrane curvature and, curiously, PLD2 is primarily find in the plasma membrane.

Several findings in our work also led us to hypothesize that there is a compensatory process by either PLD1 or PLD2 upon the other enzyme ablation: the sum of the decrease PEtOH production upon PLD1 and PLD2 ablation was less than 100% (see Chapter 2, figure 1B) and PLD2 ablation leads to increased levels of 4 PEtOH species (see Chapter 2, figure S1) and increased levels of one PA specie (see Chapter 2, figure 1D). We decided to explore the levels *Pld1*/PLD1 and *Pld2*/PLD2 mRNA (see Chapter 2, figure S2) and protein levels (see Chapter 2, figure S3) and conclude that ablating either of the PLD isoenzymes does not lead to expression upregulation of the other. One could consider other compensatory mechanisms such as localization modification, differences in co-factor modulation or post-translational modifications, such as histone acetylation, ubiquitination, phosphorylation or glycosylation. For example post-translational modification such as phosphorylation has been shown to regulate Spo14 localization and some bacterial toxins can regulate enzyme expression by modulating histone acetylation, which downregulates the NAPE-PLD (another human enzyme that exhibits PLD-like phosphodiesterase activity) promoter (Selvy et al., 2011). Moreover PLD activity *in vivo* is mediated by cellular calcium fluctuations and recruitment of PLD upon phosphatidylinositol bisphosphate or triphosphate (PIP_2 or PIP_3) production allows upstream lipid kinases or phosphatases to mediate PLD lipase activity (Selvy et al., 2011). Another fact is that PLD1 and PLD2 are phosphorylated in response to signal transduction as a regulatory mechanism and are post-translationally palmitoylated at two cysteine residues in the pleckstrin homology (PH) domain, which facilitates protein sorting into specific intracellular and plasma membrane domains including lipid rafts (Selvy et al., 2011). Interestingly, PLD1, but not PLD2, is post-translationally modified by multi-monoubiquitination, which is important for modulating the localization and curbing lipase activity, and suppression of lipase activity either by mutation of the HKD motif or the phosphatidylinositol 4,5-bisphosphate binding motif or through use of PLD-selective inhibitors impairs the ubiquitination of PLD1 (Yin et al., 2010).

Several methods have been used to study PLD activation and PLD-derived PA. Fluorescent protein fusions can localize PLD1 and PLD2, but do not differentiate their activation state. Genetically encoded probes directly visualize PA, although they cannot distinguish between different biosynthetic pools of PA. New tools for visualizing PLD signaling and PA are now emerging, in an attempt to tackle up and downstream PLD activation and the crosstalk and

compensation between PA synthesizing pathways. Raghu and colleagues applied a method of high performance liquid chromatography (HPLC)-coupled MS to determine the acyl chain composition of PA species at the *sn*–1 and *sn*–2 position, depending on ions generated by fragmentation of the corresponding PA anions that correspond to loss of one of the acyl chains. This enable assumption of the chain length and saturation of the individual fatty acid substituents in the parent phosphatidic acid molecule (Panda et al., 2018). It was also developed a chemoenzymatic, activity-based imaging method to visualize the precise subcellular locations of PLD activity with high spatiotemporal resolution, called IMPACT (Imaging Phospholipase D Activity with Clickable Alcohols via Transphosphatidylation) (Bumpus and Baskin, 2017). It relies on the PLD ability to accept azidoalcohols as reporters in a transphosphatidylation reaction and the resultant azidolipids are then fluorescently tagged, which allows visualization of cellular membranes bearing active PLD enzymes (Bumpus and Baskin, 2017). Moreover, the same laboratory created optogenetic controlled PLD (optoPLD), which is a complementary method for generating, rather than visualizing, organelle-specific PA pools (Tei and Baskin, 2020).

Although PLD1 and PLD2 catalyze the same reaction, clearly the loss of function of one and/or another generate different repercussions on hippocampal lipidome and different phenotypes (see chapter 1), therefore dismantling the idea of absolute enzyme redundancy. PLD1 and/or PLD2 deficient mice have been proposed to show reduced brain growth at 14-27 days after birth (Burkhardt et al., 2014) and *Pld2* KO mice have olfactory defects and an increased number of ectopic cerebellar Purkinje cells after 13 weeks of age (Vermeren et al., 2016). Moreover, Burkhardt et al. showed a deficit in the level of discrimination in long-term novel object recognition (NOR) test in *Pld2* and double *Pld* KO and a social recognition deficit in *Pld1* and/or *Pld2* KO (Burkhardt et al., 2014). Other authors showed that PLD2 ablation had no major behavioral deficits: Oliveira et al., evaluated spatial working memory (using a radial arm water maze paradigm) and contextual fear conditioning memory (Oliveira et al., 2010b) and Vermeren at. al evaluated rotarod and open field on *Pld2* KO animals (Vermeren et al., 2016). In chapter 2 (Santa-Marinha et al., 2020), we showed that PLD1 ablation impairs short-term object recognition memory and social exploration, since *Pld1* KO mice were less social in a hippocampus-dependent task, spending less time exploring compared to WT. In chapter 3, we showed that PLD2 ablation leads to social discrimination deficits with deficient ability to recognize a littermate and were less social in the same a hippocampus-dependent task.

Previously, Burkhardt et al. performed a partial characterization of behaviors upon ablation PLD1 and/or PLD2 in mice. Long term memory evaluated by NOR test was performed with a day-interval between exposing the animal to two equal objects and then adding a third novel (Burkhardt et al., 2014) (different from our NOR test that tested short term memory with an inter-trial of 1h). Short term memory evaluated as preference for social novelty was performed exposing an animal to an empty cage and a cage with an unknown mouse and then, after a 15 min break, a novel mouse was placed in previously empty cage and time interacting was counted (Burkhardt et al., 2014) (different from our preference for social novelty test with no inter-trial interval between the two trials). While *Pld1* KO mice showed a trend toward a deficit in the level of discrimination in long-term NOR and a preference for social novelty deficit, PLD2 deficiency caused severe impairments on preference for social novelty and object recognition (Burkhardt et al., 2014). This work is not in total agreement with ours. Although PLD1 and PLD2 ablation led to decreased social exploration, the ability to prefer a novel mouse instead of a previously met (preference for social novelty) was not impaired. One potential caveat to consider as an explanation for the partial differences in observed results could be due to the different protocols used and to not using littermate mice as controls by Burkhardt et al..

Concerning the integration of the behavioral alterations with other phenotypic alterations observed by us, the social and object recognition deficits of *Pld1* KO animals were associated with LTD decreased induction (See Chapter 2, Figure 4B, left panel) and decrease of synaptic proteins levels, namely SNAP-25 and GluN2A, in DH (see Chapter 2, Figure 5). Dorsal CA1 inhibition with muscimol, a selective GABAA receptor agonist that temporarily interrupt its function, was also shown to impair spatial and object memory (Stackman et al., 2016), although some studies conclude that the association of DH and object recognition is due to object-place recognition (Mendez et al., 2015; Oliveira et al., 2010a). It was also previously shown a role for CA1 and LTD in the acquisition of object–place configuration. Hippocampal LTD induction was associated with exploration of a new environment containing unfamiliar objects and/or familiar objects, whereas exploration of the new environment itself, in the absence of objects, impairs LTD (Kemp and Manahan-Vaughan, 2004). It agreement with our work, SNAP-25 heterozygous mice have a worse performance in the recognition of a novel object in a NOR protocol with 2h inter-trial interval and also have deficits in social behavior, with no deficits in spatial learning and memory tasks (Corradini et al., 2014). In addition to decreased levels of SNAP-25, *Pld1* KO mice have reduced LTD induction in DH, which can also be caused by the reduced levels of SNAP-25.

In fact, infusion with a C-terminal SNAP-25 fragment (proposed to block its normal functions) reduces CA3-CA1 LTD induction, but not LTP (Zhang et al., 2011) and LTD is decreased in corticostriatal preparations of SNAP-25 heterozygous mice (Baca et al., 2013). Deficits in social behavior are also associated with impaired NMDAR-mediated neurotransmission, namely with GluN2A receptors (Zoicas and Kornhuber, 2019). For example, administratioin of PEAQX, a GluN2A-preferring antagonist, decreases social interaction in adolescent rats (Green et al., 2016; Morales and Spear, 2014). On the other hand, transgenic overexpression of GluN2A in forebrain, with an increased GluN2A: GluN2B ratio, leads to reduced long-term memory function and long-term memory impairments in a olfactory recognition task. (Jacobs and Tsien, 2014). The dynamic regulation and the combination of GluN2A and GluN2B subunits are crucial for physiological properties of NMDARs and should be evaluated.

While the social and object recognition deficits caused by PLD1 ablation were correlated with the decrease of LTD (See Chapter 2, Figure 4B, left panel) and decrease of synaptic proteins in DH (see Chapter 2, Figure 5), the social deficits in *Pld2* KO animals were associated with decreased LTP in VH (see Chapter 3, Figure 2A, right panel) without alterations in synaptic proteins (see Chapter 3, Figure 3). The lack of PLD2 did not interfere with sociability and preference for social novelty (see Chapter 3, Figure 1B, 1C, S1A and S1B) but *Pld2* KO mice lost the ability to discriminate between a littermate and a strange mouse and spent less time interacting with conspecifics in this social discrimination task (see Chapter 3, Figure 1D and S1C). Curiously, the loss of the ability to discriminate between a littermate and a novel subject phenocopies the silencing of dorsal CA2 (Meira et al., 2018), proposing a mechanism of CA2 dysfunction in *Pld2* KO animals. CA2 is a hippocampal region with distinct features from CA1 and CA3, from synaptic connectivity and electrophysiological characteristics to gene expression profile and relative resistance to cell death and resistance to damage from injury and synaptic plasticity (Dudek et al., 2016; Nadler et al., 1978; Sloviter and Damiano, 1981; Zhao et al., 2007). Several classes of proteins are particularly enriched in CA2. In fact, *in situ* hybridization revealed that PLD2 is highly expressed in CA2 when compared to CA1 and CA3 (Vermeren et al., 2016). Arginine vasopressin (AVP) and oxytocin (OXT) are two hypothalamic produced neuropeptides and AVP receptor 1b (AVPR1b) and OXT receptor (OXTR) also highly expressed in CA2 pyramidal neurons (Hammock and Levitt, 2013; Hidema et al., 2016; Mitre et al., 2016; Yoshida et al., 2009; Young et al., 2006). Modification or alteration on OXT/OXTR or AVPR1b have an impact on social behavior. Decreased levels of OXT and OXTR lead to social deficits and poor social

recognition (Lee et al., 2008; Takayanagi et al., 2005) and DG and CA2/CA3 OXTR are indispensable for discrimination of social stimuli (Raam et al., 2017) and long-term social recognition memory, without any effect on sociability and preference for social novelty (Lin et al., 2018). Moreover, AVPR1b KO mice display sociability and social memory impairments (DeVito et al., 2009; Wersinger et al., 2002; Wersinger et al., 2008). It is known that PLD activity is enhanced by AVP and OXT (Coletti et al., 2000; Inamori et al., 1995; Komati et al., 2005; Li et al., 2001; Morrison et al., 1996; Naro et al., 1997). In fact, AVP increases the PEtOH formation (indicating PLD activity) and inhibition of PLD decreases AVP produced PEtOH in cultures (Kusaka et al., 1996). Moreover, TWIK-related K+ channel (TREK) 1 is a PA-sensitive K2P channel that directly binds to PLD2 and, curiously, is also another protein highly expressed in CA2 (Talley et al., 2001). Importantly, PLD2 (and not PLD1) potentiates TREK1 current through local PA production that tonically activates the channel (Comoglio et al., 2014). An upregulated current of TREK1 channel in CA2 is found in Human 22q11.2 deletion syndrome (22q11.2DS) mouse model (Df(16)A+/−), also known as DiGeorge syndrome (the greatest molecular genetic risk factor for schizophrenia). These mice also show impaired social memory, phenocopying a silent CA2 (Piskorowski et al., 2016). As discussed below, TREK1 ablation in mice have decreased LTP in the CA1 region, similarly to VH of *Pld2* KO mice, associated with recognition memory deficits (Wang et al., 2020). Considering these associations already described between PLD and AVP/OXT/TREK1, we can speculate a dysregulation on these pathways, possibly in CA2, were they are highly expressed, thus leading to the CA2 dependent impairment of littermate recall phenotype observed in *Pld2* KO mice.

One of the most important characteristics of the mammalian brain is its plasticity. It has been proposed that associative memories are stored as changes in the strength of synaptic connections between neurons, also called synaptic plasticity (Bannerman et al., 2014; Citri and Malenka, 2008). The intrinsic functionally of DH and VH can also be demonstrated by the different properties of synaptic plasticity. In our work, the DH and VH of WT mice presented different ability to produce a PP response (See Chapter 2, Figure 4C and Chapter 3, Figure 2C), a reliable signature already reported in rats (Maggio and Segal, 2007; Pinto et al., 2015). We can hypothesize that this intrinsic variability could be related with the intrinsic synaptic protein levels in DH and VH of WT animals (See Chapter 2, Figure 5). For example, whole-life exposure in rats to perfluorooctane sulfonate, which decreases the mRNA levels of AMPA receptor subunits GluA1 and GluA2, moderately suppresses PP facilitation (Zhang et al., 2019) and a study to aim the

adverse effects of copper oxide nanoparticles administration to rats revealed decrease of both PP and expression of GluN2A, but not GluN2B (Li et al., 2018) in CA1 region.

We addressed the *ex vivo* impact of PLD removal in the trisynaptic circuit in the DH and VH poles. In chapter 2 we show that PLD1 ablation reduced LTD induction in the DH after low-frequency stimulation (See Chapter 2, Figure 4B, left panel). Recently, through the use of inhibitors and *Pld1* KO mice, it was shown that PLD1, but not PLD2, is necessary for M1 (subtype of muscarinic acetylcholine receptor)-LTD induction in the mouse prefrontal cortex (Moran et al., 2019), supporting our result of impairment of LTD in DH of *Pld1* KO animals. Moreover, mechanistic target of rapamycin complex 1 (mTORC1) activation through PA derived from PLD signaling is a regulator of homeostatic signaling and PLD1 overexpression is sufficient to activate mTORC1 and alter synaptic function in cultured hippocampal neurons (Henry et al., 2018). Modulation of mTOR also modifies macroautophagy, altering the presynaptic structure and neurotransmission (Hernandez et al., 2012). The role of PLD1 and SNAP-25 has also been described in the autophagy field, since the induction of SNAP-25 in cancer cells maintains autophagic flux and autolysosomal efflux (Mu et al., 2018) and PLD1 was suggested to regulate autophagy through a possible effect in the VPS34/PI(3)P pathway (Dall'Armi et al., 2010). More recently, the PLD pathway was shown to modulate the autophagy in retinal pigment epithelium cells (Bermúdez et al., 2019). We can then speculate that the decreased levels of SNAP-25 in the DH of *Pld1* KO animals may be an effector of the role of PLD1 as a modulator of autophagy.

Electrophysiological changes in the DH of mice lacking PLD1 were accompanied by decreased levels of SNAP-25 and GluN2A. As previously discussed, the reduced LTD induction in DH of *Pld1* KO mice could be caused by the decreased levels of SNAP-25, since blocking the normal functions of this protein reduces CA3-CA1 LTD induction (Zhang et al., 2011) and SNAP-25 heterozygous mice have decreased LTD in corticostriatal preparations (Baca et al., 2013). SNAP-25 is subject to alternative splicing, producing SNAP-25a (predominant isoform in neurons in mice during embryonic and early postnatal development) and SNAP-25b (the dominant isoform as central synapses mature into adulthood) (Gopaul et al., 2020). In the first two weeks of development, rodents exhibit predominantly, or entirely, metabotropic glutamate receptor (mGluR)-dependent forms of LTD of synaptic transmission (Gopaul et al., 2020). With the change in relative levels of SNAP-25a to SNAP-25b there is upregulation NMDARs, suggesting that SNAP-25a may play a greater role in the expression of mGluR-dependent LTD, while SNAP-25b may be more important for expression of NMDAR-dependent LTD and LTP (Gopaul et al., 2020). A recent

study showed that SNAP-25a favors the expression of LTD over LTP in the developing brain in one month old animals, while SNAP-25b deficient mice displayed similar LTD as their littermate controls (Gopaul et al., 2020). These results suggest that the balance between the two isoforms has an electrophysiological impact worthy of study in the future. Based on these recent observations, an important future experiment to be performed is to assess the balance of SNAP-25a and b in *Pld* KO models, as wells as their interaction with PLD. The balance of the levels of GluN2A has also been subject of studies with alterations in hippocampal synaptic properties. For example, an increase in GluN2A levels selectively alters long term memory formation and, although it abolishes one type of protocol of LTD induction, it has no effects in a protocol similar to ours in CA1 from hippocampal slices (Cui et al., 2013). Another interesting fact is that it has been shown that LTD between the amygdala and perirhinal cortex is induced presynaptically via GluN2A-containing NMDARs (Laing and Bashir, 2015). NMDARs mediate LTP and LTD, but inconsistent results have been published, some of them highlighting the balance of GluN2A/GluN2B and others dismissing these results (Shipton and Paulsen, 2014; Wong and Gray, 2018). Once again, the balance of GluN2A/GluN2B is also an interesting line of research to be explored in *Pld* KO models.

In chapter 3 we show that PLD2 ablation impairs LTP generation in the VH after tetanic stimulation (See Chapter 3, Figure 2A, right panel) at the Schaffer collaterals. Although previous work showed no differences in LTP upon PLD2 ablation in hippocampal slices, this experiment did not take into account DH-VH differentiation (Oliveira et al., 2010b). Moreover, dorsal CA2 (a region with high levels of PLD2, as discussed before) provides important social information to ventral CA1 to support social memory (Meira et al., 2018), a region that is impaired in *Pld2* KO mice, with decreased LTP (see Chapter 3, Figure 2A, right panel). OXT and AVPR1b (highly expressed in CA2 as discussed before) are also implicated in synaptic plasticity. While OXT transiently reduces synaptic inhibition in multiple brain regions and enables long-term synaptic plasticity in the auditory cortex (Mitre et al., 2016), selective activation of AVPR1b or OXTR agonists induces significant potentiation in excitatory synaptic responses in CA2, despite its resistance to LTP (Pagani et al., 2015). Moreover, TREK1 total ablation in mice results in decreased LTP in CA1 region, which phenocopies PLD2 ablation (Wang et al., 2020). Taking into account the interaction of these proteins with PLD2, one should consider that these interactions can be affected in *Pld2* KO mice, thus contributing to LTP impairment.

Dendritic trees are crucial for the neuronal input of information (for signal reception and signal integration), being critical for neuronal functioning and they are distinctive for each specific neuronal type (Jan and Jan, 2010). Dendritic spines connect with presynaptic terminals in order to match with each other correctly, leading to functional synapses (Luo et al., 2017). The number of synapses and spines reaches its maximum point in early childhood, followed by synaptic pruning during adolescence and stabilization in adulthood (Jan and Jan, 2010). Abnormalities in dendrite growth or pruning are present in mental disorders, in the ones that manifest in early childhood, such as autism, and also in the ones that manifest in late adolescence, such as schizophrenia (Jan and Jan, 2010). In chapter 2, we characterized the hippocampal dendritic arborization in *Pld1* WT animals in a DH-VH dependent manner (See Chapter 2, Figures 3). These dendritic DH-VH natural differences in WT animals correlated with the higher protein levels of GluA1, GluN2A and GluN2BP (phosphorylated at Y1472) and lower levels of syntaxin-1A in DH when compared to VH (See Chapter 2, Figure 5). The role of these synaptic proteins on dendritic branching has been a target of study. For example, GluA1 expression promotes dendritic growth of spinal cord neurons, by recruiting SAP97, a scaffolding protein, to the cell surface (Zhou et al., 2008); tyrosine phosphorylation of GluN2B has been reported to regulate the number of dendritic spines in rats with chronic migraine (Wang et al., 2018); the pruning of dendritic branches along maturation is accompanied with reduction in GluN2B expression and a significant elevation in synaptic expression of GluN2A and PSD95 (Bustos et al., 2014); and inhibition of syntaxin-1A with antisense oligonucleotides in cultured rat dorsal root ganglion neurons or with antibodies in cultured chick retinal ganglion neuron increases neurite sprouting (Yamaguchi et al., 1996) although cleavage of syntaxin by *Clostridium botulinum* neurotoxin C1 inhibited axonal growth (Igarashi et al., 1996). Regarding the genotype, we observed a decrease in apical dendritic length of DH CA3 of *Pld1* KO mice when compared to *Pld1* WT (See Chapter 2, Figure 3B, left panel). Since the DH is highly associated with cognitive functions, the decrease in dendritic length of DH CA3 can possibly relate to the cognitive impairments observed in *Pld1* KO mice. Moreover, the lack of genotype dependent alterations in VH may explain the absence of anxious-like behavioral effects.

During dendritic development growth phase there is a large requirement of lipids and cell-autonomous production is crucial (Ziegler et al., 2017) as it is the glia-derived lipids (Nieweg et al., 2009). PLD1 and PLD2 have been implicated in the regulation of neurite growth in neural cell lines and neural stem cells (Ammar et al., 2013; Kanaho et al., 2009; Oh et al., 2007; Watanabe

et al., 2004a; Watanabe et al., 2004b; Yoon et al., 2006; Yoon et al., 2005; Yun et al., 2006; Zhu et al., 2016; Zhu et al., 2012) and also PA can differentially contribute to different neurite outgrowth conditions due to its inverted cone shaped structure and fusogenic properties (Tanguy et al., 2019; Tanguy et al., 2020b). PLD1 has been proposed to be involved in *in vitro* dendritic arborization mechanisms, although with inconsistent results. Lalli and Hall proposed that small GTPase RalB promotes neuronal branching through a pathway involving PLD, by leading to PKC-dependent phosphorylation of 43-kD growth-associated protein (GAP-43), which is implicated in branching and axonal regeneration (Lalli and Hall, 2005), but Zhu and colleagues described a negative control by PLD1 in dendritic branching in cultured hippocampal neurons, acting downstream of RhoA, one small Rho GTPase, to suppress dendritic branching. Specifically, they show that when PLD1 is knockdown from individual neurons there is increase in dendritic branching and when PLD1 is overexpressed it leads to decreased dendrite complexity (Zhu et al., 2012). On the other hand, Ammar and colleagues reported a decrease of neurite outgrowth in cultured cortical neurons from *Pld1* null mutant mice and that neuronal growth factor (NGF) induces neurite outgrowth requires phosphorylation of PLD1 by the serine-threonine kinase RSK2 in PC12 cells (Ammar et al., 2013). They also showed that PLD1 participates in the brain-derived neurotrophic factor (BDNF) signaling pathway in cortical neurons, promoting the idea of neuronal development regulation by PLD (Ammar et al., 2015). Interestingly the phosphorylation site for RSK2 is not found in PLD2 (Zeniou-Meyer et al., 2008). More recently, it was shown that knockdown of PLD1 only in astrocytes reduces dendritic branching of neurons in mixed culture composed of neuron and glia, by reducing PA in astrocytes, reducing protein kinase A activation in neurons and consequently dendritic branching (Zhu et al., 2016). Using hippocampal neurons, Luo et al., reported that overexpressing PLD1 increases both the density and the area of dendritic spines by inhibiting the ADAM10 mediated N-cadherin cleavage, while loss of function of PLD1 leads to the opposite (Luo et al., 2017), and work from the same group hypothesized the role of PLD1 in dendritic morphogenesis through the signaling link with protein kinase D1 (Li et al., 2019). Moreover, an increase in expression of PLD1 and PLD2 was related to the development of hippocampal mossy fibers (Zhang et al., 2004). Taking all of this into account, further studies should tackle the importance of PLD2, the specific role of PLD in astrocytes and how PLD-derived PA affects in DH-VH dendritic arborization differentiation.

PA can be generated by other enzymes, such as the DGK and LPAAT. DGK phosphorylates DAG to produce PA. Brain specific conditional DGKδ-KO mice showed irrational contacts with familiar

and novel objects in the NOR test and buried more marbles than controls in the marble burying test, suggesting an obsessive-compulsive behavior like phenotype, accompanied with an increase number of long axon/neurites (Usuki et al., 2016). On the other hand, DGKβ KO mice presented cognitive impairment in Y-maze and MWM tests, along with reduced LTP in CA1 and reduced branches and spines (Shirai et al., 2010). LPAAT produce PA, having as substrates LPA, an inverted cone-shaped lipid, and acyl-CoA. There are eleven LPAAT enzymes, each one responsible for the production of a distinct and specific pool of PA (Bradley and Duncan, 2018; Zhukovsky et al., 2019). Mice knock-out for LPAATδ (expressed mainly in brain and muscle) show severe dysfunctions including cognitive impairment, impaired force contractility and altered white adipose tissue accompanied by drastically lower brain content of GluN1, GluN2A and GluN2B, as well as GluA1 (Bradley et al., 2017). These results regarding PA catalyzing enzymes partly phenocopy ours and demonstrate that, although the reduction of PA impacts brain organization and function, the compensatory mechanisms and the source of PA are also crucial, with implications for neuropsychiatric pathologies.

There is also crescent clinical importance considering PLD impact in the pathophysiology of important diseases, namely neurodegenerative diseases such as AD. AD is clinically characterized by a progressive impairment of memory and other cognitive functions and it is thought that neuronal degeneration and cell loss begins in the hippocampus (Vyas et al., 2020). AD-associated behavioral deficits in animals' models are observed in hippocampal-dependent tasks, such as Morris water maze (Bergin et al., 2018; Chen et al., 2000; Rorabaugh et al., 2017), radial arm (water) maze (Klevanski et al., 2015; Oliveira et al., 2010b), contextual fear memory (Oliveira et al., 2010b), NOR (Biasibetti et al., 2017), social behavior (Hsiao et al., 2018; Kosel et al., 2019), among others (Harris et al., 2010). Curiously, reduction in investigation time, namely social investigation, has also been proposed to be present in AD mice models (Kosel et al., 2019). Along with loss of synapses and neurons, the hallmarks of AD are the extracellular Aβ deposition (generated from APP) by sequential cleavages mediated by the β-secretase β-site APP cleavage enzyme 1, BACE1, and the γ-secretase complex) as senile plaques and the intracellular accumulation of hyperphosphorylated tau as neurofibrillary tangles (Di Paolo and Kim, 2011). There are studies linking PLD1/PLD2 and AD, not only in mice models (Cai et al., 2006a; Cai et al., 2006b; Oliveira et al., 2010b), but also in other models such as *Caenorhabditis elegans*, which only expresses one PLD (Bravo et al., 2018), and in humans (Kanfer et al., 1996; Krishnan et al., 2018). The PLD pathway has been implicated AD pathogenesis as being involved

in Aβ signaling (Bravo et al., 2018; Oliveira et al., 2010b) and APP processing and trafficking (Cai et al., 2006a; Cai et al., 2006b). Moreover, PLD3 has been shown to be involved in AD pathogenesis (Cruchaga et al., 2014), with a proposed role in lysosomal functioning (Fazzari et al., 2017). Furthermore, both PLD3 and PLD4 are exonucleases regulating the inflammatory cytokine response (Gavin et al., 2018), which could be linked to the multiple genetic AD risk factors connected to immune system biology (Karch and Goate, 2015), even though, neither of them have been shown to contribute to PA production. Since both PLD1 (Bourne et al., 2019; Cai et al., 2006a; Cai et al., 2006b; Krishnan et al., 2018; Liu et al., 2009) and PLD2 (Oliveira et al., 2010b) have been implicated in the pathophysiology of AD (Bravo et al., 2018; Kanfer et al., 1996; Oliveira and Di Paolo, 2010), future experiments should tackle PLD1 in the rescue of object recognition deficits and the specific role of PLD1/PLD2 in the circuits associated with social deficits impaired in AD models (and the electrophysiological, dendritic organization and protein alterations associated with these circuits).

Parkinson's Disease is the second most common neurodegenerative disorder in the elderly, defined by the progressive death of dopaminergic neurons in the *substantia nigra pars compacta* and the presence of Lewy bodies (cytosolic inclusions with misfolded protein α-synuclein) (Conde et al., 2018). Although *in vitro* assays show no inhibitory properties of α-syn on PLD activities (Rappley et al., 2009), α-synuclein has been reported as an inhibitor of PLD1 activity (Conde et al., 2018) and *in vivo* experiments have demonstrated that α-syn is able to inhibit PLD2 activity (Gorbatyuk et al., 2010). Furthermore, it was shown that pharmacological inhibition of PLD1 activity impairs normal autophagic flux, blocking the fusion between autophagosomes and lysosomes leading to accumulation of α-synuclein in the brain and, in the same study, it was reported that *post mortem* brains obtained from Lewy Body dementia patients display diminished PLD1 expression (Park et al., 2018). Interestingly, neuronal toxicity caused by a-synuclein accumulation was rescued by overexpression of PLD1 (Park et al., 2018).

Our experiments revealed relevant social phenotypes upon PLD ablation. Autism spectrum disorders and other psychiatric disorders, such as schizophrenia, featuring social cognition deficits may have behind modifications in circuits underlying social discrimination or social interaction (Kennedy and Adolphs, 2012). In fact, PLD2, and the PLD family member PLD5, have both been linked to autism (Anney et al., 2010). There is an autism-linked SNP (rs4141463) within an intron of the mono-ADP ribosylhydrolase 2 (MACROD2) gene, a region linked to

regulation of PLD2 expression (Anney et al., 2010). Moreover, MACROD2 is associated with schizophrenia (Xu et al., 2009) and attention deficit hyperactivity disorder (Lionel et al., 2011). PLD1 plays a role in dendritic arborization organization and autism, schizophrenia and intellectual disability, also feature dendritic spine development, which leads to abnormal synapse formation and function (Glantz and Lewis, 2000; Hutsler and Zhang, 2010; Kulkarni and Firestein, 2012; Penzes et al., 2011). Taking this into account, PLD should also be studied as a susceptibility gene in these diseases.

PLD inhibition/ablation is compatible with life, so it seems intuitive that inhibiting PLD could be a useful weapon in treating conditions where PLD pathway is up regulated, for example in neurodegeneration, viral infections and cancer (Nelson and Frohman, 2015; Oliveira et al., 2010b; Yao et al., 2020). But there is still a great lack of studies regarding this subject, from *in vitro* to human genetic variations studies. Regarding neurodegenerative diseases, these are particularly challenging to diagnose, as its first symptoms can be related to normal age cognitive decline. Moreover, the fact that there are several sources of PA could be another discouraging and a reason for the reduced therapeutic studies.

Overall Conclusion

In this thesis we show that the reduction of PLD1-derived PA or PLD2-derived PA has a different impact on organization and functioning of the longitudinal hippocampal axis.

First, in chapter 2 (see Box 1), we show that PLD1 is a major hippocampal PA source when compared to PLD2. Then we demonstrate that PLD1 ablation has a higher impact on the DH, either in lipidome, reduction of LTD induction and GluN2A and SNAP-25 protein levels. Furthermore, *Pld1* KO mice show specific deficits in novel object recognition and social interaction and disruption in the DH-VH dendritic arborization differentiation in CA1/CA3 pyramidal neurons.

In chapter 3 (see Box 2), we show that PLD2 ablation has an impact on the induction of LTP of the VH and leads to deficient social discrimination and decreases social exploration.

In conclusion, we demonstrate that PLD1 and PLD2 are necessary for the proper organization and function of the longitudinal hippocampal axis. Although these two isoenzymes catalyze the same reaction, our work further supports these two PLD isoforms have complementary functions.

Box 1. Chapter 2 highlights.

CHAPTER 2 - HIGHLIGHTS:

- PLD1 is a major PA source compared to PLD2
- *Pld1* KO mice show deficits in object recognition and social exploration
- PLD1 ablation disrupts DH-VH dendritic arborization differentiation
- PLD1 ablation reduces LTD induction and GluN2A and SNAP-25 levels in the DH

Box 2. Chapter 3 highlights.

CHAPTER 3 - HIGHLIGHTS:

- *Pld2* KO mice have social discrimination and social exploration deficits
- PLD2 ablation reduces LTP induction in VH
- PLD2 ablation has no major impact on synaptic proteins

Future Perspectives

Overall, we display the importance of PLD1/PLD2 as lipidic modulators of hippocampal longitudinal axis physiology, being essential regulators of hippocampal anatomy and synaptic functioning, which dysregulation leads to phenotypical impairment.

We need to further explore compensatory mechanisms to the production of PA levels, either compensation of one isoenzyme by the other, by measuring *in vivo* PLD activity, either by other PA producing enzymes.

Since in these studies we used genetic models to PLD1/2 levels, we plan to test in the future the phenotypical behavior and synaptic functions upon acute and chronic pharmacologic inhibition.

It will be essential to explore the mechanism linking the lack of PLD2 (and also PLD1) with social behavior impairment. We look forward to tackle the relationship between OTR/AVP and their receptors, either by colocalization studies, protein quantification or acute inhibition of PLD2 and explore modifications in TREK1 induced currents.

PLD1/PLD2 ablation is responsible for learning and memory defects, therefore it would be critical to explore the role of PLD in pathophysiology of diseases related to these deficits (namely AD and mood disorders, such as depression).

Since PLD is a risk factor and enhances the pathophysiology of several diseases, such as AD, and since PLD inhibition/ablation is compatible with life, it would be important to study PLD as a therapeutical target, in an attempt to ameliorate their pathological deficits.

References

Ammar, M.R., Humeau, Y., Hanauer, A., Nieswandt, B., Bader, M.F., and Vitale, N. (2013). The Coffin-Lowry syndrome-associated protein RSK2 regulates neurite outgrowth through phosphorylation of phospholipase D1 (PLD1) and synthesis of phosphatidic acid. The Journal of neuroscience : the official journal of the Society for Neuroscience *33*, 19470-19479.

Ammar, M.R., Thahouly, T., Hanauer, A., Stegner, D., Nieswandt, B., and Vitale, N. (2015). PLD1 participates in BDNF-induced signalling in cortical neurons. Scientific reports *5*, 14778.

Anney, R., Klei, L., Pinto, D., Regan, R., Conroy, J., Magalhaes, T.R., Correia, C., Abrahams, B.S., Sykes, N., Pagnamenta, A.T.*, et al.* (2010). A genome-wide scan for common alleles affecting risk for autism. Human molecular genetics *19*, 4072-4082.

Baca, M., Allan, A.M., Partridge, L.D., and Wilson, M.C. (2013). Gene-environment interactions affect long-term depression (LTD) through changes in dopamine receptor affinity in Snap25 deficient mice. Brain research *1532*, 85-98.

Bannerman, D.M., Sprengel, R., Sanderson, D.J., McHugh, S.B., Rawlins, J.N., Monyer, H., and Seeburg, P.H. (2014). Hippocampal synaptic plasticity, spatial memory and anxiety. Nature reviews Neuroscience *15*, 181-192.

Barber, C.N., Huganir, R.L., and Raben, D.M. (2018). Phosphatidic acid-producing enzymes regulating the synaptic vesicle cycle: Role for PLD? Adv Biol Regul *67*, 141-147.

Bergin, D.H., Jing, Y., Mockett, B.G., Zhang, H., Abraham, W.C., and Liu, P. (2018). Altered plasma arginine metabolome precedes behavioural and brain arginine metabolomic profile changes in the APPswe/PS1 ΔE9 mouse model of Alzheimer's disease. Transl Psychiatry *8*, 108.

Bermúdez, V., Tenconi, P.E., Giusto, N.M., and Mateos, M.V. (2019). Lipopolysaccharide-Induced Autophagy Mediates Retinal Pigment Epithelium Cells Survival. Modulation by the Phospholipase D Pathway. Front Cell Neurosci *13*, 154.

Biasibetti, R., Almeida Dos Santos, J.P., Rodrigues, L., Wartchow, K.M., Suardi, L.Z., Nardin, P., Selistre, N.G., Vázquez, D., and Gonçalves, C.A. (2017). Hippocampal changes in STZ-model of Alzheimer's disease are dependent on sex. Behavioural brain research *316*, 205-214.

Bourne, K.Z., Natarajan, C., Perez, C.X.M., Tumurbaatar, B., Taglialatela, G., and Krishnan, B. (2019). Suppressing aberrant phospholipase D1 signaling in 3xTg Alzheimer's disease mouse model promotes synaptic resilience. Scientific reports *9*, 18342.

Bradley, R.M., and Duncan, R.E. (2018). The lysophosphatidic acid acyltransferases (acylglycerophosphate acyltransferases) family: one reaction, five enzymes, many roles. Current opinion in lipidology *29*, 110-115.

Bradley, R.M., Mardian, E.B., Bloemberg, D., Aristizabal Henao, J.J., Mitchell, A.S., Marvyn, P.M., Moes, K.A., Stark, K.D., Quadrilatero, J., and Duncan, R.E. (2017). Mice Deficient in lysophosphatidic acid acyltransferase delta (Lpaat δ)/acylglycerophosphate acyltransferase 4 (Agpat4) Have Impaired Learning and Memory. Molecular and cellular biology *37*.

Bravo, F.V., Da Silva, J., Chan, R.B., Di Paolo, G., Teixeira-Castro, A., and Oliveira, T.G. (2018). Phospholipase D functional ablation has a protective effect in an Alzheimer's disease Caenorhabditis elegans model. Scientific reports *8*, 3540.

Bumpus, T.W., and Baskin, J.M. (2017). Clickable Substrate Mimics Enable Imaging of Phospholipase D Activity. ACS central science *3*, 1070-1077.

Burke, J.E., and Dennis, E.A. (2009). Phospholipase A2 biochemistry. Cardiovascular drugs and therapy *23*, 49-59.

Burkhardt, U., Stegner, D., Hattingen, E., Beyer, S., Nieswandt, B., and Klein, J. (2014). Impaired brain development and reduced cognitive function in phospholipase D-deficient mice. Neuroscience letters *572*, 48-52.

Bustos, F.J., Varela-Nallar, L., Campos, M., Henriquez, B., Phillips, M., Opazo, C., Aguayo, L.G., Montecino, M., Constantine-Paton, M., Inestrosa, N.C.*, et al.* (2014). PSD95 suppresses dendritic arbor development in mature hippocampal neurons by occluding the clustering of NR2B-NMDA receptors. PloS one *9*, e94037.

Cai, D., Netzer, W.J., Zhong, M., Lin, Y., Du, G., Frohman, M., Foster, D.A., Sisodia, S.S., Xu, H., Gorelick, F.S.*, et al.* (2006a). Presenilin-1 uses phospholipase D1 as a negative regulator of beta-amyloid formation. Proceedings of the National Academy of Sciences of the United States of America *103*, 1941-1946.

Cai, D., Zhong, M., Wang, R., Netzer, W.J., Shields, D., Zheng, H., Sisodia, S.S., Foster, D.A., Gorelick, F.S., Xu, H.*, et al.* (2006b). Phospholipase D1 corrects impaired betaAPP trafficking and neurite outgrowth in familial Alzheimer's disease-linked presenilin-1 mutant neurons. Proceedings of the National Academy of Sciences of the United States of America *103*, 1936-1940.

Chan, R.B., Oliveira, T.G., Cortes, E.P., Honig, L.S., Duff, K.E., Small, S.A., Wenk, M.R., Shui, G., and Di Paolo, G. (2012). Comparative lipidomic analysis of mouse and human brain with Alzheimer disease. The Journal of biological chemistry *287*, 2678-2688.

Chen, G., Chen, K.S., Knox, J., Inglis, J., Bernard, A., Martin, S.J., Justice, A., McConlogue, L., Games, D., Freedman, S.B.*, et al.* (2000). A learning deficit related to age and beta-amyloid plaques in a mouse model of Alzheimer's disease. Nature *408*, 975-979.

Choi, W.S., Kim, Y.M., Combs, C., Frohman, M.A., and Beaven, M.A. (2002). Phospholipases D1 and D2 regulate different phases of exocytosis in mast cells. Journal of immunology (Baltimore, Md : 1950) *168*, 5682-5689.

Citri, A., and Malenka, R.C. (2008). Synaptic plasticity: multiple forms, functions, and mechanisms. Neuropsychopharmacology : official publication of the American College of Neuropsychopharmacology *33*, 18-41.

Clark, J.D., Schievella, A.R., Nalefski, E.A., and Lin, L.L. (1995). Cytosolic phospholipase A2. Journal of lipid mediators and cell signalling *12*, 83-117.

Coletti, D., Silvestroni, L., Naro, F., Molinaro, M., Adamo, S., and Palleschi, S. (2000). Vesicle-mediated phosphatidylcholine reapposition to the plasma membrane following hormone-induced phospholipase D activation. Experimental cell research *256*, 94-104.

Colley, W.C., Sung, T.C., Roll, R., Jenco, J., Hammond, S.M., Altshuller, Y., Bar-Sagi, D., Morris, A.J., and Frohman, M.A. (1997). Phospholipase D2, a distinct phospholipase D isoform with novel regulatory properties that provokes cytoskeletal reorganization. Current biology : CB *7*, 191-201.

Comoglio, Y., Levitz, J., Kienzler, M.A., Lesage, F., Isacoff, E.Y., and Sandoz, G. (2014). Phospholipase D2 specifically regulates TREK potassium channels via direct interaction and local production of phosphatidic acid. Proceedings of the National Academy of Sciences of the United States of America *111*, 13547-13552.

Conde, M.A., Alza, N.P., Iglesias González, P.A., Scodelaro Bilbao, P.G., Sánchez Campos, S., Uranga, R.M., and Salvador, G.A. (2018). Phospholipase D1 downregulation by α-synuclein: Implications for neurodegeneration in Parkinson's disease. Biochimica et biophysica acta Molecular and cell biology of lipids *1863*, 639-650.

Corradini, I., Donzelli, A., Antonucci, F., Welzl, H., Loos, M., Martucci, R., De Astis, S., Pattini, L., Inverardi, F., Wolfer, D.*, et al.* (2014). Epileptiform activity and cognitive deficits in SNAP-25(+/-) mice are normalized by antiepileptic drugs. Cerebral cortex (New York, NY : 1991) *24*, 364-376.

Cruchaga, C., Karch, C.M., Jin, S.C., Benitez, B.A., Cai, Y., Guerreiro, R., Harari, O., Norton, J., Budde, J., Bertelsen, S.*, et al.* (2014). Rare coding variants in the phospholipase D3 gene confer risk for Alzheimer's disease. Nature *505*, 550-554.

Cui, Z., Feng, R., Jacobs, S., Duan, Y., Wang, H., Cao, X., and Tsien, J.Z. (2013). Increased NR2A:NR2B ratio compresses long-term depression range and constrains long-term memory. Scientific reports *3*, 1036-1036.

Dall'Armi, C., Hurtado-Lorenzo, A., Tian, H., Morel, E., Nezu, A., Chan, R.B., Yu, W.H., Robinson, K.S., Yeku, O., Small, S.A.*, et al.* (2010). The phospholipase D1 pathway modulates macroautophagy. Nature communications *1*, 142-142.

DeVito, L.M., Konigsberg, R., Lykken, C., Sauvage, M., Young, W.S., 3rd, and Eichenbaum, H. (2009). Vasopressin 1b receptor knock-out impairs memory for temporal order. The Journal of neuroscience : the official journal of the Society for Neuroscience *29*, 2676-2683.

Di Paolo, G., and Kim, T.W. (2011). Linking lipids to Alzheimer's disease: cholesterol and beyond. Nature reviews Neuroscience *12*, 284-296.

Dudek, S.M., Alexander, G.M., and Farris, S. (2016). Rediscovering area CA2: unique properties and functions. Nature reviews Neuroscience *17*, 89-102.

Farooqui, A.A., and Horrocks, L.A. (2005). Signaling and interplay mediated by phospholipases A2, C, and D in LA-N-1 cell nuclei. Reproduction, nutrition, development *45*, 613-631.

Farooqui, A.A., Horrocks, L.A., and Farooqui, T. (2000). Glycerophospholipids in brain: their metabolism, incorporation into membranes, functions, and involvement in neurological disorders. Chemistry and physics of lipids *106*, 1-29.

Fazzari, P., Horre, K., Arranz, A.M., Frigerio, C.S., Saito, T., Saido, T.C., and De Strooper, B. (2017). PLD3 gene and processing of APP. Nature *541*, E1-e2.

Frohman, M.A. (2015). The phospholipase D superfamily as therapeutic targets. Trends Pharmacol Sci *36*, 137-144.

Gavin, A.L., Huang, D., Huber, C., Martensson, A., Tardif, V., Skog, P.D., Blane, T.R., Thinnes, T.C., Osborn, K., Chong, H.S.*, et al.* (2018). PLD3 and PLD4 are single-stranded acid exonucleases that regulate endosomal nucleic-acid sensing. Nature immunology *19*, 942-953.

Glantz, L.A., and Lewis, D.A. (2000). Decreased dendritic spine density on prefrontal cortical pyramidal neurons in schizophrenia. Archives of general psychiatry *57*, 65-73.

Gopaul, K.R., Irfan, M., Miry, O., Vose, L.R., Moghadam, A., Subah, G., Hökfelt, T., Bark, C., and Stanton, P.K. (2020). Developmental Time Course of SNAP-25 Isoforms Regulate Hippocampal Long-Term Synaptic Plasticity and Hippocampus-Dependent Learning. International journal of molecular sciences *21*.

Gorbatyuk, O.S., Li, S., Nguyen, F.N., Manfredsson, F.P., Kondrikova, G., Sullivan, L.F., Meyers, C., Chen, W., Mandel, R.J., and Muzyczka, N. (2010). α-Synuclein expression in rat substantia nigra suppresses phospholipase D2 toxicity and nigral neurodegeneration. Molecular therapy : the journal of the American Society of Gene Therapy *18*, 1758-1768.

Green, T.L., Burket, J.A., and Deutsch, S.I. (2016). Age-dependent effects on social interaction of NMDA GluN2A receptor subtype-selective antagonism. Brain research bulletin *125*, 159-167.

Gustavsson, L. (1995). ESBRA 1994 Award Lecture. Phosphatidylethanol formation: specific effects of ethanol mediated via phospholipase D. Alcohol and alcoholism (Oxford, Oxfordshire) *30*, 391-406.

Hammock, E.A., and Levitt, P. (2013). Oxytocin receptor ligand binding in embryonic tissue and postnatal brain development of the C57BL/6J mouse. Frontiers in behavioral neuroscience *7*, 195.

Harris, J.A., Devidze, N., Halabisky, B., Lo, I., Thwin, M.T., Yu, G.Q., Bredesen, D.E., Masliah, E., and Mucke, L. (2010). Many neuronal and behavioral impairments in transgenic mouse models of Alzheimer's disease are independent of caspase cleavage of the amyloid precursor protein. The Journal of neuroscience : the official journal of the Society for Neuroscience *30*, 372-381.

Henry, F.E., Wang, X., Serrano, D., Perez, A.S., Carruthers, C.J.L., Stuenkel, E.L., and Sutton, M.A. (2018). A Unique Homeostatic Signaling Pathway Links Synaptic Inactivity to Postsynaptic mTORC1. The Journal of neuroscience : the official journal of the Society for Neuroscience *38*, 2207-2225.

Hernandez, D., Torres, C.A., Setlik, W., Cebrián, C., Mosharov, E.V., Tang, G., Cheng, H.C., Kholodilov, N., Yarygina, O., Burke, R.E., *et al.* (2012). Regulation of presynaptic neurotransmission by macroautophagy. Neuron *74*, 277-284.

Hidema, S., Fukuda, T., Hiraoka, Y., Mizukami, H., Hayashi, R., Otsuka, A., Suzuki, S., Miyazaki, S., and Nishimori, K. (2016). Generation of Oxtr cDNA(HA)-Ires-Cre Mice for Gene Expression in an Oxytocin Receptor Specific Manner. Journal of cellular biochemistry *117*, 1099-1111.

Hiroyama, M., and Exton, J.H. (2005). Localization and regulation of phospholipase D2 by ARF6. Journal of cellular biochemistry *95*, 149-164.

Hsiao, Y.H., Chang, C.H., and Gean, P.W. (2018). Impact of social relationships on Alzheimer's memory impairment: mechanistic studies. Journal of biomedical science *25*, 3.

Huang, P., Altshuller, Y.M., Hou, J.C., Pessin, J.E., and Frohman, M.A. (2005). Insulin-stimulated plasma membrane fusion of Glut4 glucose transporter-containing vesicles is regulated by phospholipase D1. Molecular biology of the cell *16*, 2614-2623.

Hutsler, J.J., and Zhang, H. (2010). Increased dendritic spine densities on cortical projection neurons in autism spectrum disorders. Brain research *1309*, 83-94.

Igarashi, M., Kozaki, S., Terakawa, S., Kawano, S., Ide, C., and Komiya, Y. (1996). Growth cone collapse and inhibition of neurite growth by Botulinum neurotoxin C1: a t-SNARE is involved in axonal growth. The Journal of cell biology *134*, 205-215.

Inamori, K., Sagawa, N., Hasegawa, M., Itoh, H., Yano, J., and Mori, T. (1995). Activation of phospholipase D in cultured human amnion cells. Reproduction, fertility, and development *7*, 1591-1594.

Jacobs, S.A., and Tsien, J.Z. (2014). Overexpression of the NR2A subunit in the forebrain impairs long-term social recognition and non-social olfactory memory. Genes, brain, and behavior *13*, 376-384.

Jan, Y.N., and Jan, L.Y. (2010). Branching out: mechanisms of dendritic arborization. Nature reviews Neuroscience *11*, 316-328.

Jenkins, G.M., and Frohman, M.A. (2005). Phospholipase D: a lipid centric review. Cellular and molecular life sciences : CMLS *62*, 2305-2316.

Kanaho, Y., Funakoshi, Y., and Hasegawa, H. (2009). Phospholipase D signalling and its involvement in neurite outgrowth. Biochim Biophys Acta *1791*, 898-904.

Kanfer, J.N., Singh, I.N., Pettegrew, J.W., McCartney, D.G., and Sorrentino, G. (1996). Phospholipid metabolism in Alzheimer's disease and in a human cholinergic cell. Journal of lipid mediators and cell signalling *14*, 361-363.

Karch, C.M., and Goate, A.M. (2015). Alzheimer's disease risk genes and mechanisms of disease pathogenesis. Biological psychiatry *77*, 43-51.

Kemp, A., and Manahan-Vaughan, D. (2004). Hippocampal long-term depression and long-term potentiation encode different aspects of novelty acquisition. Proceedings of the National Academy of Sciences of the United States of America *101*, 8192-8197.

Kennedy, D.P., and Adolphs, R. (2012). The social brain in psychiatric and neurological disorders. Trends in cognitive sciences *16*, 559-572.

Klein, J., Chalifa, V., Liscovitch, M., and Löffelholz, K. (1995). Role of phospholipase D activation in nervous system physiology and pathophysiology. Journal of neurochemistry *65*, 1445-1455.

Klevanski, M., Herrmann, U., Weyer, S.W., Fol, R., Cartier, N., Wolfer, D.P., Caldwell, J.H., Korte, M., and Müller, U.C. (2015). The APP Intracellular Domain Is Required for Normal Synaptic Morphology, Synaptic Plasticity, and Hippocampus-Dependent Behavior. The Journal of neuroscience : the official journal of the Society for Neuroscience *35*, 16018-16033.

Komati, H., Naro, F., Mebarek, S., De Arcangelis, V., Adamo, S., Lagarde, M., Prigent, A.F., and Némoz, G. (2005). Phospholipase D is involved in myogenic differentiation through remodeling of actin cytoskeleton. Molecular biology of the cell *16*, 1232-1244.

Kosel, F., Torres Munoz, P., Yang, J.R., Wong, A.A., and Franklin, T.B. (2019). Age-related changes in social behaviours in the 5xFAD mouse model of Alzheimer's disease. Behavioural brain research *362*, 160-172.

Krishnan, B., Kayed, R., and Taglialatela, G. (2018). Elevated phospholipase D isoform 1 in Alzheimer's disease patients' hippocampus: Relevance to synaptic dysfunction and memory deficits. Alzheimer's & dementia (New York, N Y) *4*, 89-102.

Kulkarni, V.A., and Firestein, B.L. (2012). The dendritic tree and brain disorders. Mol Cell Neurosci *50*, 10-20.

Kusaka, I., Ishikawa, S.E., Higashiyama, M., Saito, T., Nagasaka, S., and Saito, T. (1996). The activation of phospholipase D participates in the mitogenic action of arginine vasopressin in cultured rat glomerular mesangial cells. Endocrinology *137*, 5421-5428.

Laing, M.D., and Bashir, Z.I. (2015). Presynaptic NR2A-Containing NMDARs Are Required for LTD between the Amygdala and the Perirhinal Cortex: A Potential Mechanism for the Emotional Modulation of Memory? eNeuro *2*.

Lalli, G., and Hall, A. (2005). Ral GTPases regulate neurite branching through GAP-43 and the exocyst complex. The Journal of cell biology *171*, 857-869.

Lee, H.J., Caldwell, H.K., Macbeth, A.H., Tolu, S.G., and Young, W.S., 3rd (2008). A conditional knockout mouse line of the oxytocin receptor. Endocrinology *149*, 3256-3263.

Li, W.Q., Luo, L.D., Hu, Z.W., Lyu, T.J., Cen, C., and Wang, Y. (2019). PLD1 promotes dendritic spine morphogenesis via activating PKD1. Mol Cell Neurosci *99*, 103394.

Li, X., Sun, W., and An, L. (2018). Nano-CuO impairs spatial cognition associated with inhibiting hippocampal long-term potentiation via affecting glutamatergic neurotransmission in rats. Toxicology and industrial health *34*, 409-421.

Li, Y., Shiels, A.J., Maszak, G., and Byron, K.L. (2001). Vasopressin-stimulated Ca2+ spiking in vascular smooth muscle cells involves phospholipase D. American journal of physiology Heart and circulatory physiology *280*, H2658-2664.

Lin, Y.T., Hsieh, T.Y., Tsai, T.C., Chen, C.C., Huang, C.C., and Hsu, K.S. (2018). Conditional Deletion of Hippocampal CA2/CA3a Oxytocin Receptors Impairs the Persistence of Long-Term Social Recognition Memory in Mice. The Journal of neuroscience : the official journal of the Society for Neuroscience *38*, 1218-1231.

Lionel, A.C., Crosbie, J., Barbosa, N., Goodale, T., Thiruvahindrapuram, B., Rickaby, J., Gazzellone, M., Carson, A.R., Howe, J.L., Wang, Z.*, et al.* (2011). Rare copy number variation discovery and cross-disorder comparisons identify risk genes for ADHD. Science translational medicine *3*, 95ra75.

Liscovitch, M., Czarny, M., Fiucci, G., Lavie, Y., and Tang, X. (1999). Localization and possible functions of phospholipase D isozymes. Biochim Biophys Acta *1439*, 245-263.

Liu, Y., Zhang, Y.W., Wang, X., Zhang, H., You, X., Liao, F.F., and Xu, H. (2009). Intracellular trafficking of presenilin 1 is regulated by beta-amyloid precursor protein and phospholipase D1. The Journal of biological chemistry *284*, 12145-12152.

Luo, L.D., Li, G., and Wang, Y. (2017). PLD1 promotes dendritic spine development by inhibiting ADAM10-mediated N-cadherin cleavage. Scientific reports *7*, 6035.

Maggio, N., and Segal, M. (2007). Striking variations in corticosteroid modulation of long-term potentiation along the septotemporal axis of the hippocampus. The Journal of neuroscience : the official journal of the Society for Neuroscience *27*, 5757-5765.

Meira, T., Leroy, F., Buss, E.W., Oliva, A., Park, J., and Siegelbaum, S.A. (2018). A hippocampal circuit linking dorsal CA2 to ventral CA1 critical for social memory dynamics. Nature communications *9*, 4163.

Mendez, M., Arias, N., Uceda, S., and Arias, J.L. (2015). c-Fos expression correlates with performance on novel object and novel place recognition tests. Brain research bulletin *117*, 16-23.

Miranda, A.M., Bravo, F.V., Chan, R.B., Sousa, N., Di Paolo, G., and Oliveira, T.G. (2019). Differential lipid composition and regulation along the hippocampal longitudinal axis. Transl Psychiatry *9*, 144.

Mitre, M., Marlin, B.J., Schiavo, J.K., Morina, E., Norden, S.E., Hackett, T.A., Aoki, C.J., Chao, M.V., and Froemke, R.C. (2016). A Distributed Network for Social Cognition Enriched for Oxytocin Receptors. The Journal of neuroscience : the official journal of the Society for Neuroscience *36*, 2517-2535.

Morales, M., and Spear, L.P. (2014). The effects of an acute challenge with the NMDA receptor antagonists, MK-801, PEAQX, and ifenprodil, on social inhibition in adolescent and adult male rats. Psychopharmacology *231*, 1797-1807.

Moran, S.P., Xiang, Z., Doyle, C.A., Maksymetz, J., Lv, X., Faltin, S., Fisher, N.M., Niswender, C.M., Rook, J.M., Lindsley, C.W.*, et al.* (2019). Biased M(1) receptor-positive allosteric modulators reveal role of phospholipase D in M(1)-dependent rodent cortical plasticity. Science signaling *12*.

Morrison, J.J., Dearn, S.R., Smith, S.K., and Ahmed, A. (1996). Activation of protein kinase C is required for oxytocin-induced contractility in human pregnant myometrium. Human reproduction (Oxford, England) *11*, 2285-2290.

Mu, Y., Yan, X., Li, D., Zhao, D., Wang, L., Wang, X., Gao, D., Yang, J., Zhang, H., Li, Y.*, et al.* (2018). NUPR1 maintains autolysosomal efflux by activating SNAP25 transcription in cancer cells. Autophagy *14*, 654-670.

Nadler, J.V., Perry, B.W., and Cotman, C.W. (1978). Intraventricular kainic acid preferentially destroys hippocampal pyramidal cells. Nature *271*, 676-677.

Naro, F., Donchenko, V., Minotti, S., Zolla, L., Molinaro, M., and Adamo, S. (1997). Role of phospholipase C and D signalling pathways in vasopressin-dependent myogenic differentiation. Journal of cellular physiology *171*, 34-42.

Nelson, R.K., and Frohman, M.A. (2015). Physiological and pathophysiological roles for phospholipase D. J Lipid Res *56*, 2229-2237.

Nieweg, K., Schaller, H., and Pfrieger, F.W. (2009). Marked differences in cholesterol synthesis between neurons and glial cells from postnatal rats. Journal of neurochemistry *109*, 125-134.

Oh, D.Y., Park, S.Y., Cho, J.H., Lee, K.S., Min do, S., and Han, J.S. (2007). Phospholipase D1 activation through Src and Ras is involved in basic fibroblast growth factor-induced neurite outgrowth of H19-7 cells. Journal of cellular biochemistry *101*, 221-234.

Oliveira, A.M., Hawk, J.D., Abel, T., and Havekes, R. (2010a). Post-training reversible inactivation of the hippocampus enhances novel object recognition memory. Learning & memory (Cold Spring Harbor, NY) *17*, 155-160.

Oliveira, T.G., Chan, R.B., Bravo, F.V., Miranda, A., Silva, R.R., Zhou, B., Marques, F., Pinto, V., Cerqueira, J.J., Di Paolo, G.*, et al.* (2016). The impact of chronic stress on the rat brain lipidome. Mol Psychiatry *21*, 80-88.

Oliveira, T.G., Chan, R.B., Tian, H., Laredo, M., Shui, G., Staniszewski, A., Zhang, H., Wang, L., Kim, T.W., Duff, K.E.*, et al.* (2010b). Phospholipase d2 ablation ameliorates Alzheimer's disease-linked synaptic dysfunction and cognitive deficits. The Journal of neuroscience : the official journal of the Society for Neuroscience *30*, 16419-16428.

Oliveira, T.G., and Di Paolo, G. (2010). Phospholipase D in brain function and Alzheimer's disease. Biochim Biophys Acta *1801*, 799-805.

Pagani, J.H., Zhao, M., Cui, Z., Avram, S.K., Caruana, D.A., Dudek, S.M., and Young, W.S. (2015). Role of the vasopressin 1b receptor in rodent aggressive behavior and synaptic plasticity in hippocampal area CA2. Mol Psychiatry *20*, 490-499.

Panda, A., Thakur, R., Krishnan, H., Naik, A., Shinde, D., and Raghu, P. (2018). Functional analysis of mammalian phospholipase D enzymes. Bioscience reports *38*.

Park, J.H., Park, J.W., Lee, J.H., Kim, D.Y., Hahm, J.H., and Bae, Y.S. (2018). Role of phospholipase D in the lifespan of Caenorhabditis elegans. Experimental & molecular medicine *50*, 8.

Penzes, P., Cahill, M.E., Jones, K.A., VanLeeuwen, J.E., and Woolfrey, K.M. (2011). Dendritic spine pathology in neuropsychiatric disorders. Nature neuroscience *14*, 285-293.

Pinto, V., Costa, J.C., Morgado, P., Mota, C., Miranda, A., Bravo, F.V., Oliveira, T.G., Cerqueira, J.J., and Sousa, N. (2015). Differential impact of chronic stress along the hippocampal dorsal-ventral axis. Brain structure & function *220*, 1205-1212.

Piomelli, D., Astarita, G., and Rapaka, R. (2007). A neuroscientist's guide to lipidomics. Nature reviews Neuroscience *8*, 743-754.

Piskorowski, R.A., Nasrallah, K., Diamantopoulou, A., Mukai, J., Hassan, S.I., Siegelbaum, S.A., Gogos, J.A., and Chevaleyre, V. (2016). Age-Dependent Specific Changes in Area CA2 of the Hippocampus and Social Memory Deficit in a Mouse Model of the 22q11.2 Deletion Syndrome. Neuron *89*, 163-176.

Raam, T., McAvoy, K.M., Besnard, A., Veenema, A.H., and Sahay, A. (2017). Hippocampal oxytocin receptors are necessary for discrimination of social stimuli. Nature communications *8*, 2001.

Raghu, P., Coessens, E., Manifava, M., Georgiev, P., Pettitt, T., Wood, E., Garcia-Murillas, I., Okkenhaug, H., Trivedi, D., Zhang, Q.*, et al.* (2009a). Rhabdomere biogenesis in Drosophila photoreceptors is acutely sensitive to phosphatidic acid levels. The Journal of cell biology *185*, 129-145.

Raghu, P., Manifava, M., Coadwell, J., and Ktistakis, N.T. (2009b). Emerging findings from studies of phospholipase D in model organisms (and a short update on phosphatidic acid effectors). Biochim Biophys Acta *1791*, 889-897.

Rappley, I., Gitler, A.D., Selvy, P.E., LaVoie, M.J., Levy, B.D., Brown, H.A., Lindquist, S., and Selkoe, D.J. (2009). Evidence that alpha-synuclein does not inhibit phospholipase D. Biochemistry *48*, 1077-1083.

Rorabaugh, J.M., Chalermpalanupap, T., Botz-Zapp, C.A., Fu, V.M., Lembeck, N.A., Cohen, R.M., and Weinshenker, D. (2017). Chemogenetic locus coeruleus activation restores reversal learning in a rat model of Alzheimer's disease. Brain : a journal of neurology *140*, 3023-3038.

Rose, K., Rudge, S.A., Frohman, M.A., Morris, A.J., and Engebrecht, J. (1995). Phospholipase D signaling is essential for meiosis. Proceedings of the National Academy of Sciences of the United States of America *92*, 12151-12155.

Santa-Marinha, L., Castanho, I., Silva, R.R., Bravo, F.V., Miranda, A.M., Meira, T., Morais-Ribeiro, R., Marques, F., Xu, Y., Point du Jour, K.*, et al.* (2020). Phospholipase D1 Ablation Disrupts

Mouse Longitudinal Hippocampal Axis Organization and Functioning. Cell reports *30*, 4197-4208.e4196.

Scott, S.A., Xiang, Y., Mathews, T.P., Cho, H.P., Myers, D.S., Armstrong, M.D., Tallman, K.A., O'Reilly, M.C., Lindsley, C.W., and Brown, H.A. (2013). Regulation of phospholipase D activity and phosphatidic acid production after purinergic (P2Y6) receptor stimulation. The Journal of biological chemistry *288*, 20477-20487.

Selvy, P.E., Lavieri, R.R., Lindsley, C.W., and Brown, H.A. (2011). Phospholipase D: enzymology, functionality, and chemical modulation. Chemical reviews *111*, 6064-6119.

Shipton, O.A., and Paulsen, O. (2014). GluN2A and GluN2B subunit-containing NMDA receptors in hippocampal plasticity. Philosophical transactions of the Royal Society of London Series B, Biological sciences *369*, 20130163.

Shirai, Y., Kouzuki, T., Kakefuda, K., Moriguchi, S., Oyagi, A., Horie, K., Morita, S.Y., Shimazawa, M., Fukunaga, K., Takeda, J.*, et al.* (2010). Essential role of neuron-enriched diacylglycerol kinase (DGK), DGKbeta in neurite spine formation, contributing to cognitive function. PloS one *5*, e11602.

Sloviter, R.S., and Damiano, B.P. (1981). Sustained electrical stimulation of the perforant path duplicates kainate-induced electrophysiological effects and hippocampal damage in rats. Neuroscience letters *24*, 279-284.

Stackman, R.W., Jr., Cohen, S.J., Lora, J.C., and Rios, L.M. (2016). Temporary inactivation reveals that the CA1 region of the mouse dorsal hippocampus plays an equivalent role in the retrieval of long-term object memory and spatial memory. Neurobiology of learning and memory *133*, 118-128.

Strange, B.A., Witter, M.P., Lein, E.S., and Moser, E.I. (2014). Functional organization of the hippocampal longitudinal axis. Nature reviews Neuroscience *15*, 655-669.

Takayanagi, Y., Yoshida, M., Bielsky, I.F., Ross, H.E., Kawamata, M., Onaka, T., Yanagisawa, T., Kimura, T., Matzuk, M.M., Young, L.J.*, et al.* (2005). Pervasive social deficits, but normal parturition, in oxytocin receptor-deficient mice. Proceedings of the National Academy of Sciences of the United States of America *102*, 16096-16101.

Talley, E.M., Solorzano, G., Lei, Q., Kim, D., and Bayliss, D.A. (2001). Cns distribution of members of the two-pore-domain (KCNK) potassium channel family. The Journal of neuroscience : the official journal of the Society for Neuroscience *21*, 7491-7505.

Tanguy, E., Costé de Bagneaux, P., Kassas, N., Ammar, M.R., Wang, Q., Haeberlé, A.M., Raherindratsara, J., Fouillen, L., Renard, P.Y., Montero-Hadjadje, M.*, et al.* (2020a). Mono- and Poly-unsaturated Phosphatidic Acid Regulate Distinct Steps of Regulated Exocytosis in Neuroendocrine Cells. Cell reports *32*, 108026.

Tanguy, E., Wang, Q., Moine, H., and Vitale, N. (2019). Phosphatidic Acid: From Pleiotropic Functions to Neuronal Pathology. Frontiers in Cellular Neuroscience *13*.

Tanguy, E., Wang, Q., and Vitale, N. (2020b). Role of Phospholipase D-Derived Phosphatidic Acid in Regulated Exocytosis and Neurological Disease. Handbook of experimental pharmacology *259*, 115-130.

Tei, R., and Baskin, J.M. (2020). Spatiotemporal control of phosphatidic acid signaling with optogenetic, engineered phospholipase Ds. The Journal of cell biology *219*.

Thakur, R., Panda, A., Coessens, E., Raj, N., Yadav, S., Balakrishnan, S., Zhang, Q., Georgiev, P., Basak, B., Pasricha, R.*, et al.* (2016). Phospholipase D activity couples plasma membrane endocytosis with retromer dependent recycling. eLife *5*.

Ueno, N., Murakami, M., and Kudo, I. (2000). Functional crosstalk between phospholipase D(2) and signaling phospholipase A(2)/cyclooxygenase-2-mediated prostaglandin biosynthetic pathways. FEBS letters *475*, 242-246.

Usuki, T., Takato, T., Lu, Q., Sakai, H., Bando, K., Kiyonari, H., and Sakane, F. (2016). Behavioral and pharmacological phenotypes of brain-specific diacylglycerol kinase δ-knockout mice. Brain research *1648*, 193-201.

van Meer, G. (2005). Cellular lipidomics. The EMBO journal *24*, 3159-3165.

Vermeren, M.M., Zhang, Q., Smethurst, E., Segonds-Pichon, A., Schrewe, H., and Wakelam, M.J. (2016). The Phospholipase D2 Knock Out Mouse Has Ectopic Purkinje Cells and Suffers from Early Adult-Onset Anosmia. PloS one *11*, e0162814.

Vitale, N., Caumont, A.S., Chasserot-Golaz, S., Du, G., Wu, S., Sciorra, V.A., Morris, A.J., Frohman, M.A., and Bader, M.F. (2001). Phospholipase D1: a key factor for the exocytotic machinery in neuroendocrine cells. The EMBO journal *20*, 2424-2434.

Vyas, Y., Montgomery, J.M., and Cheyne, J.E. (2020). Hippocampal Deficits in Amyloid-β-Related Rodent Models of Alzheimer's Disease. Frontiers in neuroscience *14*, 266.

Wang, W., Kiyoshi, C.M., Du, Y., Taylor, A.T., Sheehan, E.R., Wu, X., and Zhou, M. (2020). TREK-1 Null Impairs Neuronal Excitability, Synaptic Plasticity, and Cognitive Function. Molecular neurobiology *57*, 1332-1346.

Wang, X.Y., Zhou, H.R., Wang, S., Liu, C.Y., Qin, G.C., Fu, Q.Q., Zhou, J.Y., and Chen, L.X. (2018). NR2B-Tyr phosphorylation regulates synaptic plasticity in central sensitization in a chronic migraine rat model. The journal of headache and pain *19*, 102.

Watanabe, H., Yamazaki, M., Miyazaki, H., Arikawa, C., Itoh, K., Sasaki, T., Maehama, T., Frohman, M.A., and Kanaho, Y. (2004a). Phospholipase D2 functions as a downstream signaling molecule of MAP kinase pathway in L1-stimulated neurite outgrowth of cerebellar granule neurons. Journal of neurochemistry *89*, 142-151.

Watanabe, H., Yokozeki, T., Yamazaki, M., Miyazaki, H., Sasaki, T., Maehama, T., Itoh, K., Frohman, M.A., and Kanaho, Y. (2004b). Essential role for phospholipase D2 activation downstream of ERK MAP kinase in nerve growth factor-stimulated neurite outgrowth from PC12 cells. The Journal of biological chemistry *279*, 37870-37877.

Wenk, M.R. (2005). The emerging field of lipidomics. Nature reviews Drug discovery *4*, 594-610.

Wersinger, S.R., Ginns, E.I., O'Carroll, A.M., Lolait, S.J., and Young, W.S., 3rd (2002). Vasopressin V1b receptor knockout reduces aggressive behavior in male mice. Mol Psychiatry *7*, 975-984.

Wersinger, S.R., Temple, J.L., Caldwell, H.K., and Young, W.S., 3rd (2008). Inactivation of the oxytocin and the vasopressin (Avp) 1b receptor genes, but not the Avp 1a receptor gene, differentially impairs the Bruce effect in laboratory mice (Mus musculus). Endocrinology *149*, 116-121.

Wong, J.M., and Gray, J.A. (2018). Long-Term Depression Is Independent of GluN2 Subunit Composition. The Journal of neuroscience : the official journal of the Society for Neuroscience *38*, 4462-4470.

Xu, B., Woodroffe, A., Rodriguez-Murillo, L., Roos, J.L., van Rensburg, E.J., Abecasis, G.R., Gogos, J.A., and Karayiorgou, M. (2009). Elucidating the genetic architecture of familial schizophrenia using rare copy number variant and linkage scans. Proceedings of the National Academy of Sciences of the United States of America *106*, 16746-16751.

Yamaguchi, K., Nakayama, T., Fujiwara, T., and Akagawa, K. (1996). Enhancement of neurite-sprouting by suppression of HPC-1/syntaxin 1A activity in cultured vertebrate nerve cells. Brain research *740*, 185-192.

Yao, Y., Wang, X., Li, H., Fan, J., Qian, X., Li, H., and Xu, Y. (2020). Phospholipase D as a key modulator of cancer progression. Biological reviews of the Cambridge Philosophical Society.

Yin, H., Gui, Y., Du, G., Frohman, M.A., and Zheng, X.L. (2010). Dependence of phospholipase D1 multi-monoubiquitination on its enzymatic activity and palmitoylation. The Journal of biological chemistry *285*, 13580-13588.

Yoon, M.S., Cho, C.H., Lee, K.S., and Han, J.S. (2006). Binding of Cdc42 to phospholipase D1 is important in neurite outgrowth of neural stem cells. Biochemical and biophysical research communications *347*, 594-600.

Yoon, M.S., Yon, C., Park, S.Y., Oh, D.Y., Han, A.H., Kim, D.S., and Han, J.S. (2005). Role of phospholipase D1 in neurite outgrowth of neural stem cells. Biochemical and biophysical research communications *329*, 804-811.

Yoshida, M., Takayanagi, Y., Inoue, K., Kimura, T., Young, L.J., Onaka, T., and Nishimori, K. (2009). Evidence that oxytocin exerts anxiolytic effects via oxytocin receptor expressed in serotonergic neurons in mice. The Journal of neuroscience : the official journal of the Society for Neuroscience *29*, 2259-2271.

Young, W.S., Li, J., Wersinger, S.R., and Palkovits, M. (2006). The vasopressin 1b receptor is prominent in the hippocampal area CA2 where it is unaffected by restraint stress or adrenalectomy. Neuroscience *143*, 1031-1039.

Yun, D.H., Jeon, E.S., Sung, S.M., Ryu, S.H., and Kim, J.H. (2006). Lysophosphatidylcholine suppresses apoptosis and induces neurite outgrowth in PC12 cells through activation of phospholipase D2. Experimental & molecular medicine *38*, 375-384.

Zeng, X.X., Zheng, X., Xiang, Y., Cho, H.P., Jessen, J.R., Zhong, T.P., Solnica-Krezel, L., and Brown, H.A. (2009). Phospholipase D1 is required for angiogenesis of intersegmental blood vessels in zebrafish. Developmental biology *328*, 363-376.

Zeniou-Meyer, M., Liu, Y., Béglé, A., Olanich, M.E., Hanauer, A., Becherer, U., Rettig, J., Bader, M.F., and Vitale, N. (2008). The Coffin-Lowry syndrome-associated protein RSK2 is implicated in calcium-regulated exocytosis through the regulation of PLD1. Proceedings of the National Academy of Sciences of the United States of America *105*, 8434-8439.

Zhang, Q., Liu, W., Zhao, H., Zhang, Z., Qin, H., Luo, F., and Niu, Q. (2019). Developmental perfluorooctane sulfonate exposure inhibits long-term potentiation by affecting AMPA receptor trafficking. Toxicology *412*, 55-62.

Zhang, X.L., Upreti, C., and Stanton, P.K. (2011). Gbetagamma and the C terminus of SNAP-25 are necessary for long-term depression of transmitter release. PloS one *6*, e20500.

Zhang, Y., Huang, P., Du, G., Kanaho, Y., Frohman, M.A., and Tsirka, S.E. (2004). Increased expression of two phospholipase D isoforms during experimentally induced hippocampal mossy fiber outgrowth. Glia *46*, 74-83.

Zhao, M., Choi, Y.S., Obrietan, K., and Dudek, S.M. (2007). Synaptic plasticity (and the lack thereof) in hippocampal CA2 neurons. The Journal of neuroscience : the official journal of the Society for Neuroscience *27*, 12025-12032.

Zhou, W., Zhang, L., Guoxiang, X., Mojsilovic-Petrovic, J., Takamaya, K., Sattler, R., Huganir, R., and Kalb, R. (2008). GluR1 controls dendrite growth through its binding partner, SAP97. The Journal of neuroscience : the official journal of the Society for Neuroscience *28*, 10220-10233.

Zhu, Y.B., Gao, W., Zhang, Y., Jia, F., Zhang, H.L., Liu, Y.Z., Sun, X.F., Yin, Y., and Yin, D.M. (2016). Astrocyte-derived phosphatidic acid promotes dendritic branching. Scientific reports *6*, 21096.

Zhu, Y.B., Kang, K., Zhang, Y., Qi, C., Li, G., Yin, D.M., and Wang, Y. (2012). PLD1 Negatively Regulates Dendritic Branching. The Journal of neuroscience : the official journal of the Society for Neuroscience *32*, 7960-7969.

Zhukovsky, M.A., Filograna, A., Luini, A., Corda, D., and Valente, C. (2019). The Structure and Function of Acylglycerophosphate Acyltransferase 4/ Lysophosphatidic Acid Acyltransferase Delta (AGPAT4/LPAAT δ). Frontiers in cell and developmental biology *7*, 147.

Ziegler, A.B., Thiele, C., Tenedini, F., Richard, M., Leyendecker, P., Hoermann, A., Soba, P., and Tavosanis, G. (2017). Cell-Autonomous Control of Neuronal Dendrite Expansion via the Fatty Acid Synthesis Regulator SREBP. Cell reports *21*, 3346-3353.

Zoicas, I., and Kornhuber, J. (2019). The Role of the N-Methyl-D-Aspartate Receptors in Social Behavior in Rodents. International journal of molecular sciences *20*.